THE GEOLOGY AND FRACTURING OF THE SPRABERRY FORMATION IN MIDLAND, GLASSCOCK, UPTON, AND REAGAN COUNTIES WEST TEXAS

by

WILLIAM BENFORD FARRINGTON

B.C.E., Cornell University
(1947)

M.S., Cornell University
(1949)

SUBMITTED IN PARTIAL FULFILLMENT
OF THE REQUIREMENTS FOR THE
DEGREE OF DOCTOR OF
PHILOSOPHY

at the

MASSACHUSETTS INSTITUTE OF
TECHNOLOGY

June 1953

Department of Geology, May 18, 1953

Thesis Supervisor

Chairman, Departmental Committee on
Graduate Students

ABSTRACT

THE GEOLOGY AND FRACTURING OF THE SPRABERRY FORMATION IN MIDLAND, GLASSCOCK, UPTON, AND REAGAN COUNTIES, WEST TEXAS

William B. Farrington

Submitted to the Department of Geology on May 18, 1953 in partial fulfillment of the requirements for the degree of Doctor of Philosophy.

The Spraberry formation of Permian Leonard age consists, in the southern Midland basin, of about 1000 feet of siltstone and shale. The oil producing horizons have a very low permeability and owe their producing ability to closely spaced vertical fractures. The productive trend is a very large stratigraphic trap on the flank of a westward dipping monocline.

The variation of thickness of the formation and the areal changes of lithology indicate the east or southeast as the source of Spraberry sediments. During Spraberry deposition the Midland Basin appears to have had the characteristics of a stagnant basin. The sediments in the Upper Spraberry have a median diameter of 0.0056 mm which is in the coarse silt range of the Wentworth scale. The sorting is good. The fossils are almost entirely pelagic and occur only at infrequent intervals. The calcium carbonate and organic content of the sediments is high and reducing conditions are indicated.

About half of the well cores made in the Spraberry contain fractures down their length which divide them into two almost equal parts. Measurement of core diameters across and parallel to fractures shows an apparent fracture opening of about 0.002". A differential horizontal stress of 600 p.s.i. could also produce the effect of an apparent fracture opening. Of the cores with single fractures which were studied, over 75% had the fracture within 1/10 inch of the centerline of the core. Calculations from production and Hydrafrac treatment data show that the lateral extent of the fractures opened artificially must be several hundred feet. Release of hydrostatic pressure applied in a pressure vessel produced a few "artificial" fractures showing that a direction of incipient weakness exists in some of the specimens and that some of the fractures are not open in the formation. The major fracture set trends N 25° E with a more poorly developed set of fractures crossing the main set. This fracture pattern was duplicated in warped plate glass by means of compressive stresses applied in two directions.

Aug. 13, 1953

Physical tests on the siltstone show that the value of Young's modulus is strongly dependent on the applied stress. Poisson's ratio is similarly dependent on stress and has a very low value indicative of a very brittle material. Samples were found to creep under prolonged high stress. The Mohr diagram construction was used to analyze rupture conditions under confining pressures. The rupture stress required is much larger when confining pressure acts.

Thesis Supervisor: Dr. Walter L. Whitehead

TABLE OF CONTENTS

Chapter		Page
I	Introduction	1
	1. Acknowledgements	1
	2. Statement of Problem	1
	3. Previous Work	2
	4. Method of Collecting and Filing Data	3
	A. Microfilm	3
	B. Punched Cards	5
	5. Materials Available for Study	7
II	Reservoir Performance	8
	1. General Geology of the Formation	8
	A. Stratigraphy	8
	B. Structure	9
	2. Reservoir Characteristics	11
	A. Permeability	11
	Upper Spraberry	11
	Statistical Analysis	12
	Lower Spraberry	13
	Conclusions	13
	B. Porosity	17
	Upper Spraberry	17
	Lower Spraberry	17
	Effect of Fractures	20
	C. General Production Data	21
	3. Completion Practices	23
	A. Hydrafrac and Strata-frac	24
	B. Conclusions from Hydrafrac Data	26
	Number of Fractures	26
	Extent of Fracturing	26
	Fracture Stress	27
	C. Other Completion Practices	30
	Acid Flushing of Fractures	30
	Cementing Practices	31
III	Basin Characteristics	32
	1. General Shape of Basin	32
	2. Isopachous Maps	32
	A. Base of Dean to Top of Spraberry	33
	B. Isopachous Map of the Clearfork Formation	34
	C. Isopachous Map of San Andreas and Grayburg	34
	D. Summary of Whole Section	35

TABLE OF CONTENTS
-2-

Chapter		Page
	3. Sedimentology	36
	A. General Methods of Study	36
	B. Grain Size Analyses	38
	Method of Making Count	38
	Treatment of Data	39
	Results	43
	Conclusions	45
	C. Grain Shape	46
	D. Minerology	47
	E. Depositional Fabric	47
	Theory of Grain Orientation	47
	General Description of Equipment	49
	Results	51
	Conclusions	54
	F. Lithofacies Map of Spraberry	55
	G. Other Sedimentary Features	57
	Micro-Laminations	57
	Concretions	57
	4. Paleontology	58
	5. Paleogeography	59
	A. Construction of Paleogeologic Maps	59
	B. Discussion of Paleogeographic Maps of Spraberry	61
	6. Conclusions about Basin Characteristics	62
IV	Fracture Study	64
	1. Relation of Fractures to Centers of Cores	64
	A. Method of Study	64
	B. Results of Study	65
	C. Significance of Results	66
	2. Fracture Dimensions	68
	A. Direct Measurement of Widths Theory	68
	Method of Study	69
	Results	69
	Conclusions	70
	B. Calculation of Lateral Extent	74
	3. Discussion of Fracture Formation	77

TABLE OF CONTENTS
-3-

Chapter		Page
	4. Pressure Vessel Work	79
	A. General Theory.	79
	B. Analysis of Stresses.	82
	The Mohr Diagram.	83
	C. General Description of Equipment.	89
	D. Choice of Pore Fluid.	90
	E. Time Required for Test.	94
	F. Results	95
	Whole cores	95
	Previously Fractured Cores.	97
	G. Conclusions	98
	5. Orientation of Fractures	99
	A. Magnetic Core Orientation	99
	Theory.	99
	Results	101
	B. Orientation of Fractures from Production Data.	101
	6. Mechanics of Fracture Formation.	103
	A. Evidence that Fractures are Joints.	103
	B. Relation to Joints in Surrounding Areas.	104
	C. Mechanical Reproduction of Fractures	105
V	Physical Tests of Spraberry Cores	108
	1. Desired Information.	108
	2. Methods of Testing and Results	109
	A. SR-4 Gages.	109
	B. Destructive Tension and Compression Tests.	111
	Compression	111
	Tension	113
	C. Cantilever Tests.	115
	D. Tests with Mechanical Gages	122
	E. Torsional Tests	127
	3. Significance of Physical Tests	128
VI	Summary of Conclusions.	131
	References.	133
	Appendix "A". Description of Photoelectric Orientation Instrument	144
	Appendix "B". Description of Pressure Vessel	155
	Biographical Note	165

LIST OF FIGURES

		After Page
1.	Location Map	5
2.	Four County Area	6
3.	Stratigraphic Correlation Chart	8
4.	Structure Map - Top of Spraberry	9
5.	Principal Oil Fields	10
6.	Permeability Distribution in Upper Spraberry	11
7.	Permeability Distribution in Lower Spraberry	13
8.	Porosity of Upper Spraberry	17
9.	Porosity of Lower Spraberry	17
10.	Typical Gel Injection Pressure Curve	25
11.	Isopach Map - Base of Dean to Top of Spraberry	33
12.	Isopach Map - Clearfork	34
13.	Isopach Map - San Andreas to Grayburg	34
14.	Isopach Map - Base of Dean to Top of Grayburg	35
15.	Upper Spraberry Grain Size Analyses	43
16.	Histogram of 12 Upper Spraberry Grain Analyses	44
17.	Cumulative Curve of Total of Upper Spraberry Analyses	45
18.	Angular Relation between Grain Orientation and Fractures	53
19.	Lithofacies Map	55
20.	Paleogeographic Map - Top of Spraberry	60
21.	Paleogeographic Map - Base of Dean	60

LIST OF FIGURES
-2-

		After Page
22.	Relation of Fractures to Core Centers	65
23.	Frequency Distribution of Fracture Sizes	70
24.	Effect of Stress on Apparent Fracture Opening	72
25.	Change of Pressure Distribution with Time	80
26.	Mohr Circle	83
27.	Mohr Circles for the Three Principal Planes	84
28.	Mohr Envelope and Failure Circles for Steel	85
29.	Mohr Envelope and Failure Circles for Upper Spraberry	86
30.	Mohr Diagram for Existing Conditions	88
31.	Orientation of Fractures from Magnetic Poles of Cores	101
32.	Load vs. Deflections for First Cantilever Test	120
33.	Load vs. Deflections for Second Cantilever Test	120
34.	Stress vs. Strain for Upper Spraberry Core Loaded Perpendicular to Bedding	125
35.	Stress vs. Young's Modulus for Upper Spraberry Core Loaded Perpendicular to Bedding	126
36.	Stress vs. Poisson's Ratio for Upper Spraberry Core Loaded Perpendicular to Bedding	126
37.	Photoelectric Amplifier Circuit	145
38.	Pressure Vessel	155

LIST OF PLATES

		After Page
1.	Punched Card	4
2.	Punched Cards and Equipment	4
3.	Photomicrograph Equipment	37
4.	Photomicrographs of Spraberry Thin Sections	46
5.	Photomicrographs of Spraberry Thin Sections	47
6.	Photomicrographs of Spraberry Thin Sections	47
7.	Photographs of Spraberry Polished Sections	47
8.	Photograph and photomicrograph of Micro-laminations	57
9.	Photographs of Concretions	57
10.	Photomicrographs of Radiolaria	58
11.	Photomicrographs of Radiolaria	58
12.	Typical Spraberry Cores	64
13.	Core Measuring Equipment	64
14.	Unusual Fractures from Pressure Vessel	95
15.	Artificial Fractures in Glass	105
16.	Use of SR-4 Gages. Broken Test Pieces	110
17.	Arrangement of Equipment for Cantilever Test	115
18.	Grain Orientation Equipment	147
19.	Whole Thin Section Analyzer	149
20.	Pressure Vessel	159
21.	Auxiliary Vessel Equipment	161.

LIST OF TABLES

		Page
I	Distribution of Permeabilities in the Upper Spraberry	14
II	Distribution of Permeabilities in the Lower Spraberry	15
III	Distribution of Porosity in the Upper Spraberry	18
IV	Distribution of Porosity in the Lower Spraberry	19
V	Distribution of Grain Sizes 28 feet below Top of Upper Spraberry	40
VI	Distribution of Grain Sizes 96 feet below Top of Upper Spraberry	40
VII	Distribution of Grain Sizes 159 feet below Top of Upper Spraberry	41
VIII	Distribution of Grain Sizes in 12 Upper Spraberry Cores	42
IX	Grain Orientation Data by Photoelectric Method	52
X	Deviation of Fractures from Core Centers	67
XI	Distribution of Fracture Widths	71
XII	Tests of Ultimate Compressive Stress	112
XIII	Tests of Ultimate Tensile Stress	114
XIV	First Cantilever Test	117
XV	Second Cantilever Test	119
XVI	Compression Test Perpendicular to Bedding with Dial Gages	125

CHAPTER I

INTRODUCTION

1. ACKNOWLEDGEMENTS

The writer is indebted to Dr. W. L. Whitehead for suggesting the study of the Spraberry formation and for helpful ideas as the work progressed. Thanks are also extended to the Sunray Oil Corporation for contributing well cores and well data and to Carter Research Laboratories, the California Research Corporation, the Humble Oil Company, the Phillips Petroleum Co., and the Sohio Petroleum Company for general information. Many consulting geologists gave valuable information and made useful suggestions. Particular thanks are due to George Gibson, E. Russell Lloyd, Victor Ogden, J. W. Skrabanek and W. A. Waldschmidt.

2. STATEMENT OF PROBLEM

The Spraberry formation of West Texas contains a large petroleum reserve which could not be produced economically if it were not for fractures in the formation. The permeability of the matrix of the reservoir rock is so low that very little oil would flow from each well if it were not for the system of fractures. Fractured reservoirs have recently

been found to be more common than was once thought, and the future oil possibilities in many areas may depend on an understanding of the operation and geological conditions of such reservoirs.

There is some difference of opinion among operators in the Spraberry trend concerning the condition of the fractures in the formation. Some believe the fractures are incipient and are not opened until after drilling or completion of the well, while others believe the fractures are generally open naturally in the formation. There is general agreement that the fractures play an important part in oil production.

This paper presents some of the relations of the fractures to the general regional geology as well as some methods of studying the nature of the fractures themselves. The area covered is shown on Figure 1 and is known as the "four county area" or merely as the southern part of the trend.

3. PREVIOUS WORK

The first oil production from the Spraberry formation was in January, 1949, and general development of the area was slow until 1950. In the comparatively short time since the opening of the field a great deal of research has been

done by oil companies and consulting geologists. Of course, much of this work has never been published, and much of that which has deals with engineering rather than geological aspects of the field. However, a great number of short articles have been published, which can be combined with some data from the oil companies to give a good overall picture of the trend.

Considerable attention has been devoted to the fractures themselves, their orientation, their effective size and engineering practices needed to best utilize these fractures. General structure, lithology, and production data, and the relations of these to the fractures have all been the subjects of published articles. A great deal of attention has been devoted to the new completion practices developed especially for fractured reservoirs.

One of the first phases of the present study was the collection, correlation, and synthesis of all available information. Some of the structure maps presented were pieced together from information obtained from many sources, both published and unpublished.

4. METHOD OF COLLECTING AND FILING DATA

A. MICROFILM

During the month of June, 1952, the writer made a trip to gather well cores and information. Geologists and oil

companies were visited in Tulsa, Midland, Abilene, Dallas, and Houston. For reasons of economy it was necessary to make the trip as short as possible. Since the manual transcription of data and information is a lengthy process and is subject to human error, it was decided to copy all information photographically on microfilm. To accomplish this the writer mounted his 35 mm Exacta camera on a portable stand. When disassembled the whole setup could be carried conveniently in a briefcase. This portability was particularly useful on the rare occasions when it was not possible to borrow material overnight and copy it in a hotel room. The microfilm was generally developed in a portable tank on the same day as its exposure and then filed in cylindrical cans and labelled.

All published articles were also recorded on 35 mm microfilm in the same manner. This was especially useful for this particular problem since most of the published information consists of journal articles only two or three pages in length.

The microfilm could be scanned directly by placing it in a photographic enlarger and projecting onto a white cardboard. This was a convenient method for cataloguing the data or reading material which would not be used again. More pertinent information was projection printed and mounted on punched cards as explained below.

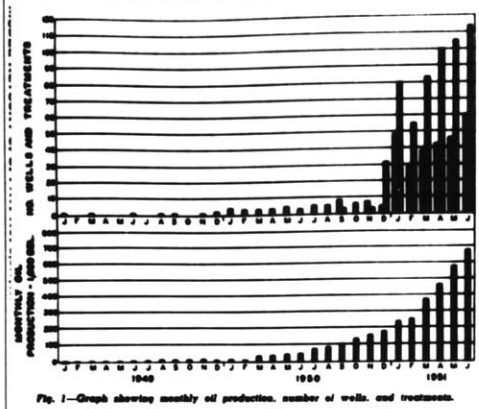


Fig. 1—Graph showing monthly oil production, number of wells, and treatments.

Hydrafrac Operations

by Waldo L. Grossmann

Division engineer, Halliburton Oil Well Cementing Co., Midland, Tex.

Application of the Hydrafrac process to wells completing from the Spraberry formation was begun during the last part of 1950. The Hydrafrac process consists of preparing a viscous gel to which a special sand is added and pumping this material into the producing formation at a rate which will develop sufficient hydraulic force to produce and or extend a fracture. The gel must be of an unstable character to revert to a thin fluid, such that it may be recovered from the well, leaving the introduced sand in the fracture as a propping agent. In order to insure the reversion of gel to a fluid, breaker chemicals are mixed with crude oil and flushed into the formation behind the gel. The success of these treatments has been closely associated with the current expanding drilling and development program along an area commonly referred to as the "Spraberry trend."

RESULTS of all treatments have varied considerably. Probably one of the best indicators of the general success of the process is the 1,046 treatments performed. Additional experience in the several means of Hydrafrac application will better enable evaluation as to the best possible method of treatment.

The solid bars in the upper portion of Fig. 1 show the number of wells completed each month for 15 Spraberry fields from January 1949 through June 1951. The cross-hatched bars indicate the number of Hydrafrac treatments each month during this period. From this graph, it may be noted that the rapid development of the Spraberry has been closely associated with the introduction of the Hydrafrac treatments.

Oil production by months is shown in the lower portion of Fig. 1 for the same fields for the same period. Current production has exceeded the rate of 1 million barrels per month.

Mixing of Material

The gel consists of a mixture of kerosine, water, and oil-soluble soap. Kerosine is used because it is generally a reliable standard fluid. The small volume of water is added to insure a breakdown of the gel. The oil-soluble soap is the gelling agent. The size of treatment is often called a two, three, or four-batch job. A batch includes the following materials: 750 gal. of kerosine plus the necessary chemicals to form the gel. The gelling agent is a time-and-temperature-sensitive material; consequently, the kerosine should be at a proper temperature for mixing. This requires the use of a steam unit during the winter months.

After the mixture has gelled properly, it is ready to be pumped into the well. As it is being pumped into the well the special sand is added, normally in the amount of 400 lb. per batch or about ½ lb. per gal. The breaker fluid consists of crude oil and a small amount of special chemical. The normal amount of breaker fluid used is twice the amount of gel fluid.

Although the addition of water to the gel should insure a breakdown of the gel within a reasonable time in wells with bottom-hole temperatures above 115 to 125 F., it was originally felt desirable to follow the gel with an external breaker fluid as additional insurance. For wells with lower bottom-hole temperatures, an internal breaker chemical is added to the gel. After the gel and breaker fluid have been displaced into the formation, the normal practice is to close the well in and allow the fluids to remain static for a minimum period of 8 to 12 hours. After this time, the gel should have become fluid and the well may be swabbed or pumped in order to be placed on production.

Method of Treatment Application

The various methods of treatment application from September 1950 through September 1951 are indicated in Table 1.

The method of performing a Hydrafrac treatment may be generally classified as an open-hole or a casing-perforation treatment. Open-hole treatments may be divided into two general classifications either with a packer or without a packer. Three different types of packer arrangements may be used. These are:

1. Packer set in casing—treat the open hole below casing shoe to total depth.

2. Single formation packer set in open hole, generally treat from packer to total depth. Treatments of open hole above packer to casing shoe have generally resulted in a fishing job.

3. Straddle-type formation packer with one or both elements set in the open hole—treat open hole between the two packer elements.

Most every one is familiar with the general design and mechanical operation of conventional hookwall casing packers and formation anchor packers. However, the hydraulically operated straddle packer is a relatively new tool originally designed for Hydrafrac operations. All of the open-hole and some of the casing-perforation treatments through a straddle packer have used this hydraulically operated tool which is set by pump pressure applied from the surface.

TABLE 1—METHOD OF TREATMENT APPLICATION

	Open hole					Casing perf		
	With packer			No packer				
	Formation							
	Casing packer	anchor-packer	Straddle packer	Tubing	Casing	Casing packer	Straddle packer	Total No treatments
1950—								
September	1	1				1		3
October								6
November		3						4
December	9	9	17			2	2	41
1951—								
January	7	10	44			10		70
February	4	10	32			7	3	54
March	10	14	33			11	3	82
April	10	11	33			4	4	109
May	11	11	33			3	10	105
June	11	11	33			11	3	116
July	11	11	33			13		144
August	10	11	33	2		12		172
September	14	10	17	1	1	4	2	138
Total	274	260	489	3	1	89	29	1,046

The main features of this tool are—

1. Available in two sizes;

drill pipe operates the circulating valve.

9. As many as five treatments

The average is about three treatments per well.

The treatment of open hole without the use of a packer has been a recent development. This method has been used in order to eliminate the loss of pumping horsepower as tubing friction. Injection rates of 10 to 15 bbl. per minute with surface pressures from 1,300 to 1,500 psi. have been obtained using this procedure.

Treatments through casing perforations whether of the single casing packer or straddle-packer type were generally performed on two classes of wells. First, dry holes or depleted wells from pre-Permian formations and, second, new wells. In wells of the first type, it was necessary to set casing through the Spraberry to test or produce these lower formations. Most of the earlier casing per-

PUNCHED CARD

PLATE 1



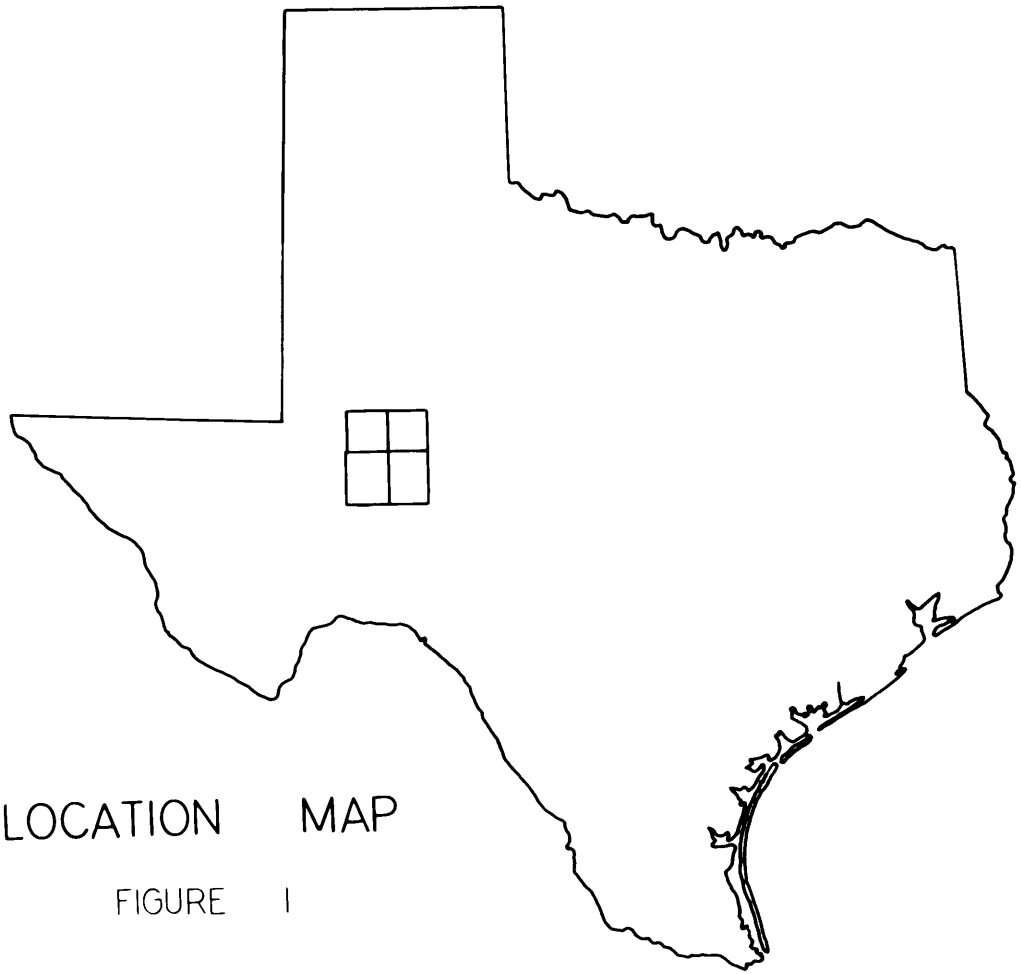
PUNCHED CARDS AND EQUIPMENT

PLATE 2

B. PUNCHED CARDS

All data deemed to be of use in this study was filed on hand-sorted punched cards. The results of the writer's laboratory work were also recorded on the punched cards. Since the total number of headings under which information would be classified was not expected to exceed one hundred, a direct code was chosen. Plate 1 shows the form of card used and the approximate size which is 5" x 8". The double rows of holes numbered 1 to 28 and 35 to 50 were used for the direct code. Three methods of punching are possible with the double row of holes; a shallow punch notches the edge of the card into the outer row of holes; a deep punch notches to the inner row of holes; and an intermediate punch connects the two rows of holes. Since this number of headings was not required, it was decided to use only deep and shallow punches, both of which could be made with the same hand punch. In each of the numbered categories the deep punch was used for information dealing directly with the Spraberry formation, while the shallow punch indicated that the card contained information of a general nature under the particular category. Both of these are shown on plate 1.

In addition to the direct code, the margins of the cards were notched for the first three letters of the author's name, the year and month of publication, and the general



LOCATION MAP

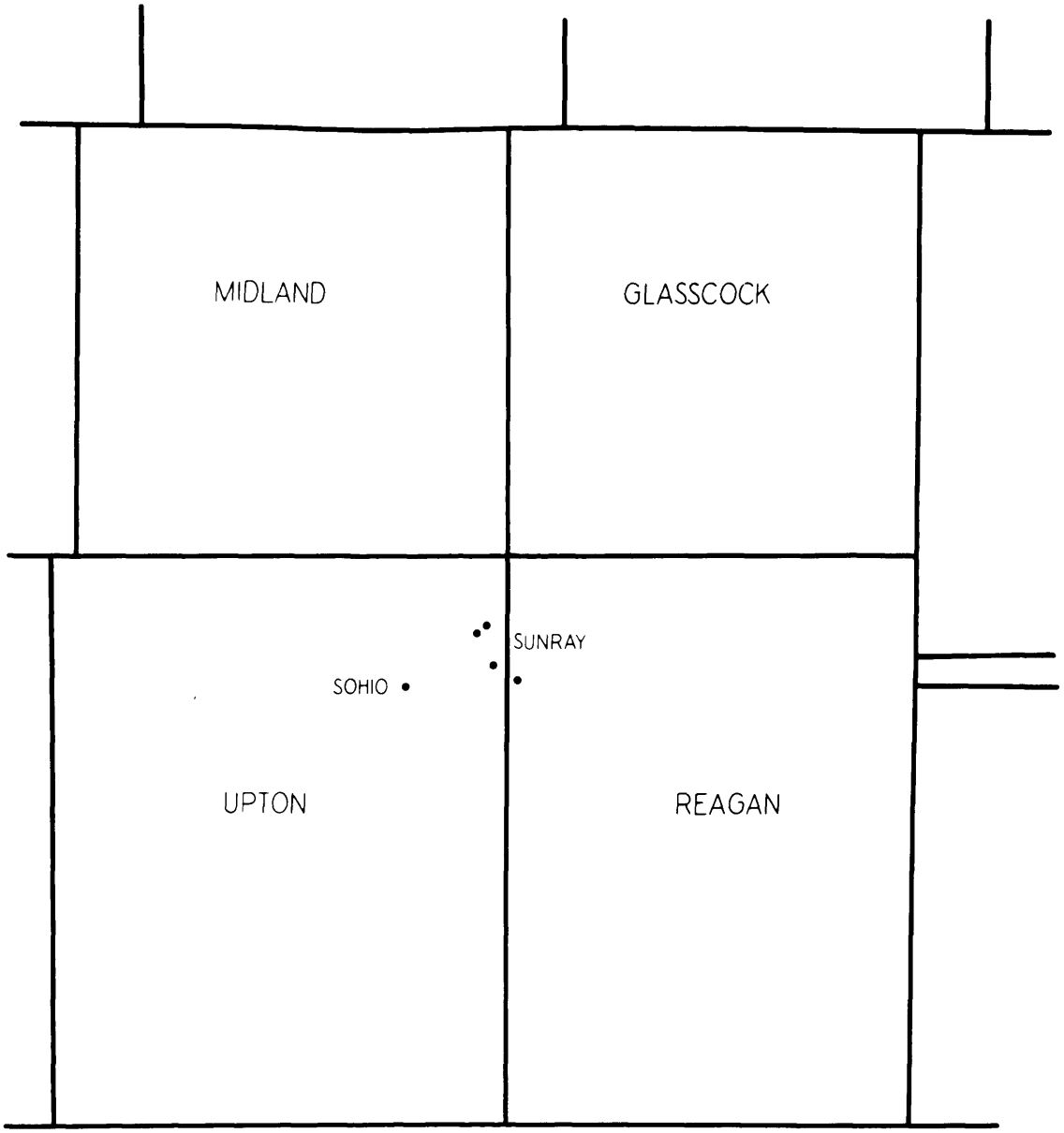
FIGURE 1

category for the source of the material. If a particular set of data or an article required more than a single card a special hole was notched out of each card in the set.

To separate the cards in any one category it was necessary only to pass a knitting needle through the stack of cards at the indicated hole and lift the whole stack of cards away from those in the desired category, which then dropped out. Since it was generally not convenient to handle a stack of cards more than an inch and a half or two inches high at one time, it became necessary to make several passes with the needle as the total number of cards increased.

The portion of the microfilmed data which was to be placed on the punched cards was projection printed onto thin white printing paper to the exact size required for mounting on the punched cards. The prints were then trimmed to size and mounted on the punched card with dry mounting tissue. It was found that three pages of journal articles could be put on a single card by mounting prints on both sides of the card. A reading glass was sometimes found to be convenient in reading the prints but was not entirely necessary. All of the punched card equipment is shown in Plate 2.

It was found that the extra thickness of the cards caused by the photographs did not affect the efficacy of the sorting process. It is felt that the time required to record photographically as outlined above is far less than



FOUR COUNTY AREA

FIGURE 2

by manual transcription, and the accuracy is absolute. The handwritten cards containing results of laboratory work were interspersed with the other cards without causing any interference in the sorting operation.

5. MATERIALS AVAILABLE FOR STUDY

While in Tulsa the writer was allowed to select core samples from the residue cores of three wells of the Sunray Oil Corporation. The selected samples were carefully packed and sent back to Cambridge by the writer for laboratory examination. Fifty-four core samples were selected. The Sunray Oil Corporation also supplied porosity and permeability data for four wells. The general locations of these wells are shown on Figure 2, but it is the company's wish that their exact identities should not be revealed.

The cores selected are almost all from the siltstones which are the producing horizon. Two of the cores are from the shale overlying the producing horizon, but none are from the thin limy horizons of the Middle Spraberry member.

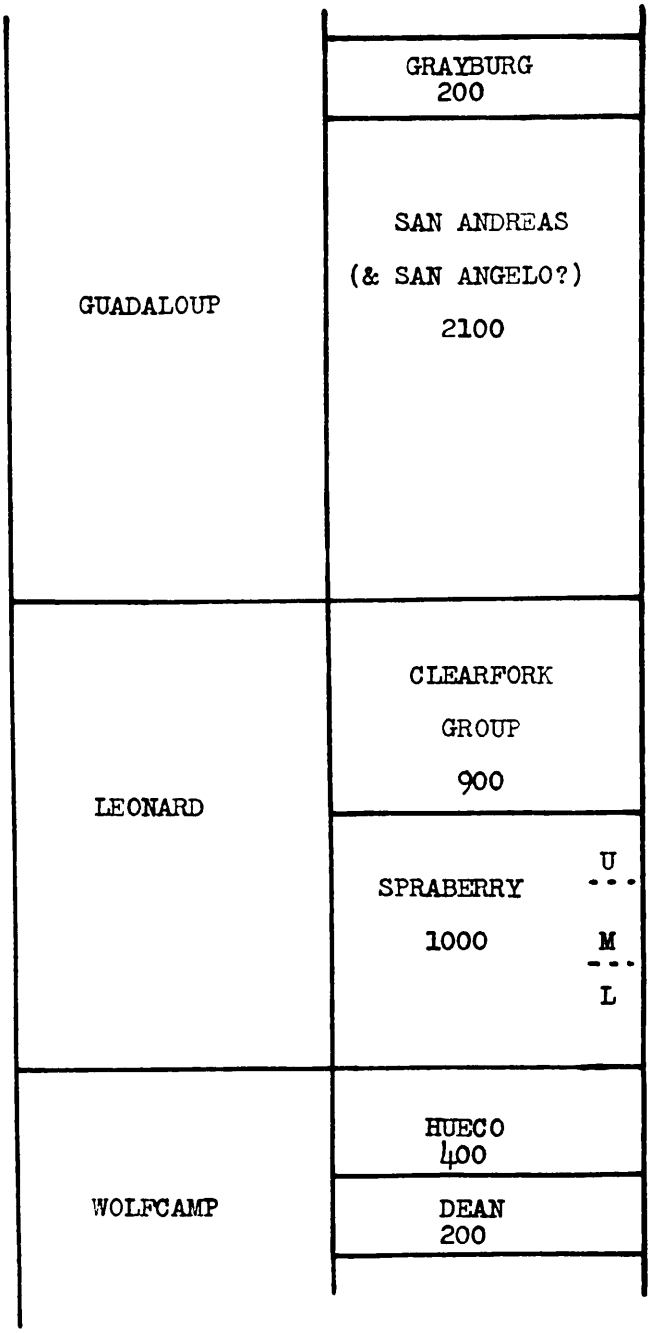
CHAPTER II

RESERVOIR PERFORMANCE

1. GENERAL GEOLOGY OF THE FORMATION

A. STRATIGRAPHY

The Spraberry formation consists of about 1000 feet of hard sandstone and shale with some limestone. Its stratigraphic position is shown in Figure 3 along with the approximate thicknesses of other formations in the center of the four county area. The Spraberry formation itself can be subdivided into an upper, middle, and lower part. The Upper Spraberry averages about 250 feet in thickness and consists of fine grained silty sandstone or siltstone with interspersed silty shale. The Upper Spraberry member thickens slightly toward the west. The Middle Spraberry averages about 350 feet in thickness and consists chiefly of black shales with one thick sandstone member occurring near the center. The lower member has a thickness of 400 to 500 feet and is similar lithologically to the upper member. The lower member thickens toward the west and south to a greater extent than either of the upper two members. The upper and lower members each become slightly more limy toward the top with little change of grain size.



CORRELATION CHART FOR FOUR COUNTY AREA WITH APPROXIMATE THICKNESSES IN FEET

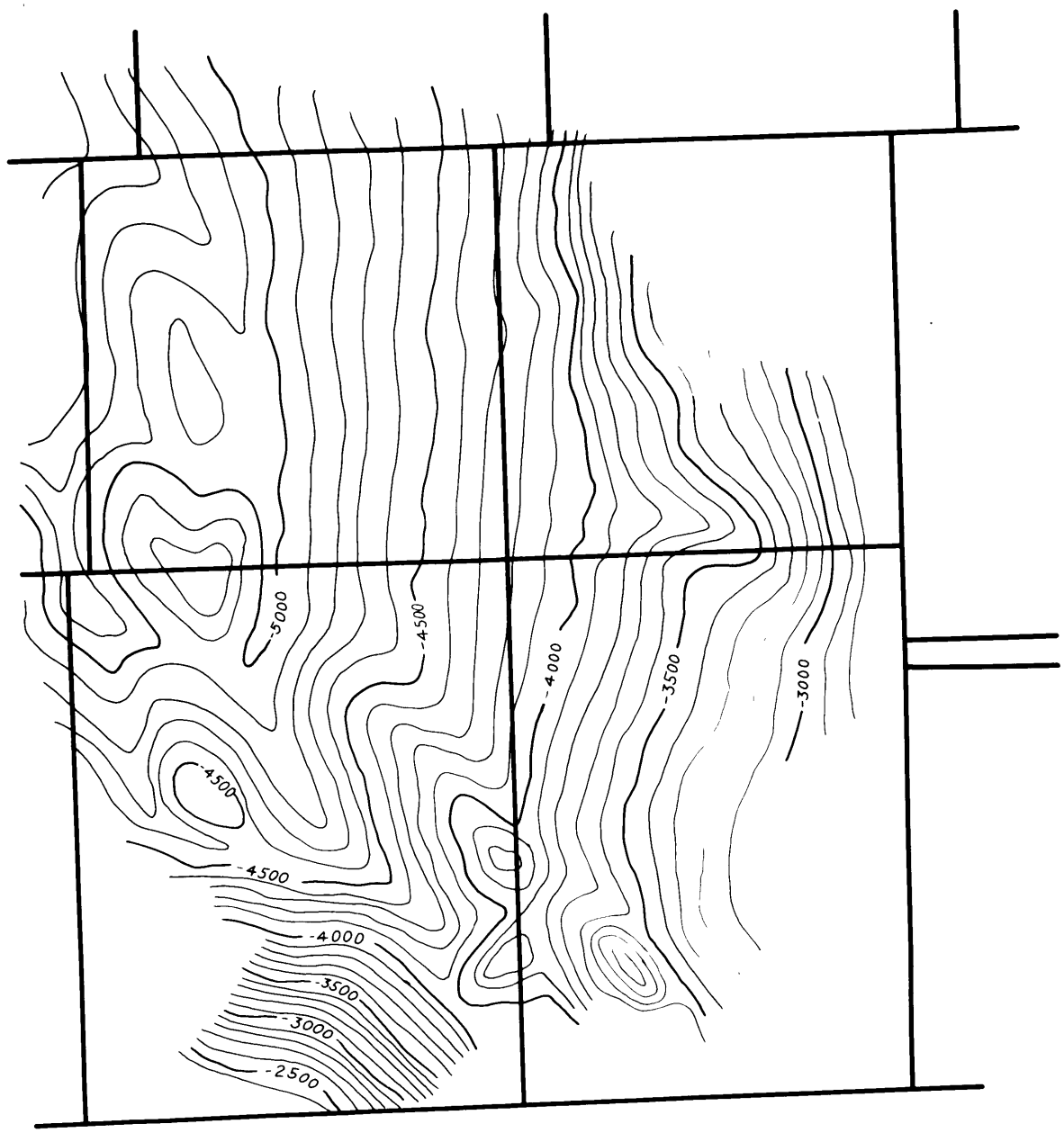
FIGURE 3

The Spraberry trend producing area is essentially a large stratigraphic trap whose limits are controlled by porosity and permeability changes due to facies changes and reduction in the intensity of fracturing. In the four county area there are over twenty separate fields (Bartley, 1951,b) which are all in this same monoclinal, westward dipping area of higher permeability and porosity. The Benedum field in east central Upton County is the only field exhibiting any appreciable structural closure.

There appear to be no large interruptions in deposition during Spraberry time and the transitions from sandstone to shale are more or less gradational. Toward the western part of the area there appears to be a fusion of the Lower and Middle Spraberry and no lithologic break can be discerned in some localities.

B. STRUCTURE

Figure 4 is a regional map with 100 foot contours showing the structure on the top of the Spraberry formation. The regional structure is a broad westward dipping monocline with average dips of about 50 feet per mile. Figure 5 shows the principal oil fields in the four county area. A comparison of the producing areas with the structure map shows that all of the fields except Benedum are associated with broad west-plunging noses on the regional monocline.



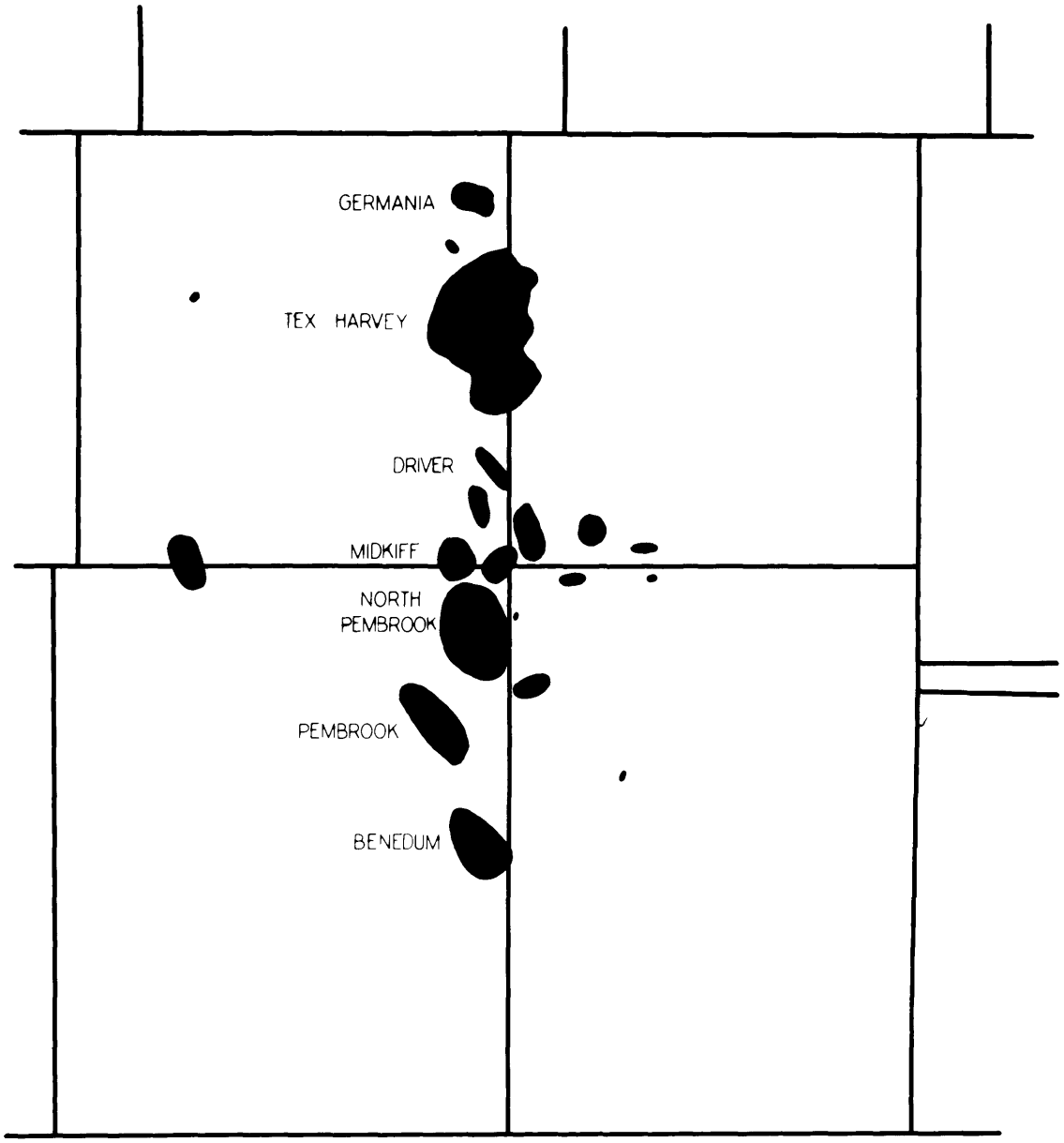
STRUCTURE MAP

TOP OF SPRABERRY

FIGURE 4

These fields have a maximum closure of less than 30 feet. The Benedum field has a closure of about 195 feet and is the result of sedimentation over a faulted Ellenburger (Ordovician) structure. Most of the fields shown produce from the Upper Spraberry, but a few in the southern part of the area produce from the Lower Spraberry or from both horizons. Both of the producing horizons become more calcareous toward the east and thus become less permeable and have lower porosity. Also there is less fracturing toward the east. Westward the members become more shaly and a little more limy, but the westward limit of production is controlled by an indefinite water table at about the minus 4500 foot contour. The regional dip was developed mostly after late Guadaloup time as will be shown in Chapter III. (See also Figure 135, Eardley, 1951)

The fractures are well developed along the producing belt in the area shown and continue for a similar distance into the next four counties to the north but are not so well developed in the northern part of the trend. The fractures are not so well developed to the east, but it is believed that the limit of production is controlled more by facies changes than by the lack of fractures. The fractures continue past the producing area to the west, but little information is available in this non-commercial area. A detailed study of some of the features of these fractures is presented in Chapter IV.



PRINCIPAL OIL FIELDS

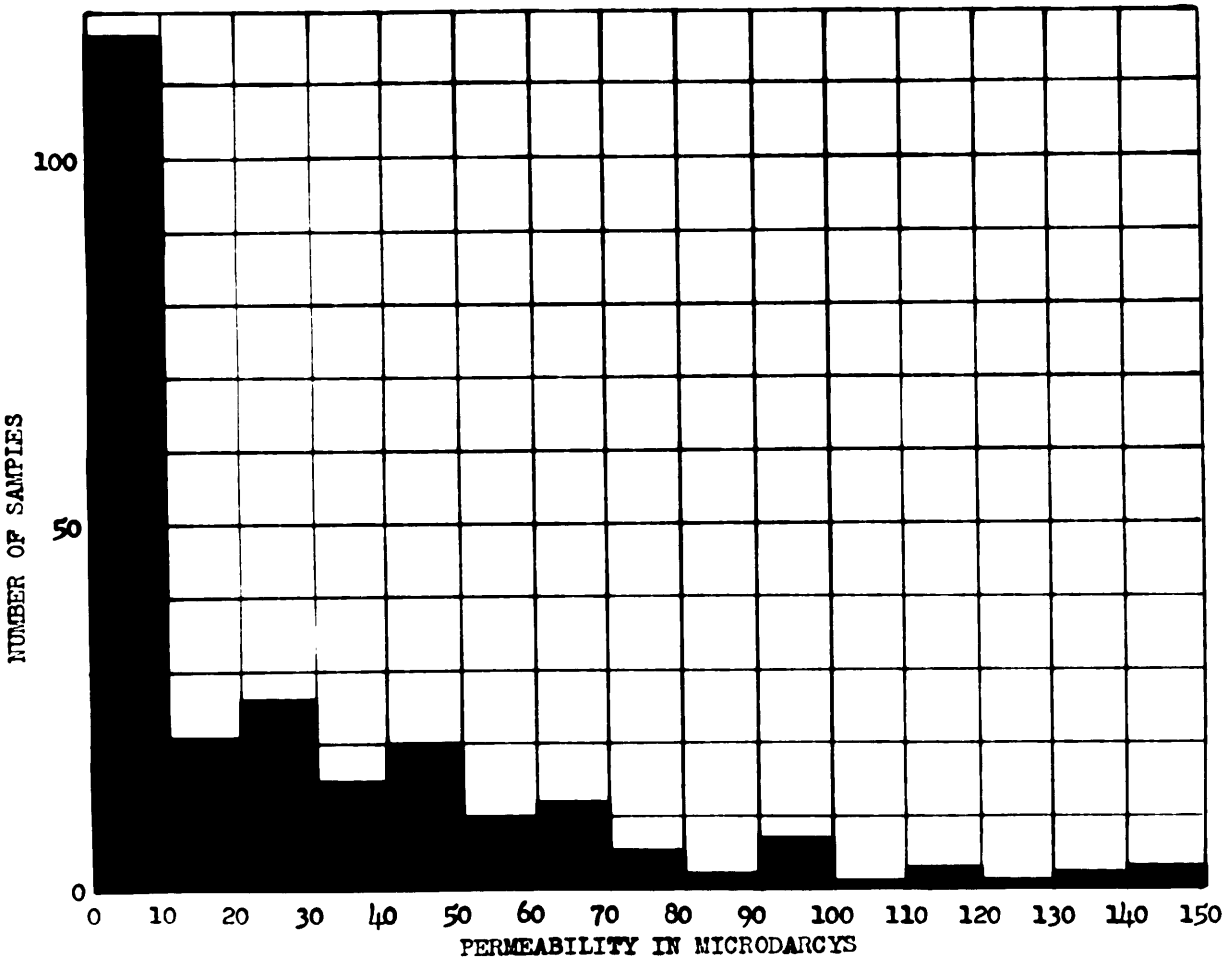
FIGURE 5

2. RESERVOIR CHARACTERISTICS

A. PERMEABILITY

One of the most striking features of the Spraberry producing zones is the very low permeabilities. The permeability of the rock matrix ranges from 0.002 to 2.5 millidarcys with by far the greater number tending toward the lower limit. Many of the higher permeabilities are the result of fractures or partial fractures in the test samples.

Upper Spraberry. Table I is a compilation of tests on 249 cores from the Upper Spraberry and shows the number of tests falling into each permeability interval. This data was supplied by the Sunray Oil Corporation and represents tests made on two closely spaced wells. The permeability interval used is 10 microdarcys. A few samples fall beyond the range of the table, but these values are not included since it is felt that many of these higher permeability values are the result of fractures. In fact many of the samples with higher permeabilities were indicated to have fractures by the technicians making the tests. Only six tests were excluded aside from those of cores definitely labelled as showing fractures. These were all in the same range of values as the fractured samples and had values completely isolating them from the lower permeability values finally used.



PERMEABILITY DISTRIBUTION IN THE UPPER SPRABERRY

FIGURE 6

From Table I it can be computed that the average permeability of the Upper Spraberry member is 30.4 microdarcys. This was computed by considering that all the samples were concentrated at the centers of the permeability ranges. Since the data was not given closer than 0.01 millidarcys there was no other choice. The computations for the average permeability are not shown on the table.

Statistical Analysis. The last three columns of Table I are part of the computations for standard deviation, σ. The third column gives e, the deviation of the center of each permeability range from the mean value of permeability found above. The fourth column gives the square of e, while the last column gives the total of the squares of deviation from the mean for all the values in each permeability range. Then standard deviation can be found from the formula

$$\sigma = \left(\frac{\sum_{o}^{n} e^2}{n - 1} \right)^{1/2}$$

Since e is the deviation from the mean rather than from the correct value, which is not known, one degree of freedom is lost and the standard deviation will thus be larger. For this reason n - 1 is used in the equation rather than n. Substituting the values from the table into the formula the standard deviation is found to be 37.8 microdarcys.

From the standard deviation the probable error of the mean can be found from the formula below given by Eshbach

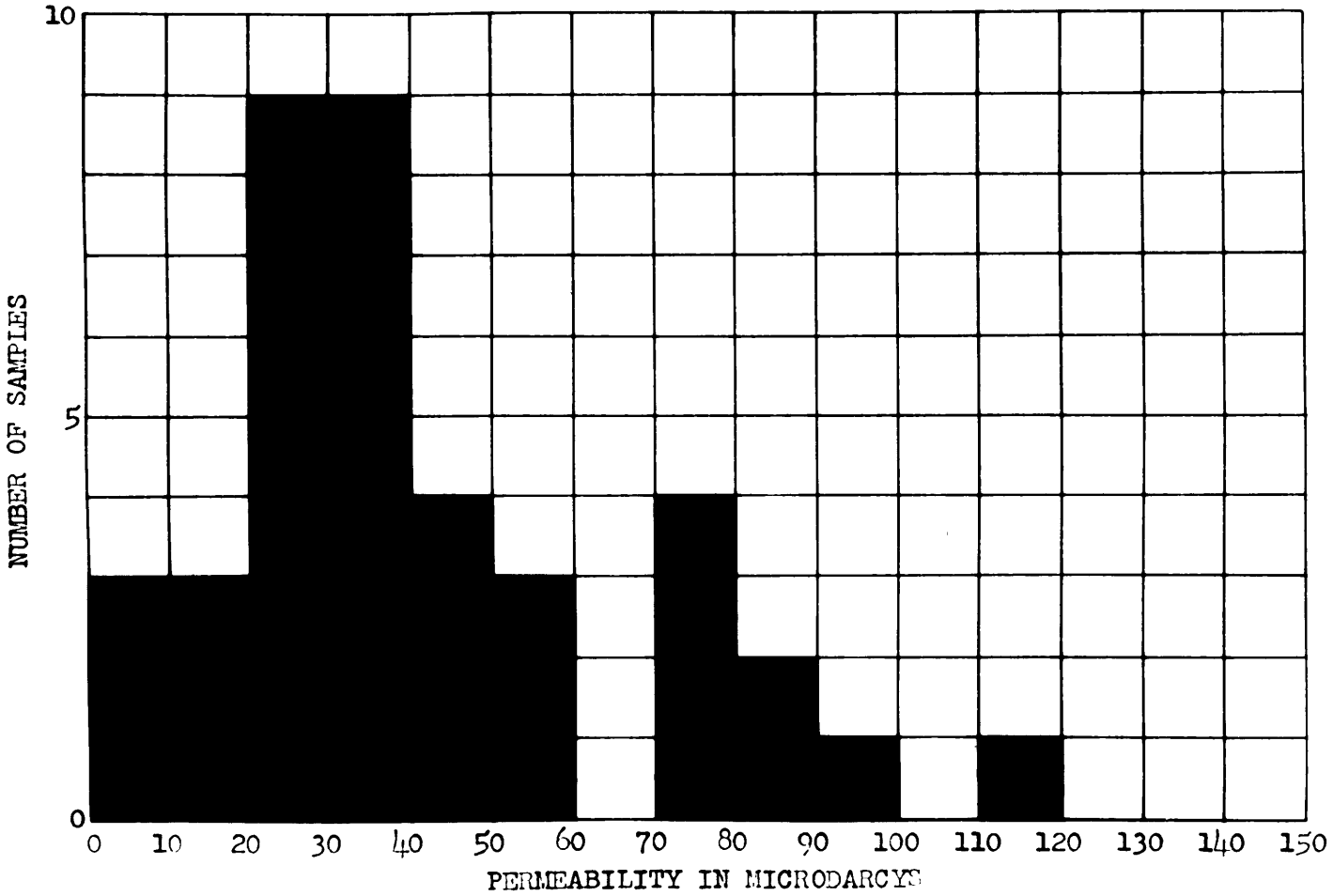
(1949, p. 2-126)

$$r_m = 0.6745 \times \left(\frac{1}{n}\right)^{1/2} \times \sigma.$$

The probable error is found to be 1.6 microdarcys. The average value of permeability in the Upper Spraberry should thus be given as 30.4 ± 1.6 microdarcys. The data of Table I is plotted on Figure 6 in the form of a histogram.

Lower Spraberry. In a similar manner Table II gives the results of 61 tests on the Lower Spraberry from two wells which are in close proximity to the two used for the Upper Spraberry analysis. One additional test was not used because of fractures noted by the technician. Unlike the higher permeability tests for the upper member, the permeabilities over 100 microdarcys are quite evenly distributed and represent a fairly large portion (38%) of the total number of tests. The average permeability is 250 ± 28 microdarcys and the standard deviation is 323 microdarcys. The data shown on Table II is plotted as a histogram on Figure 7.

Conclusions. The standard deviations of both sets of permeability data are quite large due to the influence of the few scattered tests of higher permeability. If it were assumed that these are the result of microfractures in the test samples, and computations were based on only the main peaks of the curves, (values below about 100 microdarcys) then the standard deviation would be considerably



PERMEABILITY DISTRIBUTION IN THE LOWER SPRABERRY

FIGURE 7

Table I

Distribution of Permeabilities in the Upper Spraberry

Permeability Range - μd.	No. of Samples	e	e^2	ne^2
0-10	117	- 25.4	642	75,050
10-20	21	- 15.4	237	4,980
20-30	26	- 5.4	29	754
30-40	15	+ 4.6	21	315
40-50	20	+ 14.6	213	4,260
50-60	10	+ 24.6	594	5,940
60-70	12	+ 34.6	1,181	14,180
70-80	5	+ 44.6	1,970	9,850
80-90	2	+ 54.6	2,980	5,960
90-100	7	+ 64.6	4,170	29,200
100-110	1	+ 74.6	5,570	5,570
110-120	3	+ 84.6	7,180	21,540
120-130	1	+ 94.6	8,930	8,930
130-140	2	+ 104.6	10,920	21,840
140-150	3	+ 114.6	13,100	39,300
150-160	0	+ 124.6	15,500	0
160-170	0	+ 134.6	18,100	0
170-180	0	+ 144.6	20,900	0
180-190	2	+ 154.6	23,900	47,800
190-200	0	+ 164.6	27,100	0
200-210	2	+ 174.6	30,500	61,000
	249			356,469

average = 30.4 microdarcys

Table II

Distribution of Permeabilities in the Lower Spraberry

Permeability range - μd.	No. of Samples	e	e^2	ne^2
0-10	3	- 245	60,000	180,000
10-20	3	- 235	55,200	165,600
20-30	9	- 225	50,600	455,400
30-40	9	- 215	47,100	423,900
40-50	4	- 205	41,900	167,600
50-60	3	- 195	38,000	114,000
60-70	0	- 185	34,200	0
70-80	4	- 175	30,600	122,400
80-90	2	- 165	27,200	54,400
90-100	1	- 155	24,000	24,000
110	1	- 140	19,600	19,600
210	1	- 40	1,600	1,600
240	2	- 10	100	200
270	1	+ 20	400	400
350	1	+ 100	10,000	10,000
390	2	+ 140	19,600	39,200
450	1	+ 200	40,000	40,000
470	1	+ 220	48,400	48,400
590	1	+ 340	115,500	115,500
700	2	+ 450	203,000	406,000
710	1	+ 460	211,500	211,500
740	1	+ 490	240,000	240,000
790	1	+ 540	292,000	292,000
810	1	+ 560	314,000	314,000
870	1	+ 620	384,000	384,000
890	1	+ 640	410,000	410,000
910	1	+ 660	436,000	436,000
950	1	+ 700	490,000	490,000
990	1	+ 740	548,000	548,000
1000	1	+ 750	562,500	562,500
	61			6,276,200

average = 250 microdarcys

less. This would also reduce the permeability of the upper member to 23.5 microdarcys, and that of the lower member to 38.5 microdarcys. The large percentage of very low values for the upper member is probably due to an admixing of very fine silt or clay sized particles with the grains which would normally form the matrix of the rock. Many very thin clay laminations are common in parts of the upper member, (see Plate 8, top) but are not so common in the lower one.

These very low values of permeability would indicate a production of only 3 to 5 barrels of oil per day for a well producing from a thirty foot oil horizon. The increase of permeability due to fractures cannot be measured in the laboratory since the samples are too small and the fractures are probably not in the same condition as when in the reservoir. Fairly good productions from many wells indicate that the fractures play an important part in aiding flow of oil toward the well. The increase in ease of flow because of fractures should probably not be called permeability since the fractures do not occur throughout the whole rock mass, but appear instead as openings at discrete locations. Thus flow along fractures should be treated as flow along a parallel-walled channel using proper hydraulic equations. In Chapter IV this method is used to find the lateral extent of fractures from well production data.

B. POROSITY

Upper Spraberry. The porosity of the Upper Spraberry averages about 10% while the lower member averages two or three percent higher. Table III tabulates the results of 278 porosity determinations made on Upper Spraberry cores from two wells (Sunray, 1952). The number of samples falling into each 1% porosity interval are shown along with the computations required to find the standard deviation and probable error of the average. The average value is computed from the values of each of 278 individual determinations which were given to the second decimal place in percent porosity. The average is 9.95% and the standard deviation,

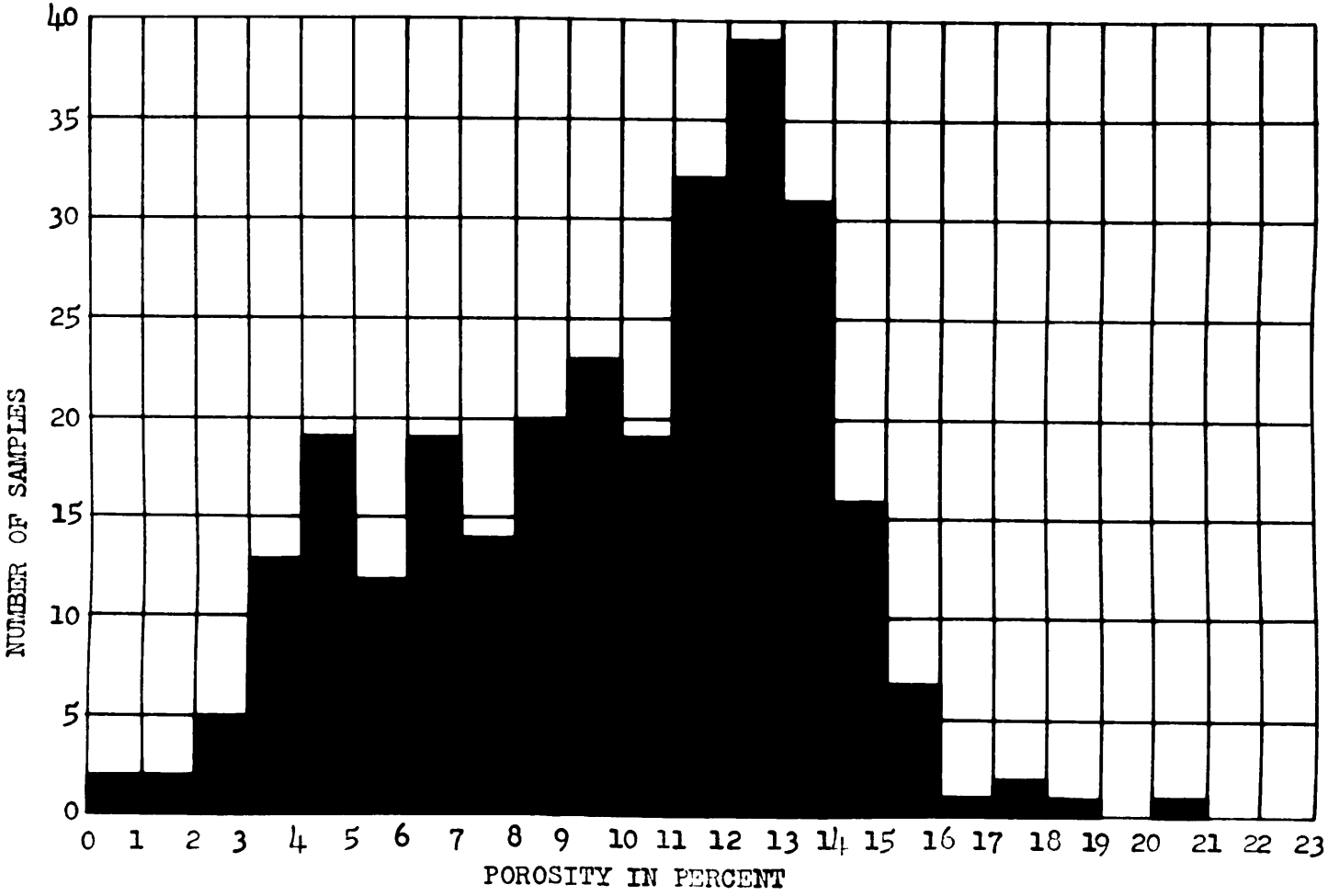
$$\sigma = \left(\frac{3951}{277}\right)^{1/2} = 3.78\%.$$

From this the probable error of the mean can be computed

$$r\bar{m} = .6745 \times \left(\frac{1}{278}\right)^{1/2} \times 3.78 = 0.15\% .$$

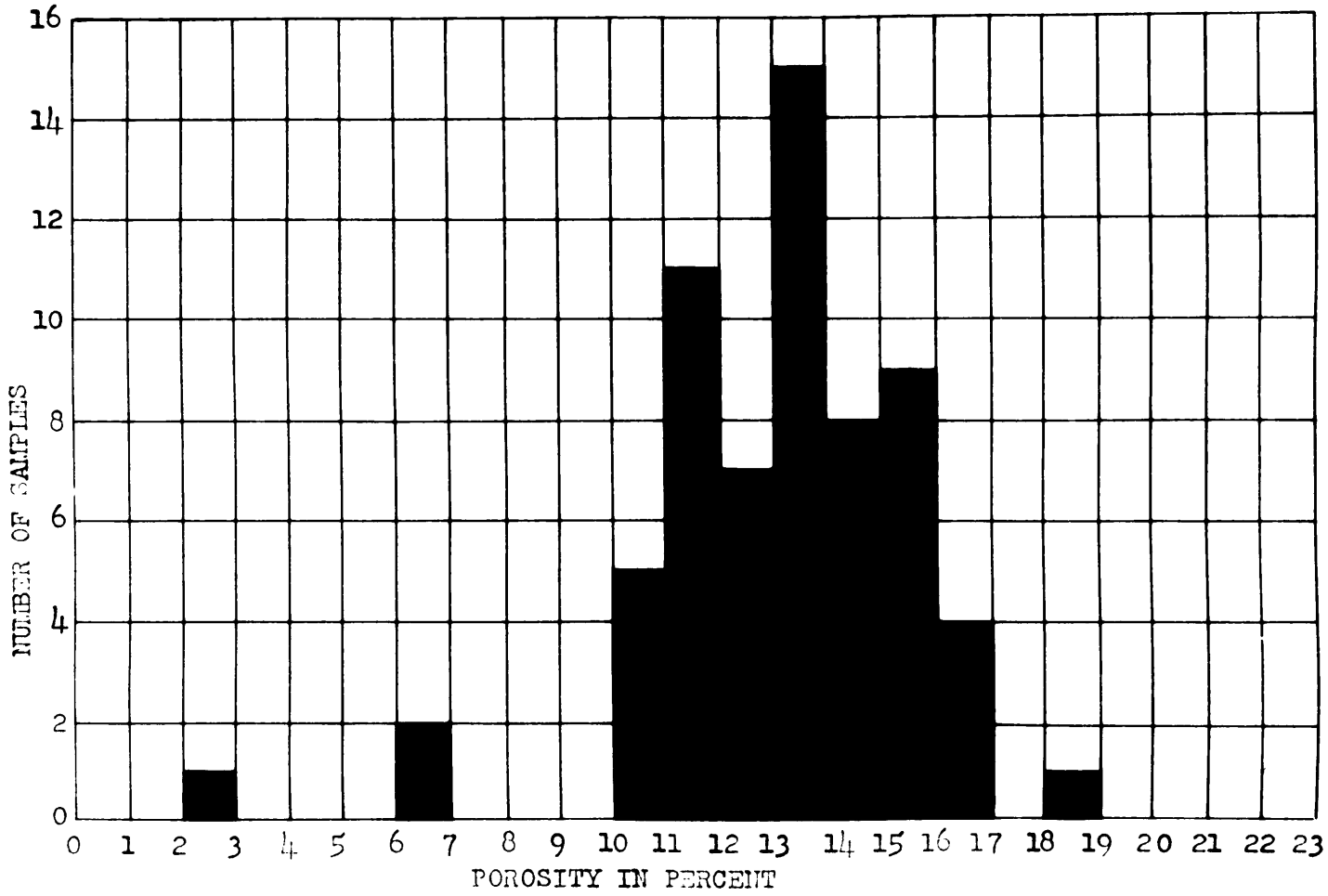
The method of computation and reasoning are the same as for the permeability analyses and are described there.

Lower Spraberry. In a like manner Table IV was prepared for 61 tests of porosity on Lower Spraberry cores from two wells in close proximity to the two wells used for the Upper Spraberry analysis. The average for these tests is 12.65 $\pm$ 0.22% porosity with a standard deviation of 2.61%. Tables III & IV are plotted as histograms on Figures 8 and 9, respectively.



POROSITY OF UPPER SPRABERRY

FIGURE 8



POROSITY OF LOWER SPRABERRY

FIGURE 9

Table III

Distribution of Porosity in the Upper Spraberry

Porosity in %	No. of Samples	e	e^2	ne^2
0-1	2	- 9.45	89.30	178.6
1-2	2	- 8.45	71.40	142.8
2-3	5	- 7.45	55.50	305.5
3-4	13	- 6.45	41.60	540.8
4-5	19	- 5.45	29.70	564.3
5-6	12	- 4.45	19.80	237.6
6-7	19	- 3.45	11.90	226.1
7-8	14	- 2.45	6.00	84.0
8-9	20	- 1.45	2.10	42.0
9-10	23	- .45	.20	4.6
10-11	19	+ .55	.30	5.7
11-12	32	+ 1.55	2.40	76.8
12-13	39	+ 2.55	6.50	253.5
13-14	31	+ 3.55	12.60	390.6
14-15	16	+ 4.55	20.70	331.2
15-16	7	+ 5.55	30.80	215.6
16-17	1	+ 6.55	42.90	42.9
17-18	2	+ 7.55	57.00	114.0
18-19	1	+ 8.55	73.10	73.1
19-20	0	+ 9.55	91.20	0.0
20-21	1	+ 10.55	111.30	111.3
	278			3951.0

average = 9.95%

Table IV

Distribution of Porosity in the Lower Spraberry

Porosity in %	No. of Samples	e	e^2	ne^2
0-1	0			
1-2	0			
2-3	1	- 10.15	103.23	103.2
3-4	0			
4-5	0			
5-6	0			
6-7	2	- 6.15	37.82	75.6
7-8	0			
8-9	0			
9-10	0			
10-11	5	- 2.15	4.62	23.1
11-12	11	- 1.15	1.32	14.5
12-13	7	- .15	.02	.1
13-14	15	+ .85	.72	10.8
14-15	8	+ 1.85	3.42	27.4
15-16	9	+ 2.85	8.12	73.0
16-17	4	+ 3.85	14.82	59.3
17-18	0			
18-19	1	+ 5.85	34.22	34.2
	63			421.2

average = 12.65%

The porosity of the lower member is somewhat greater than that of the upper member while the standard deviation is less. This indicates a more uniform grading of material in the lower member and less changes in the character of the sedimentation. The fine shaly material in the upper member mentioned previously would fill in interstices in the larger grains and reduce porosity. Also a small change in the quantity of fine material deposited would cause large swings in the porosity determinations since the fine particles would fall almost entirely into space which would otherwise be void.

Effect of Fractures. There is considerable mention in the literature of the reservoir storage volume afforded by the fractures. It is this writer's belief that the volume of storage space increase because of fractures is negligible. If a cored sample of reservoir rock contained an open fracture, then this fracture should be visible when the core is examined. While incipient fractures or microfractures might escape detection, it must be assumed that any fracture actually open in the ground to the extent, say of 0.0005 inches or larger, would be visible. Thus the proportion of open fractures in the rock in the natural state cannot exceed the proportion actually seen in the cores. While some cores contain multiple fractures, these are more than offset by those which contain none. This gives an upper limit of one fracture per 3 1/2 inch core.

In Chapter IV are presented the results of 83 direct measurements of the sizes of the fracture openings. These measurements indicate that the fractures are open on the average less than 0.002 inches in the ground. As explained in the discussion accompanying the results, these measurements may have an explanation other than that the fractures were actually open in the ground. However, they give a maximum value for the average fracture opening and can be used as such for the purpose of finding the volume of storage space in fractures.

These results show that the maximum amount of fracture openings is 0.002 inches in 3 1/2 inches or 0.00057 inches width of fracture openings per linear inch perpendicular to the fractures. This amounts to 0.057% effective porosity increase or a little more than one-half of one percent of the average matrix porosity found above.

C. GENERAL PRODUCTION DATA

The separate oil fields within the four county area are quite similar in most respects. The original reservoir pressures were all between 2300 and 2400 p.s.i.g. in the upper zone when corrected to a datum of 4400 feet subsea (Christie and Blackwood, 1952). The narrow range of pressures indicates that the original pressures may have been equal in all areas. The small differences noted are probably due

to variations in the methods of testing or the times when different fields were tested. The initial pressures of wells in fields which have been in operation for some time are lower than the field's original pressure showing that there is intercommunication between wells. It has been shown (Christie and Blackwood, 1952) that in the Driver field there was a drop of initial pressure of new wells completed amounting to 100 p.s.i.g. per month.

The saturation pressure averages about 1900 p.s.i. while the dissolved gas-oil ratio is about 750 cu.ft. per barrel. It is believed that the gas will become an increasingly important factor in the economic development of the area since it contains a good percentage of higher hydrocarbons (Carlson, 1952, c.).

Since the Spraberry has a dissolved gas drive and contains some water admixed with the oil, recovery will be low. Estimates of ultimate recovery run from 10% to 30% of the oil in place originally. However, as the fields develop more and more gas will be produced and the gas recovery may be expected to reach 80%. A 90 foot pay with a porosity of 10% and recovery of 10% would yield 1300 barrels of oil per acre, assuming an oil saturation of 25% and a reservoir volume factor of 1.4. These conditions are close to what can be expected from the Upper Spraberry as a lower limit. Most estimates of recoverable oil are double this with some ranging as high as 10,000 barrels per acre. Since the possible

acreage of the trend may reach 3,000,000 acres, and the proved acreage is approaching 1,000,000 acres, it can be seen that this is one of the largest oil areas in the world, with reserves measured in billions of barrels. This means also that a low recovery means that an even larger quantity of oil will be left behind in the reservoir. Secondary recovery by water drive is excluded by the low permeability of the formation. Proper knowledge and use of the fractures may point the way to greater recovery. Because of the fact that the Spraberry fields decline in pressure quite rapidly, there will be an early need for secondary production.

The potential productions of many wells fall in the neighborhood of 300 barrels of oil per day, but few wells can make their allowable over a prolonged period. The areal distribution of wells having equal potentials is discussed in the chapter on fractures.

3. COMPLETION PRACTICES

New completion practices have been developed especially to deal with fractured reservoirs. The purpose of the new techniques, as for the older ones, is to increase the area of contact of the well and the rock matrix. These new methods will be described here because of their use in learning about fractures.

A. HYDRAFRAC AND STRATA-FRAC

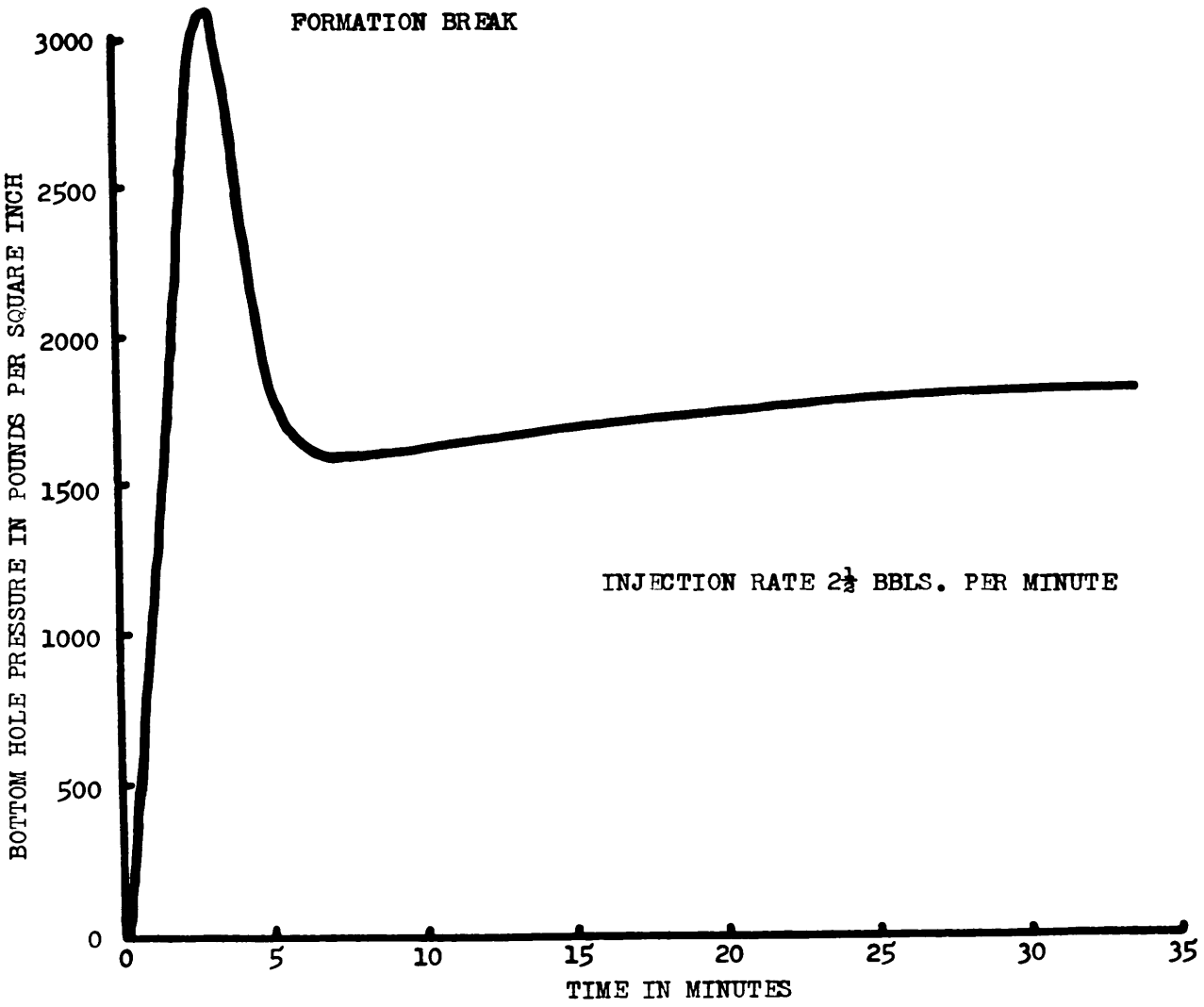
If flow of oil into the Spraberry wells were dependent only on the low permeability matrix of the rock, there would be very little production. The loss of reservoir pressure near the well would be large and production would be limited by the ability of the oil to flow into the well through the matrix of the rock in close proximity to the well bore. If one or more open fractures extended from the well to a considerable distance into the formation, the oil could flow into these fractures at many points along their length and then flow easily to the well. The new well completion techniques open these fractures by hydrostatic pressure applied through a viscous gel. The gel flows along the opened fractures carrying with it uniformly graded sand which later props the fractures open. The gel is caused to revert to a sol by means of a breaker fluid which is injected into the well after the gel. The fluid then flows back out of the well leaving the sand grains behind. Two of the most popular commercial treatments using this principle are "Hydrofrac" (Clarck, 1948) and "Strata-frac" (Moore & Ousterhout, 1952).

The viscosity of the gel is quite critical. A thin fluid would flow rapidly into the formation with the result that the applied pressure would be dissipated over a considerable distance and not cause a concentrated pressure near the well. Besides this a large flow would be required to

maintain the pressure necessary. A gel which was too viscous would not be able to flow along the small fractures once they were opened. The viscosity of the gel, the quantity of gel, the rate of flow into the formation, the quantity and grain size of the sand, as well as the quantity of breaker fluid must all be determined for each new area. In studying Spraberry fractures the size of the sand grains and the pressures required are of greatest interest. Generally the rate of pumping the gel into the formation is held constant while the pressure is recorded during the time the injection takes place.

In the upper Spraberry the pressure rises rapidly at the beginning of the injection to a peak called the "formation break" occurring at about 3000 p.s.i. at the bottom of the hole. The pressure then drops back rapidly to a fairly constant value which is about half of the peak value. The injection rate is usually about 2 1/2 to 3 barrels per minute. The general appearance of a pressure versus time curve for a Spraberry Hydrofrac treatment is shown in Figure 10. In some cases no formation break or peak is observed before the constant pressure part of the curve.

Ottawa sand is used in the Spraberry formation. This sand is of very uniform size and passes a twenty mesh per inch screen while it is retained on a thirty mesh screen.



TYPICAL GEL INJECTION PRESSURE CURVE

FIGURE 10

Thus the grains must have an average diameter of 0.020 inches.

B. CONCLUSIONS FROM HYDRAFRAC DATA

Number of Fractures. Some inferences can be drawn from the information presented above and on Figure 10. There is only one fracture opened as is indicated by the fact that there is only one formation break. It is not possible for the pressure to cause a second fracture in a direction parallel to an existing fracture just as it is not possible for tension on a laboratory test specimen to cause two parallel breaks. The ordinate of the level portion of the curve is the pressure required to hold the fracture open to at least 0.020 inches. Where the fracture is completely open in the ground no formation break is noted on the curves (Figure 10) and the only pressure required is that to open the fractures. If the fractures were partly open to start with the pressure required would not be so great. The average reduction of pressure due to this cause cannot be great since the average fracture opening size is not over 0.002 inches (see Chapter IV) while the Ottawa sand averages about 0.020 inches.

Extent of Fracturing. It is possible to make some estimate of the extent to which the gel enters the formation. The treatment in Figure 10 involves 3000 gallons which is a

fairly large treatment. Many wells are treated with 1500 or 2250 gallons although treatments as large as 8000 gallons have been known in the four county area. If it is assumed that the 3000 gallons is injected into a 90 foot section of the pay then the length of fracture opened is

$$l = \frac{3000 \times 12}{7.48 \times 0.020 \times 90} = 2675 \text{ feet.}$$

If the fracture were opened in each direction this would be a little over 1300 feet each way. With a forty acre spacing this is roughly the distance to the next well. However, since the major fracture pattern is at an angle of about 41° with the section lines, the effect on the nearest wells would be a minimum. Some interaction between diagonal wells has been noted during production, and this is discussed in Chapter IV.

The calculation just completed assumes that there is no gel lost into the matrix of the formation. Since some is lost in this manner and into connecting fractures, the extent of fracturing cannot be expected to be as great as 1300 feet. On the other hand, there is reason to believe that fractures do not extend in both directions.

Fracture Stress. Most wells along the Spraberry trend encounter the producing horizon at a depth of 7000 feet below the surface. At this depth the rock is under a vertical compressive stress of about 7000 p.s.i. due to the overburden.

Tests on Spraberry samples (see Chapter V) show that at this stress the rock has a value of 0.07 for Poisson's ratio and the modulus of elasticity (or Young's modulus) is only slightly greater in the horizontal direction than perpendicular to the bedding. These data indicate a horizontal compressive stress under 700 p.s.i. The actual horizontal stress is probably much greater than this due to the influence of creep.

The effective tensile stress required to fracture the formation can be derived from the pressure peak or formation break value on Figure 10. Later under the discussion of the Mohr diagram (Chapter IV) it will be shown that a tensile break is possible even under a net compressive stress. For this reason the term effective tensile stress has been used since it represents a reduction in compressive stress at least in part and possibly entirely. Consider a horizontal slab of the formation of unit thickness and great lateral extent. Hydrofrac pressure, P, in a well of radius R acts outward radially in all directions. The radial rock pressure on the outside of an annular ring whose inner diameter is the well bore and whose outer radius is R + d would be $P \times R/(R + d)$. Thus the net radial pressure on this ring of width d would be the difference of pressure between P and the pressure on the outer surface, or $P \times d/(R + d)$. The hoop tension in the annular ring would be $R \times P \times d/(R+d)$.

The stress in the annular ring would be the total tension just found divided by the ring's cross sectional area. Since the slab is of unit thickness the area is d. Thus the stress, f, can be found by the formula

$$f = \frac{PR}{R + d} .$$

If the ring is considered to be very narrow and the dimension d approaches zero then f = P. After the fracture has started out from the well bore there would be a concentration of stress at the end of the fracture so that the extension of the fracture would not require a stress much greater than what would be required to widen an existing fracture. The actual stress required to initiate a fracture is probably not as great as the bottom-hole pressure as indicated above. Since some of the gel flows into the formation, the transfer of stress from the fluid to the rock does not occur at a single surface but over a certain width out from the well. This has the effect of reducing the effective pressure and of causing dimension d to have a considerable width.

The horizontal portion of the curve of Figure 10 indicates the pressure required to open and hold the fracture open. It was shown above that this pressure would not differ materially from that of a fracture already open. It is of interest to note that the pressure required to open a fracture to any given width is not much greater than that required

to merely separate the two walls of the fracture. The reason for this is that the compression can take place over a great width laterally from the fracture. To shorten a 500 foot sample of the formation by 0.020 inches would require a compressive stress of only 10 p.s.i. A 5000 foot sample would require only 1 p.s.i. It is hard to estimate the extent of the rock mass affected but it must be in the same order of magnitude as the planar dimensions of the fracture. This means that the pressure indicated must be equal to the horizontal compressive stress except for the effect of fluid friction. That the fluid friction cannot be large is shown on Figure 10 by the fact that there is only a slight increase in the pressure as the fluid flows farther into the fracture.

C. OTHER COMPLETION PRACTICES

Acid Flushing of Fractures. Some Spraberry cores have been observed to be filled with calcite. For this reason acid flushing under pressure has been used as a Spraberry completion technique. The filled fractures are not abundant and the results do not appear to be as good as with the formation fracturing methods (Bristol and Helm, 1951).

The Dowell Corporation, Midland, Texas, has developed a completion technique combining the effects of acid with a gel fracturing treatment. The trade name for their process is "Strata-frac" (Moore and McCormick, 1951; Moore and Ousterhout, 1952).

Cementing Practices. Many instances are known of discovering cement in fractures many feet below the point where casing was set. In one case cement was found to extend 90 feet into the formation along fractures. In some instances the cement was found by later coring to have opened and filled fractures to a thickness of over a quarter of an inch (Senning, 1951, photograph p. 128; Gibson, 1951). This supports the conclusion that the pressure required to widen a fracture is not much more than that required to open it at all. The cement opens fractures in the same way as the gel but does not flow out again. These difficulties have lead to the practice of using no greater pressure or larger volume of cement than necessary when setting casing.

CHAPTER III

BASIN CHARACTERISTICS

1. GENERAL SHAPE OF BASIN

The Spraberry producing trend lies generally in a north south direction in the Midland Basin portion of the Permian Basin. The Midland Basin is about 75 miles wide, 165 miles long and represents an accumulation of about 7000 feet of sediments. The longer axis of the basin roughly parallels the present producing trend. On the west of the Midland Basin is the Central Basin Platform which was elevated during the Pennsylvanian, while on the east is the Eastern Platform. On the basis of size and shape and the fact that it is located on the craton, the Midland Basin should be classed as an autogeosyncline.

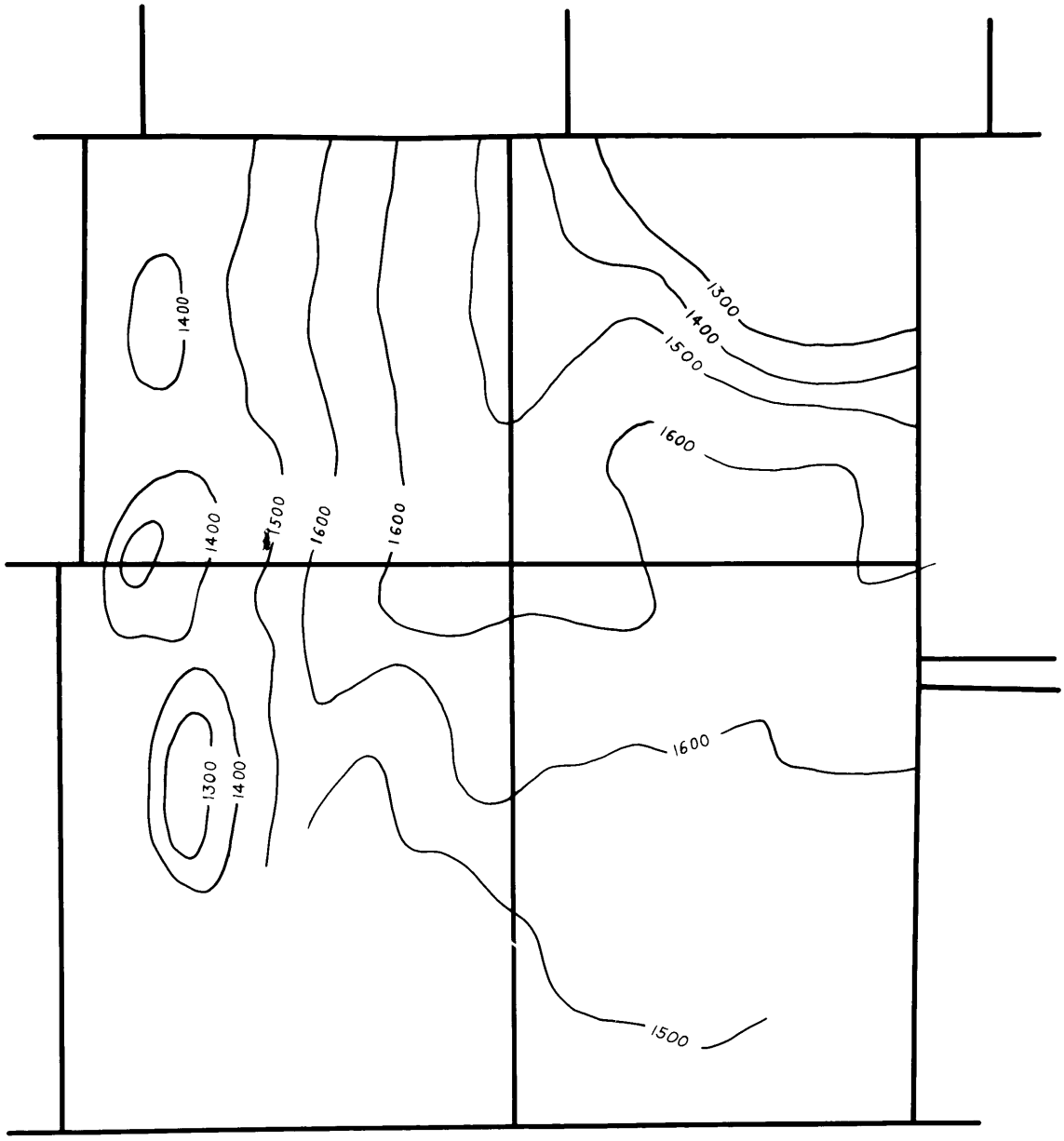
2. ISOPACHOUS MAPS

Several isopachous maps were drawn to show the variations of thickness of the Spraberry and overlying formations. These maps are useful as a means of determining the source direction of the sediments and as an indication of the general basin configuration. The information for these maps was obtained from well descriptions obtained from oil companies and isopach data of smaller areas.

A. BASE OF DEAN TO TOP OF SPRABERRY

It was not possible to make an isopachous map of the Spraberry formation alone because of the lack of available information. Many well scattered descriptions of wells gave an indication of the top and of the base of the interval from the base of the Dean sandstone to the top of the Spraberry. This interval has a thickness of about 1600 feet while the Spraberry alone would be about 1000 feet. The added interval is similar to the Spraberry in many respects, and the whole section can be considered as a unit for this purpose. The resulting map is shown in Figure 11.

The greatest thickness is seen to occur near the center of the area under study but does not occur as a sharp maximum. The broad area of maximum thickness indicates a broad, even bottomed surface of deposition. The sediments appear to have come from the east or southeast and were carried northward through Midland county. Thinning toward the west and northeast may be an indication of shallower quiet waters. The paleogeographic maps drawn near the beginning and at the end of the period under discussion (Figures 21 and 20, respectively) show that these were shallower areas. The lithofacies map of the Spraberry (Figure 19) shows that the deposits in these areas were more shaly and limy than those near the center of the basin. The source of these Lower Leonard sediments may have been



ISOPACH MAP

BASE OF DEAN TO TOP OF SPRABERRY

FIGURE II

the Marathon Uplift which became emergent during Wolfcamp time. Some coarse sands and conglomerates of this age are found in wells some distance to the south of the basin. Part of the sediments may have come from the Ouachitas.

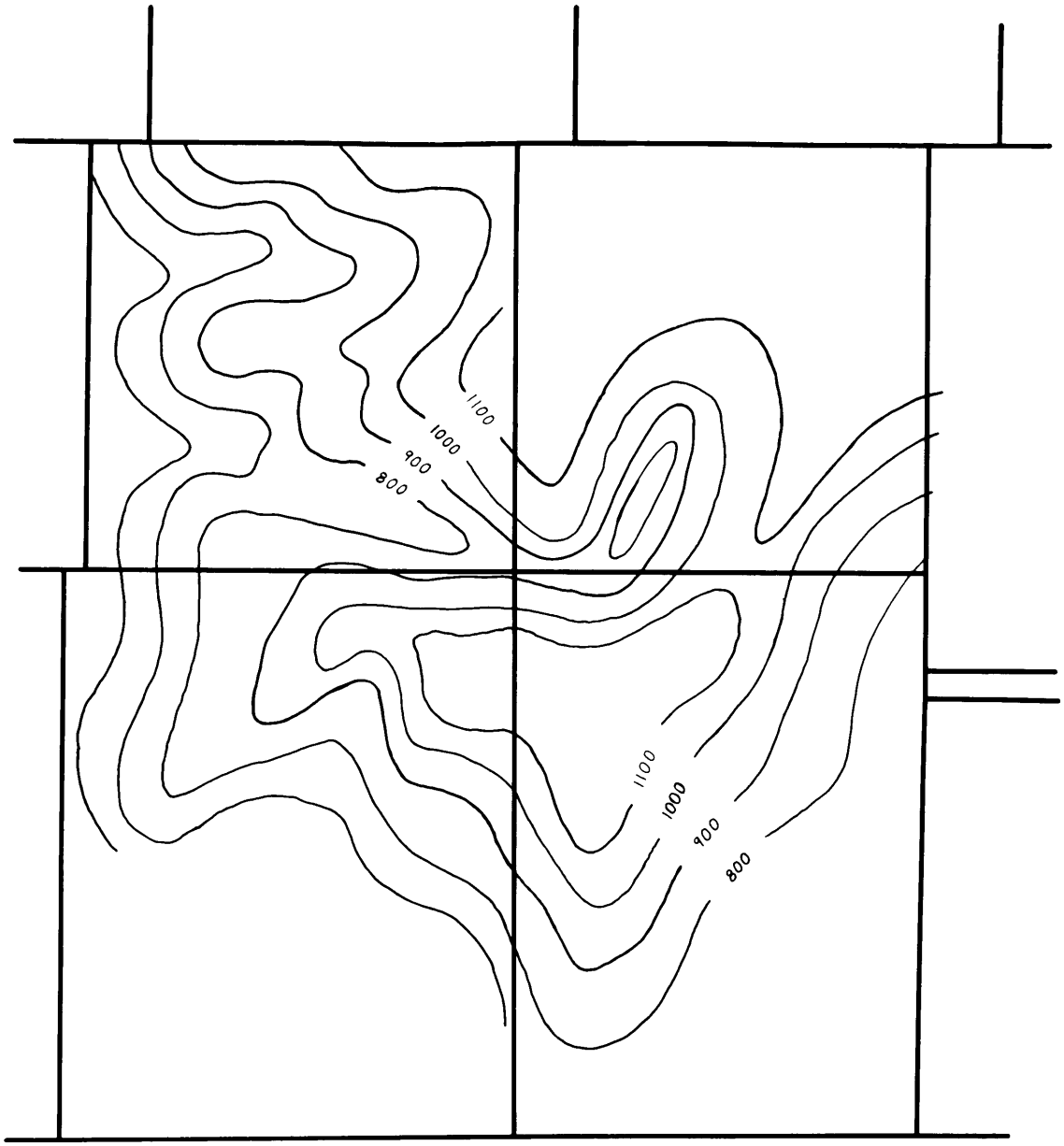
B. ISOPACHOUS MAP OF THE CLEARFORK FORMATION

Figure 12 is an isopachous map of the Clearfork formation which lies over the Spraberry. The Clearfork is Upper Leonard in age. The map shows a general thickening toward the northeast as well as a thickening at the center of the basin. The western edge of the area still shows a uniform decrease of thickness as it did during Spraberry time.

While some sediments may still have been coming into the basin from the Marathon uplift, the direction of thickening indicates that the source of the sediments may have been the Wichitas. There is evidence of folding and overthrusting in the Wichita system during Late Leonard time (Eardley, 1951).

C. ISOPACHOUS MAP OF SAN ANDREAS AND GRAYBURG

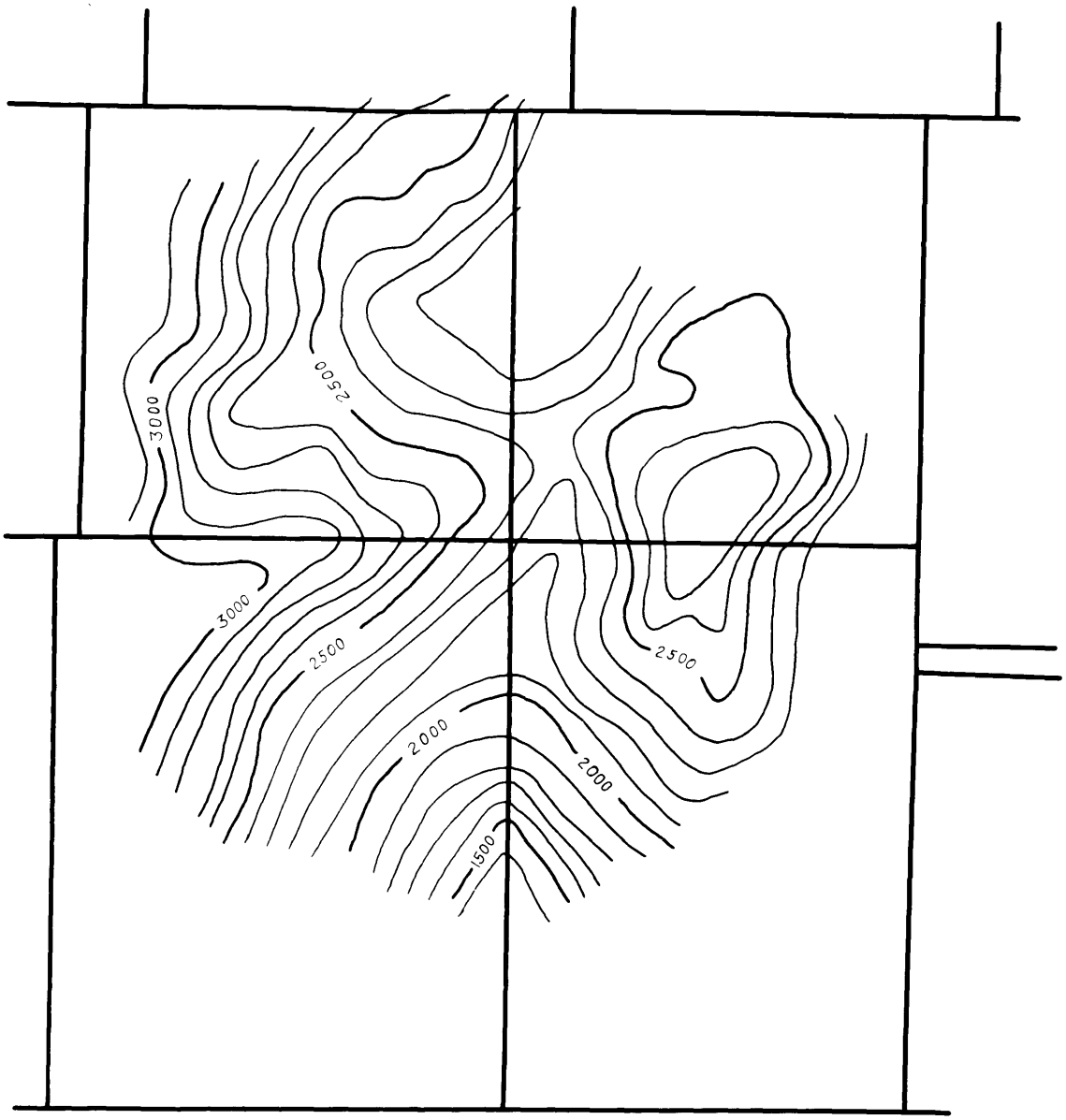
Figure 13 is an isopachous map of the total thickness of the San Andreas and Grayburg formations. There is a marked thinning southward along the Upton and Regan county boundary. In a distance of twenty miles the thickness drops from 2300 feet to 1400 feet. The thinning is of limited extent in the east-west direction and is "V" shaped in cross



ISOPACH MAP

CLEARFORK

FIGURE 12



ISOPACH MAP

SAN ANDREAS AND GRAYBURG

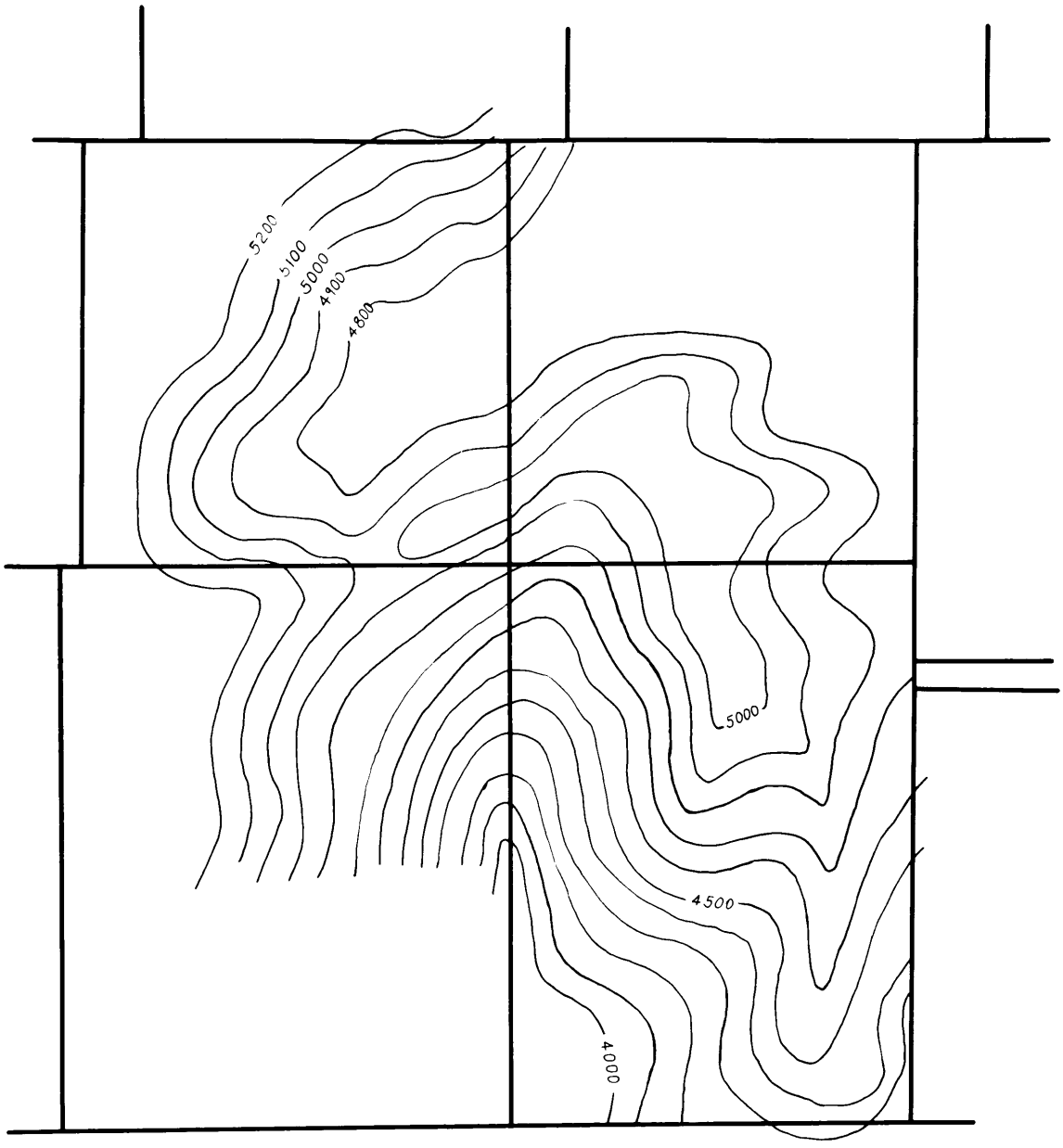
FIGURE 13

section. It would appear that such a configuration is the result of erosion rather than of deposition. There is a general thickening of the strata toward the west and a lesser thickening which represents the deepest part of the basin in the east central portion of the area. The source of the sediments appears to have been the Florida Mountains of southwestern New Mexico, the Hueco Mountains and the Diablo Mountains which are near El Paso, and possibly Pedernal Range in central New Mexico. The Pedernal Range was emergent during early and middle Permian times while the other ranges were emergent throughout the Permian (Eardley, 1951, Plate 9 and pp. 230 to 233).

The thinning may be the result of erosion resulting from an uplift at the time of the renewed uplift of the Marathon Range in late Guadaloup time. This erosion may have been submarine rather than subaerial.

D. SUMMARY OF WHOLE SECTION

Figure 14 is an isopachous map of the whole section discussed above from the base of the Dean to the top of the Grayburg. It is merely a summation of the thicknesses of Figures 11, 12 and 13. The overall thickening is toward the west indicating that this is the major direction of sedimentation. The erosional feature discussed above appears prominently on this map because of the San Andreas and Grayburg section in which it occurred represents almost



ISOPACH MAP

BASE OF DEAN TO TOP OF GRAYBURG

FIGURE 14

half the total thickness. It is accentuated also by the southward thinning of the Clearfork. Throughout this time some sediments must have been coming from the Ouachita system to the east which was overthrust in late Wolfcamp and late Leonard time. The direction of thickening indicates that these were not dominant sources. The largest amounts of sediments for the three sections discussed above were, in order from base to top, from the southeast or east, the northeast, and the west.

In spite of variations in the direction and quantity of sediments, the area of greatest accumulation near the center of the basin showed only minor shifts in location. This low portion of the basin was a negative area surrounded by areas which were intermittently positive during most of the Permian.

3. SEDIMENTOLOGY

A. GENERAL METHODS OF STUDY

The available cores from the three wells indicated on Figure 2 were examined by means of 41 thin sections cut both perpendicular and horizontal to the bedding. Descriptions of well sections obtained from oil companies and from several published sources were used to piece together the lithofacies map shown in Figure 19.

Most of the photomicrographs were taken with the writer's Exacta camera mounted onto a Leitz petrographic microscope by means of commercially available extension tubes. This equipment is shown on Plate 3. The Exacta camera is standard except for the ground glass in the hooded viewfinder which has a clear center spot. This gives a brighter and more critical reflex image on which to focus and is almost indispensable at high powers. The use of 35 mm film reduced cost to a minor factor. Also the ability to work in a lighted room is a great convenience. Low power polished section pictures were taken with this equipment or with the regular camera lens and extension tubes.

It is sometimes difficult to obtain uniform illumination of the field of view when making low power thin section photomicrographs. Some of these were made by mounting the thin section directly in an Omega D2 enlarger and projection printing onto cut film in a photographic darkroom. This method is useful when crossed nicols are not required. Plain light is used to a greater extent when taking photomicrographs of sediments than when working with hard rocks.

It was decided that grain size analyses could be made best on photographs. It was found that it was easier to work on a negative print of a photograph made from a slide in plain light rather than to work on a positive or regular print. In this way the quartz grains appeared dark on a



PHOTOMICROGRAPH EQUIPMENT

PLATE 3

lighter background and were somewhat easier to see and measure. The prints were also easier to make than regular prints. Again the thin sections were mounted directly in an enlarger. A very short focus lens was used, and the enlarger was raised and projected onto printing paper placed on the floor. Direct negative prints of 80 diameters magnification and 9 x 11 inches in size were made in this way.

B. GRAIN SIZE ANALYSES

Method of Making Count. Individual grain diameters were counted by making two parallel closely spaced lines in two mutually perpendicular directions on the negative prints described above. All grains whose projected areas were more than half inside the parallel ruled lines were included in the count. It is felt that this method eliminated the natural tendency to count less small grains. The thin sections used in this work were all cut horizontally or parallel to bedding. It is assumed that in normal sedimentation in quiet waters the shortest dimensions of most grains will be vertical when the grains are deposited. Thus in the projections used the longest and intermediate axes are generally visible. For this reason the shortest visible axis was the one chosen as giving the best indication of average grain size. Since most of the grains are fairly

equant, the difference would not be large no matter what grain dimension were used. The count was made by recording the numbers of grains found between each grade limit on the Wentworth particle size classification.

Treatment of Data. Grain size distribution of sediments is generally recorded on either a histogram or a cumulative curve. A histogram is a form of bar graph which plots weight percent in each size range on the ordinate against size range on the abscissa. The cumulative curve plots the total weight percent larger than a given size against the grain size. Thus the envelope enclosing the separate bars or blocks of the histogram is roughly equal, mathematically, to the first derivative of the cumulative curve; that is it plots the slope of the cumulative curve.

Each successively larger size range on the Wentworth scale has an average grain diameter which is twice that of the preceding smaller range. Thus in two adjacent ranges with equal weights of grains, the range with smaller grain size has eight times as many grains. This assumes that the average density of the two ranges is the same, an assumption which will seldom cause trouble. In this case the grains measured were all quartz. It becomes apparent that to convert grain count data to relative weight percent the number of grains in each successively smaller size range must be divided by successively larger powers of eight. The method of doing this is shown on Tables V, VI, VII, and VIII.

Table V
Distribution of Grain Sizes 28 feet below Top of Upper Spraberry

Range in mm	No. of Grains	Divisor	Relative wt.	Weight %
1/4 - 1/8	0	1/8	0.0	0.0
1/8 - 1/16	3	1	3.00	31.1
1/16 - 1/32	26	8	3.25	33.7
1/32 - 1/64	183	64	2.87	29.8
1/64 - 1/128	216	512	.42	4.4
1/128-	483	4096	.10	1.0
	911		9.64	100.0

Table VI
Distribution of Grain Sizes 96 feet below top of Upper Spraberry

Range in mm	No. of Grains	Divisor	Relative wt.	Weight %
1/4 - 1/8	1	1/8	8.0	48.1
1/8 - 1/16	5	1	5.0	30.1
1/16 - 1/32	21	8	2.52	15.2
1/32 - 1/64	65	64	1.02	6.1
1/64 - 1/128	30	512	.06	.4
1/128-	81	4096	.02	.1
	203		16.62	100.0

Table VII

Distribution of Grain Sizes 159 feet below top of Upper Spraberry

Range in mm	No. of Grains	Divisor	Relative wt.	Weight %
1/4 - 1/8	0	1/8	0	0.0
1/8 - 1/16	2	1	2.00	36.1
1/16 - 1/32	19	8	2.47	44.6
1/32 - 1/64	51	64	.80	14.5
1/64 - 1/128	118	512	.23	4.1
1/128-	149	4096	.04	0.7
	339		5.54	100.0

Table VIII

Distribution of Grain Sizes in 12 Upper Spraberry Cores

Range in mm	No. of Grains	Divisor	Relative wt.	Weight %
1/4 - 1/8	2	1/8	16.00	14.1
1/8 - 1/16	33	1	33.00	29.2
1/16 - 1/32	329	8	41.15	36.4
1/32 - 1/64	1231	64	19.25	17.0
1/64 - 1/128	1653	512	3.24	2.9
1/128-	1713	4096	.42	.4
	4961		113.06	100.0

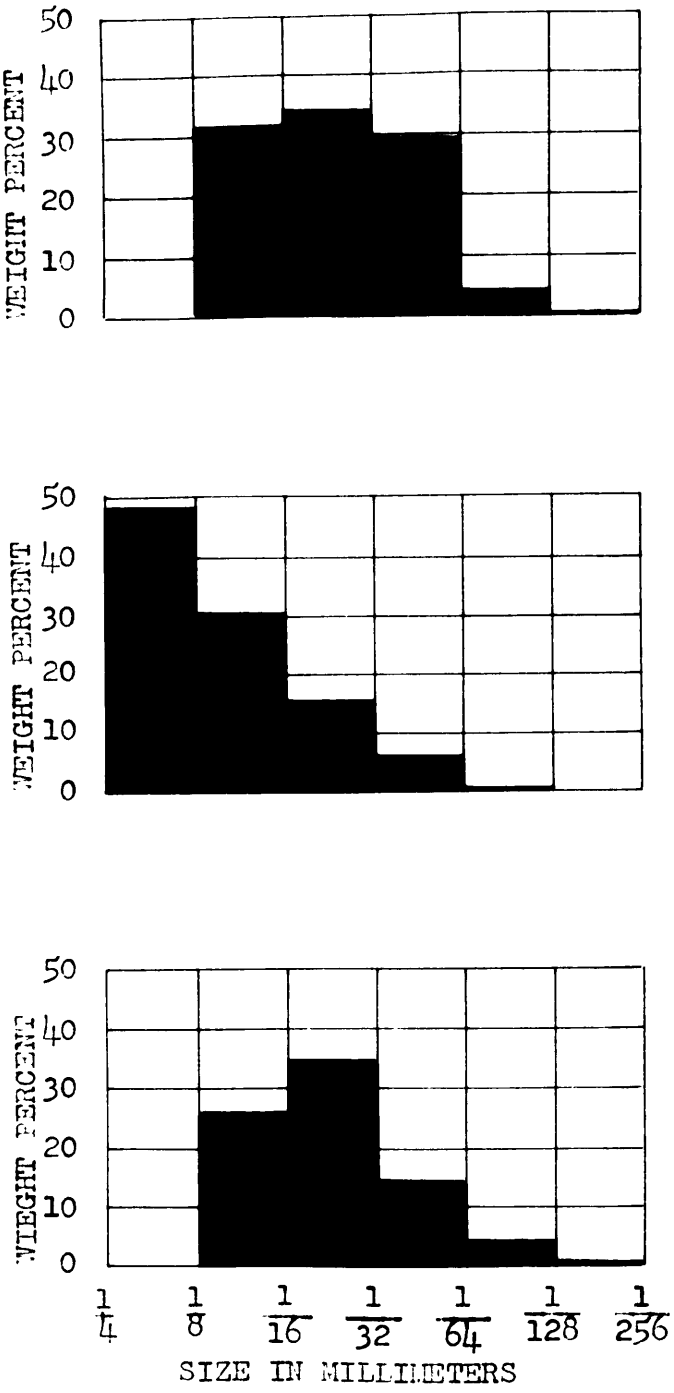
Computations for Cumulative Curve

Range in mm	Weight %	Cumulative % at	Size in mm
		0.0	1/4
1/4 - 1/8	14.1	14.1	1/8
1/8 - 1/16	29.2	43.3	1/16
1/16 - 1/32	36.4	79.7	1/32
1/32 - 1/64	17.0	96.7	1/64
1/64 - 1/128	2.9	99.6	1/128
1/128-	.4	100.0	1/256 ?
	100.0		

The actual numbers of grains are divided by numbers which are in inverse proportions to the weights of the individual grains in each range. The same result would have obtained if the number of grains in each range were multiplied by the average weight of the individual grains in that range; i.e. the cube of the diameter.

Twelve Upper Spraberry samples were analyzed in this way. In each case the count was continued until about twenty grains were included in the coarse silt range, 1/16 to 1/32 mm. This was done in order to give sufficient control in the coarser end of the scale. Large numbers of grains in the finer ranges have very little effect on the histogram or on the median grain size. In all cases except two the median size fell in the coarse silt range.

Results. The three samples shown in Tables V, VI and VII were selected to show the range of distributions found and were selected from widely spaced intervals in the formation. Table V shows that great numbers of fine grains must be counted in some samples in order to get a representative sample of grains in the median range and coarser. Table VI shows the results of having a single grain in the fine sand range, 1/4 to 1/8 mm. In order to obtain a representative distribution of the coarser grains a total of two or three thousand grains would be needed. This weight distribution cannot be considered to be that of a representative sample since almost one half of the weight is

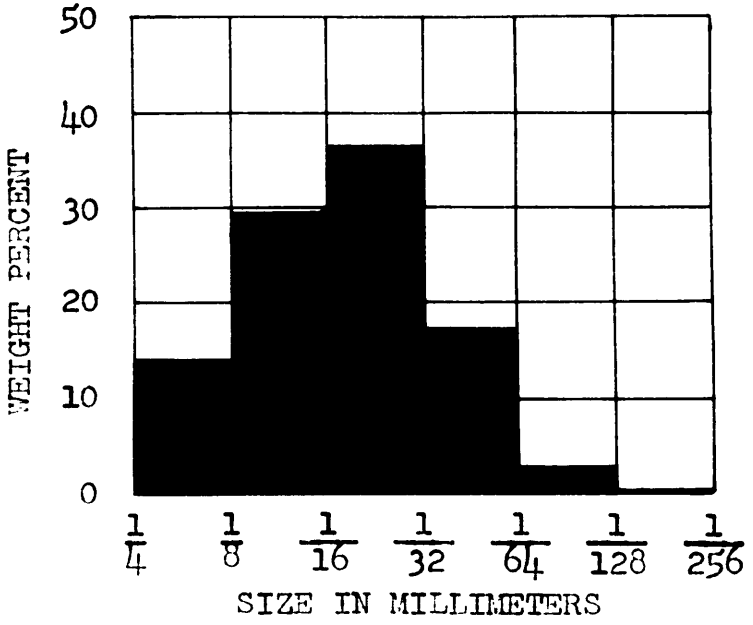


UPPER SPRABERRY GRAIN SIZE ANALYSES

FIGURE 15

represented by a sihgle grain. The sample is included here to show the number of grains required in using this method. Table VII shows grain size distribution in a sample about 70 feet from the bottom of the Upper Spraberry. The median size is intermediate between those of the first two samples. While the distribution appears normal a third of the sample depends on two grains. However, with this sample a change of one grain either way would not move the median from the coarse silt range. The histograms resulting from the weight percents found in these tables are presented in Figure 15.

Since none of the individual grain counts could give a reliable idea of the grain size distribution without including an unreasonably large number of grains, Table VIII is included to give an overall grain size distribution in the Upper Spraberry. The sum of the number of grains in each range for the twelve samples is given. This table is the result of counting 4961 grains. Even with this large number of grains over 14% of the total comes from 2 grains, showing that the coarse end of the scale is still in doubt. The two individual analyses which included these large grains were the only samples whose median size fell in the very fine sand classification. The other ten fell in the coarse silt range, 1/16 to 1/32 mm. The summed weight percents of Table VIII are plotted as a histogram on Figure 16.



TOTAL OF 12 UPPER SPRABERRY GRAIN SIZE ANALYSES

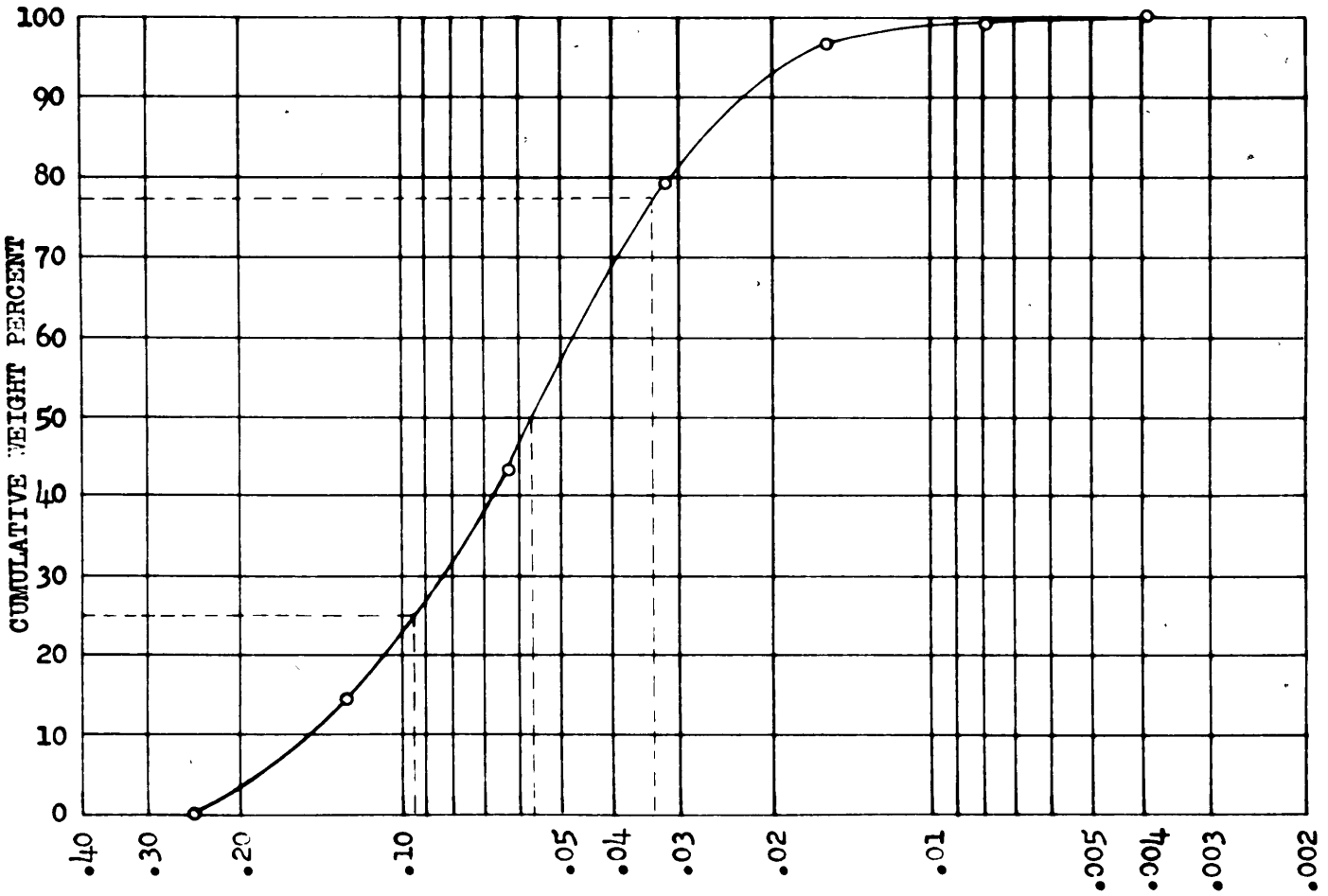
FIGURE 16

The data necessary for plotting a cumulative curve is given below Table VIII, and the resulting curve is shown on Figure 17. From this curve the median diameter is seen to be 0.0056 mm or a little less than 1/16 of a mm. The sorting coefficient is given by this equation (Trask, 1932, p. 72).

$$So = (Q_1/Q_3)^{1/2},$$

where Q_1 is the size at the first quartile and Q_3 is the size at the third quartile. From the curve the values of Q_1 and Q_3 are obtained and the sorting coefficient found to be 1.70. As would be expected this sorting coefficient is higher than the values found for eight of the individual counts. However, the variation between the coefficient found above and that of the individual samples is small since the size distributions of all of the individual samples are similar. If the average sizes of the 12 separate samples were greatly different from each other, the overall sorting coefficient found above would be very high indicating poor sorting, even though each sample by itself were well sorted. In the Spraberry the sorting and uniformity of grain size are such that even the overall sorting coefficient falls well below the value of 2.5, which Trask (1932) gives as the value below which sediments can be considered well sorted.

Conclusions. Based on the results of the grain count data the median diameter of the quartz grains in the Upper Spraberry member is 0.0056 mm which is near the coarser end



CUMULATIVE CURVE OF TOTAL OF UPPER SPRABERRY ANALYSES

FIGURE 17

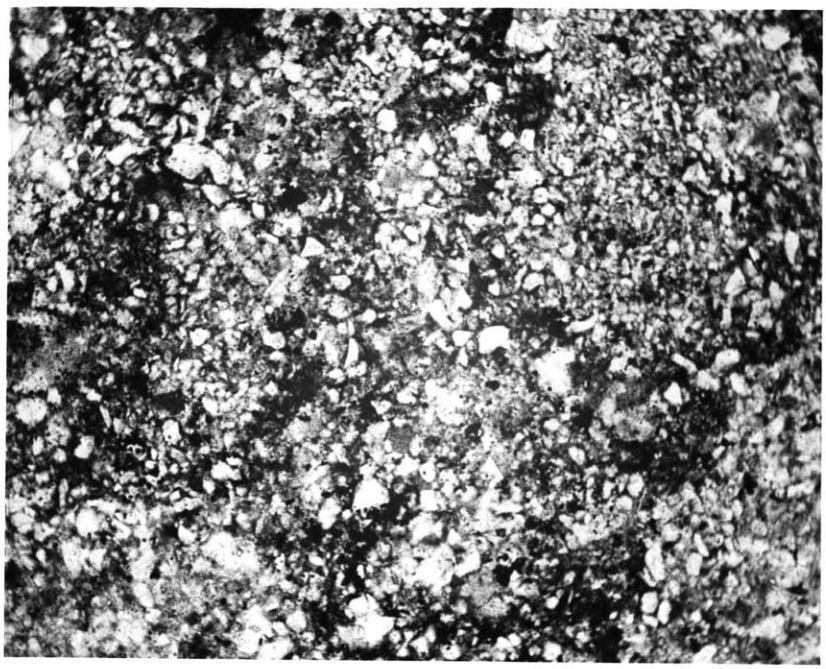
of the coarse silt classification on the Wentworth scale. The sorting coefficient, So, is somewhat better than 1.70, which indicates a well sorted sediment.

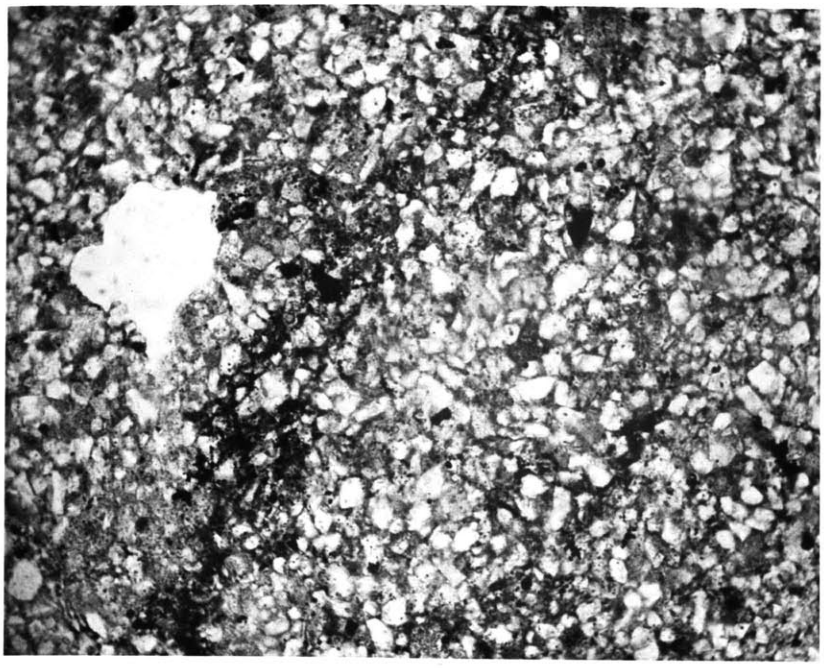
C. GRAIN SHAPE

By visual observation an estimate of particle roundness and sphericity were made. The roundness of particles averaged about 0.3 while the sphericity was about 0.75 or 0.80. The low value of roundness does not necessarily indicate a short distance of transport because of the smallness of the particles and the fact that the grains are quartz. It has been shown (Pettijohn, 1949, p. 396) that quartz grains suffer very little abrasion even with particle sizes of 1 mm, which is over ten times the size of the average Spraberry grains.

It is felt that the sphericity of the grains indicates that their source rocks were not strongly metamorphosed. A shear deformation would have had a tendency to cause an elongation of the quartz grains (Fairbairn, 1949).

Plate 4 shows two typical photomicrographs from the Upper Spraberry. These were both taken in ordinary light and show the angularity and roundness of the grains. The thin sections for these pictures were cut parallel to the bedding.





Typical Spraberry thin sections cut parallel to bedding. Plain light X 65.

PHOTOMICROGRAPHS OF SPRABERRY THIN SECTIONS

PLATE 4

D. MINERALOGY

Almost all of the detrital grains found in the Spraberry are quartz although a few grains of tourmaline and some detrital limestone has been noted. Plate 5 at the top shows a few detrital limestone grains in plain light. Some of these grains show secondary enlargement when examined under crossed nicols. Some of the grains are dolomitic.

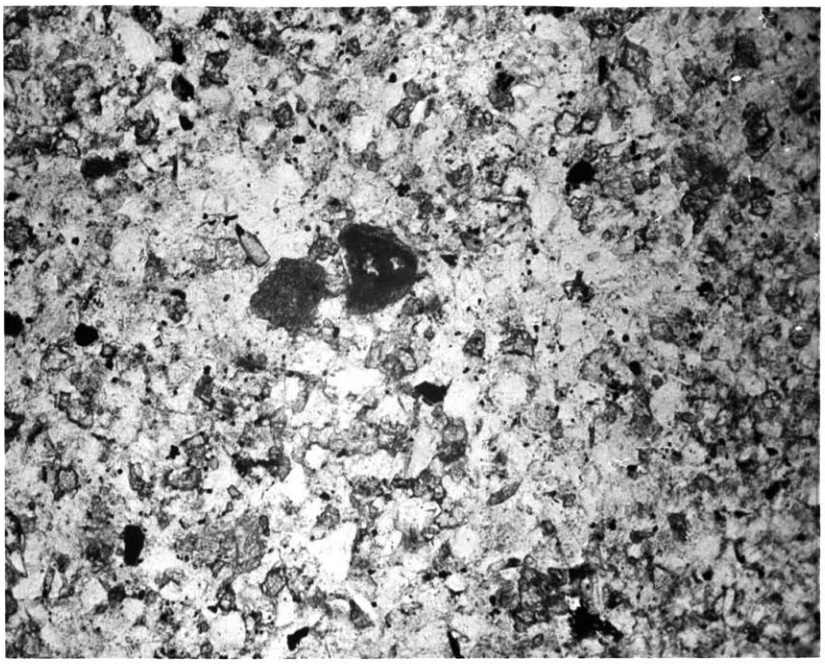
A considerable quantity of organic matter, iron, and fine clay minerals are present. Plate 5 at the bottom shows flocculation of small iron nodules and some clay. Plate 6 at the top shows lath-like growths of limonite or gothite (?) while the bottom photomicrograph shows an iron filled fracture.

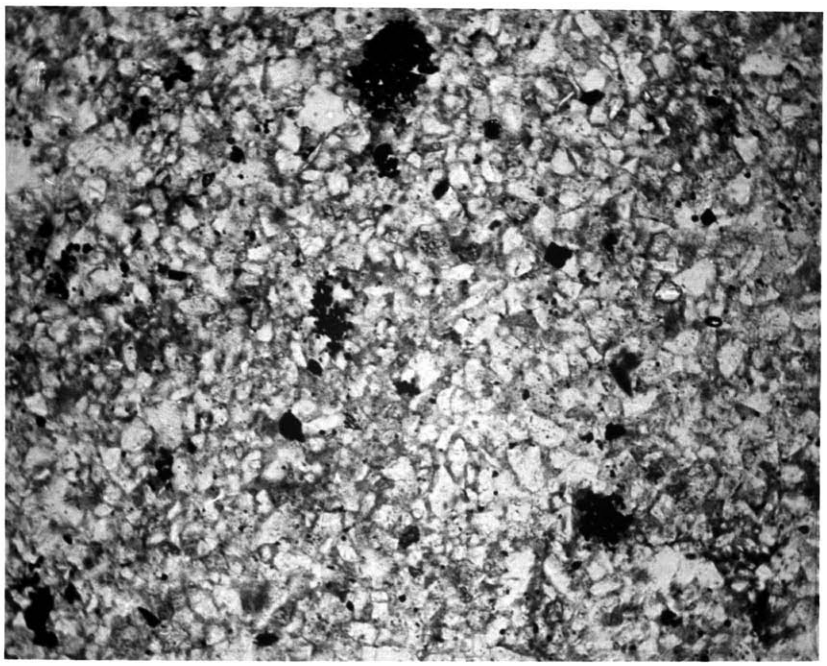
A great deal of secondary calcite is seen both as a cement and as fracture filling. Pyrite crystals and pyrite or marcasite replacement of shells is also noted in occasional fossiliferous nodules. See Plate 7. Authigenic hydromica or sericite is seen in some sections as well as some plagiclose feldspar which appears to be authigenic.

E. DEPOSITIONAL FABRIC

Grain orientation was studied in sections parallel to bedding to learn whether the quartz grains had any preferred orientation.

Theory of Grain Orientation. It has been noted that quartz grains often have their long axes parallel to their optic axes (Fairbairn, 1949, pp. 17-18 and 118). Quartz crystals in normal unrestricted growth have their long axes parallel to their

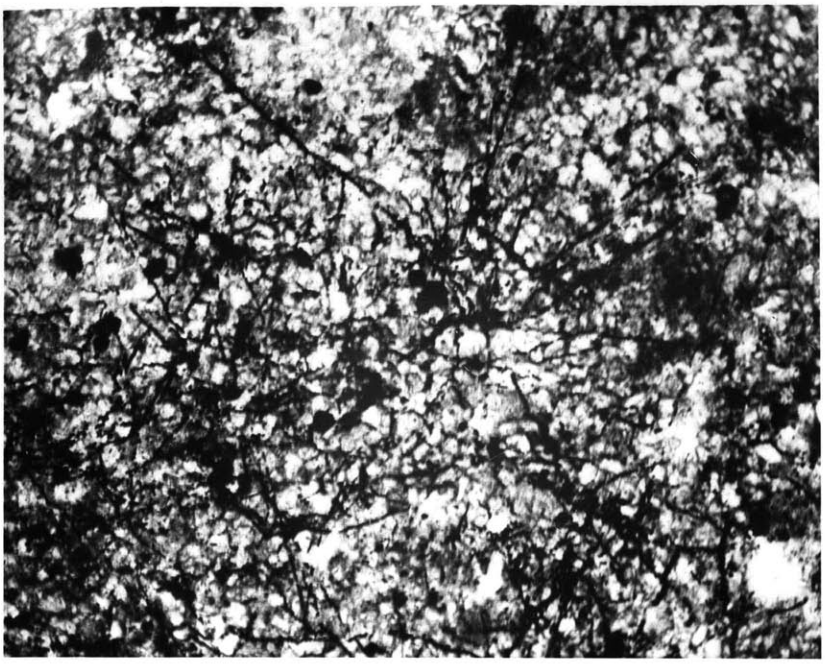




Both thin sections cut parallel to bedding. Plain light X 65.
Upper Picture: Limestone fragments
Lower Picture: Flocculated nodules

PHOTOMICROGRAPHS OF SPRABERRY THIN SECTIONS

PLATE 5



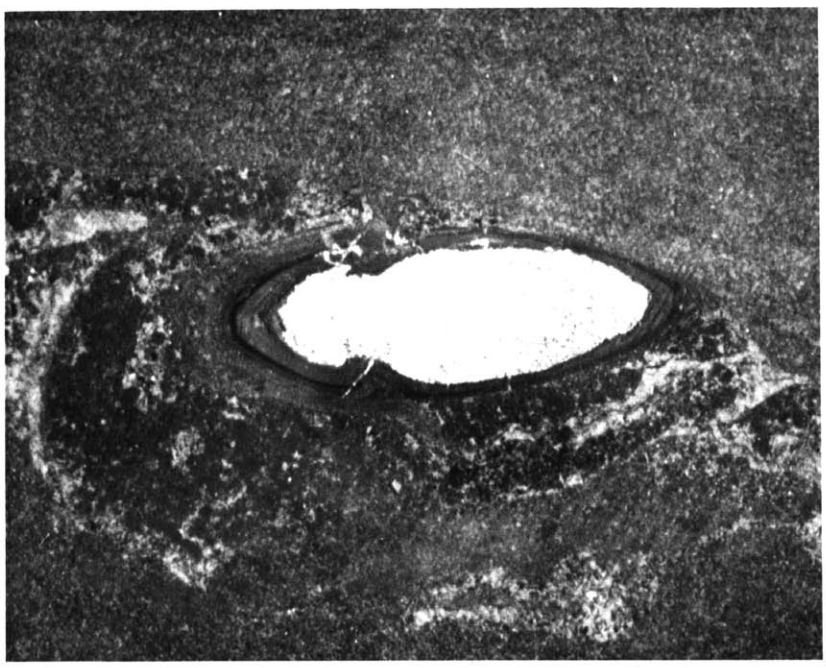


Spraberry thin sections cut parallel to the bedding showing organic matter and iron. Plain light X 65.

PHOTOMICROGRAPHS OF SPRABERRY THIN SECTIONS

PLATE 6





Photographs showing pyrite and marcasite replacement of shells.
Upper Picture: Plain light X I8
Lower Picture: Plain light X 6

PHOTOGRAPHS OF SPRABERRY POLISHED SECTIONS

PLATE 7

optic axes. Experiments by Griggs and Bell (1938) showed that the greatest number of quartz crystals broke parallel to the optic axes in crushing experiments. The direction of the break was dependent on the direction of the crushing force with respect to the crystal axes, but the greatest proportion of breaks were parallel or nearly parallel to the prism faces of the crystal.

When an elongate grain is deposited in flowing water there is tendency for the long axis to become aligned with the current direction. The reason for this is that the grain's velocity is generally somewhat less than that of the water and rotation occurs so that the force of the water against the grain is a minimum. Thus if crystals which are optic axis long are deposited in flowing water there should be a preferred orientation for the optic axes. Unless the water is very turbulent grains will almost always deposit so that the shortest axis is vertical. Therefore the bedding planes will almost always show a preferred shape orientation which is quite pronounced unless the grains are very equant; i.e. have a sphericity approaching unity. The degree of preferred orientation horizontally is determined not only by grain shape but also by the force and persistence of the flowing water. Thus information about the mobility of the depositing water can be obtained from an examination of grain orientations in sections cut parallel to bedding.

Where the currents are stronger and the grain sizes larger current direction and force can be learned from vertical thin sections by an examination of imbricated structure and other features. This does not apply to the Spraberry.

Grain orientation can be determined by an individual grain count. If the preferred orientation is quite marked this can be done by including a reasonable number of grains. Where the preferred orientation is slight a much larger number of grains must be included in the count to obtain reliable results. With an insufficient number of grains a weak orientation might not even be suspected.

If a large proportion of grains have their optic axes parallel to the long axis of the grain, the orientations can be determined by the extinctions of the grains under a petrographic microscope. If there is a preferred orientation of a portion of the grains in the field at one time, then there will be variations in the total quantity of light being transmitted as the microscope stage and thin section are rotated. If this light could be accurately measured the results would represent the total light transmission of many grains and very weak orientations, such as are found in Spraberry sediments, could be observed.

General Description of Equipment. In order to measure the variations of light transmission through a thin section rotated on the stage of a petrographic microscope, the

writer designed a special photoelectric amplifier and photocell mount. The design, construction and operation of the equipment is fully discussed in Appendix A, and only a brief description will be given here. Directly over the microscope and shielded from any outside light was placed a vacuum type photoelectric tube. This phototube is connected to a sensitive bridge circuit so designed that the variations of light intensity can be amplified. Variations of light intensity of 0.1% can be read as the microscope stage is rotated. The microscope was generally used on a medium power so as to include a fairly large number of grains. On low power there were reflections of light from the top of the thin section which interferred with the operation of the instrument.

It was found that there were slight variations in the direction of orientation when different portions of the same thin section were tested. This was much more noticeable for the weaker orientations. However, the magnitude of the preferred orientation did not vary much over the extent of any one thin section. In order to obtain a better average for the direction of orientation of each thin section a new device was constructed to replace the petrographic microscope. This equipment incorporated a light source, two ground glass surfaces, two condensing lenses, polaroid polarizer, rotating stage for the thin section, polaroid analyzer, collecting lenses, and a phototube.

This new piece of equipment was connected to the same bridge circuit amplifier. The light transmitted by the entire area of a thin section could be analyzed with this new equipment. It is described and illustrated in Appendix A.

The thin sections with a preferred direction of extinction transmit the least light whenever the preferred direction is parallel to either the polarizer or analyzer. Thus there are four minima and four maxima for each complete rotation. A direct analysis of grain orientation would show only two. Herein lies the main drawback to this method of analysis.

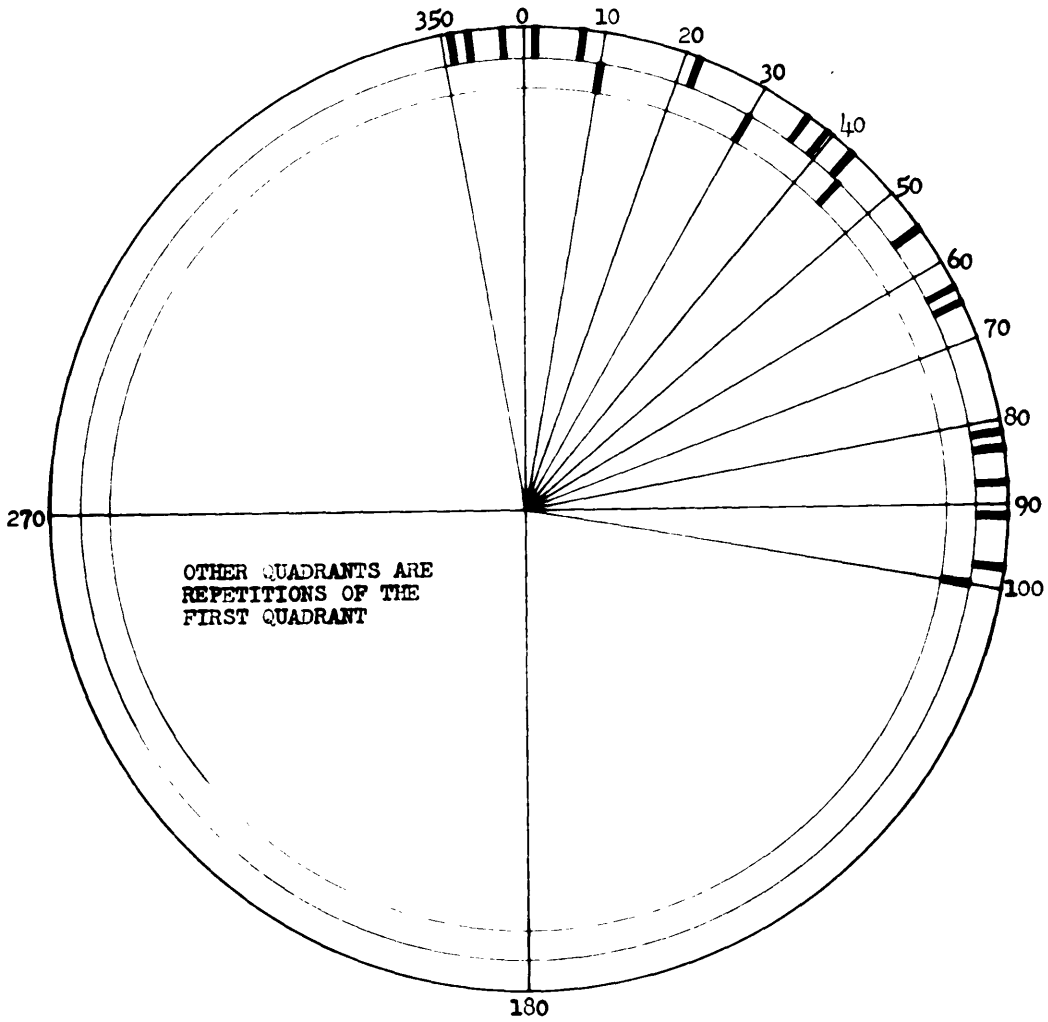
Results. Each thin section was analyzed to give two kinds of information, the direction of orientation of extinction with respect to the fracture direction, and the magnitude of the orientation in terms of variation of light output. All thin sections were carefully oriented with the fracture direction for those cores which exhibited fractures. Table IX below gives the results of this study for 22 thin sections, 17 of which were oriented by fractures. The angles are measured clockwise on the thin section from the fracture toward the next minimum. Each thin section was placed on the rotating stage in the correct relation with respect to top and bottom even though some slides had to be mounted upside down. The light variations are given as the percent of variation with respect to the maximum transmission. Two of the slides oriented by fractures gave no observable grain orientation.

Table IX
Grain Orientation Data by Photoelectric Method

Feet below top Upper Spraberry	Orientation with Fractures	Magnitude of Variation, %
8	65	5.3
24	39	5.2
39	83	3.9
48	55	4.7
56	87	4.1
63	--	under 0.2
70	--	6.2
90	36	2.3
114	none	under 0.2
129	--	2.1
132	81	4.1
144	21 (?)	1.0
145	01	6.4
158	07	2.1
165	43	4.3
179	--	1.5
188	63	0.8
201	none	under 0.2
Lower Spraberry		
7	10	8.0
30	44	3.4
39	30	4.2
114	--	2.1
Average		3.28

It was possible to obtain a preferred extinction in 19 of the samples tested but only 15 of these were from cores containing fractures and hence had a reference direction. Of those for which orientations were obtained 12 were in the Upper Spraberry and 3 were in the Lower Spraberry. When studying the data presented in the table, it should be remembered that the values near 0 degrees are repeated again above 90 degrees. Since minima occur four times each cycle at 90 degree intervals, the readings recorded in the table for the first quadrant are repeated in the other three quadrants. This data is shown plotted on Figure 18. The maximum number of readings in any 20 degree interval for the Upper Spraberry is 5 and this occurs at the interval whose center is at 0 (or 90, 180 etc.). No other 20 degree interval has over 3 points. There are not enough points in the lower member to give much information. The average variation of light intensity was 3.28%.

Several measurements were made on sections cut perpendicular to the bedding. These all showed extinction orientation parallel to the bedding and variations ranging from 9% to 26%. This indicates the correctness of the assumption that many grains are optic axis long. To learn something of the sensitivity of the method a thin section of a slightly deformed quartzite was tested. The petrofabric diagram for this thin section had previously been made by Brace (1953) with a universal stage, and this was



OUTER CIRCLE FOR UPPER SPRABERRY INNER CIRCLE FOR LOWER SPRABERRY

FRACTURE DIRECTION IS 0°

ANGULAR RELATION BETWEEN GRAIN ORIENTATION AND FRACTURES

FIGURE 18

used for comparison. The petrofabric diagram had a weak orientation showing a maximum of 3% of the quartz axes in a 1% area in two areas of about 2% of the diagram near the edges and opposite each other. This was surrounded by an irregular 2% area of larger extent. The orientation device indicated a variation of 12% with two of the minima parallel to the line connecting the maxima on the petrofabric diagram and two perpendicular thereto.

Conclusions. The number of tests made on the cores is insufficient to draw many conclusions. The fact that the greatest number of orientation tests indicated grain orientations which are either parallel or perpendicular to the fracture direction may be coincidence. It may also be the result of having the fracture direction parallel to the length of the slide glass. There is a tendency to fine grind the thin sections to a greater extent parallel to the length. This might have a tendency to remove grains whose long directions were at orientations other than parallel to the length.

It is questionable whether grain orientation in an area as small as a thin section can give information about the general current direction because of cross currents and eddies which are almost always present in large bodies of water even with low current velocities. Also any hydroplastic penecontemporaneous slumping would tend to orient

grains with their long dimensions perpendicular to the direction of the slumping motion. This phenomena has not been observed in the Spraberry formation.

The magnitude of the variations recorded should bear some relation to the force of the depositing current even if the orientation is the result of deposition by an eddy or cross current of the main flow. The average variation of 3.28% found in Table IX represants a very small degree of orientation. Thus weak currents and quiet waters are indicated.

F. LITHOFACIES MAP OF SPRABERRY

Figure 19 is a lithofacies map prepared for the four county area from specific well log data obtained from several consulting geologists and from the Sohio Petroleum Corporation. The map is based on the ratios of the total thicknesses of the end members indicated on the map. The interval covered is the whole Spraberry formation. The map was prepared by the method outlined by Krumbein and Sloss (1951, pp. 269 to 276). The total thicknesses of sandstone, silt and shale, and limestone were found for the wells for which adequate information was available. Next to each well on the working map were placed the computed values for the clastic ratio and the sand-shale ratio.



LITHOFACIES MAP

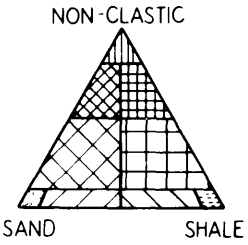


FIGURE 19

These two ratios were found thus:

$$\text{Sand-Shale Ratio} = \frac{\text{Sandstone}}{\text{Siltstone \& Shale}}$$

$$\text{Clastic Ratio} = \frac{\text{Sandstone, Siltstone \& Shale}}{\text{Limestone}}$$

On the map a line was drawn to indicate the best estimate of the loci of points whose sand-shale ratio was 1. Near the center of the basin another line was drawn to indicate a sand-shale ratio of 1/8. Then another set of lines were drawn to indicate clastic ratios of 1/4, 1, and 8. The areas formed by the intersections of these two sets of ratio lines represent the areas of the different lithologic facies. Eight of the possible nine facies on the triangle diagram are represented. The sand end member is the only facies not represented.

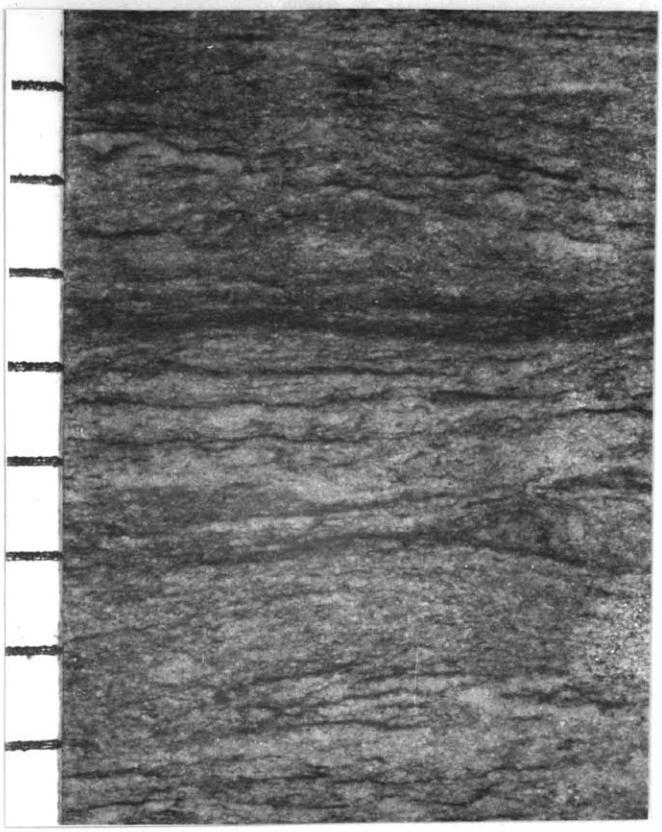
The map shows that the largest part of the area is predominantly shale or sandy shale (silt or sandy silt). The clastic sediments become more coarse toward the east indicating that this was the source direction. This checks fairly well with the evidence presented by the isopachous map of Figure 11. The isopachous map included not the Spraberry alone but also the underlying sediments to the base of the Dean sandstone. The indications from that map were that the sediments came from the southeast rather than the east.

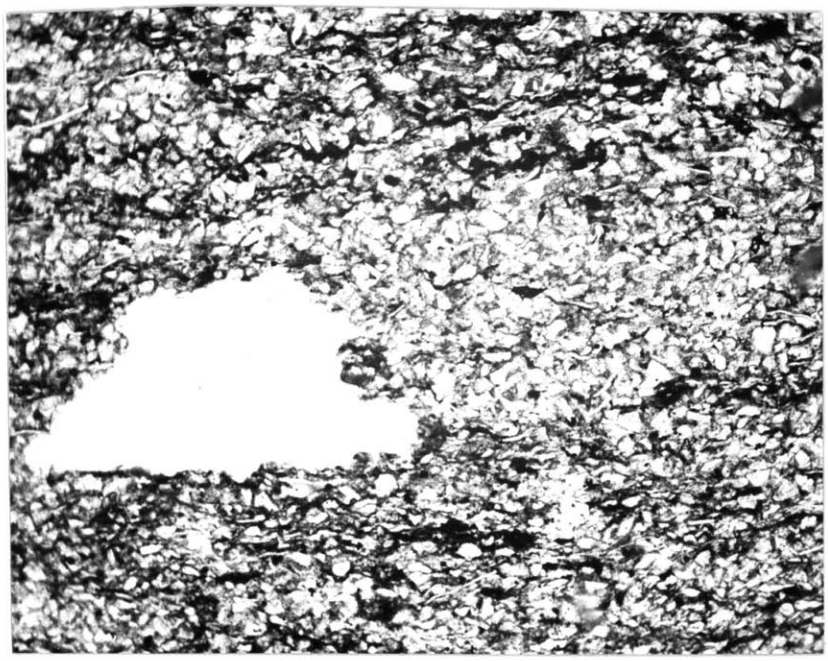
The clastic ratio is seen to decrease toward the northeast and toward the southwest. These were quite shallower shelves favoring limestone deposition.

G. OTHER SEDIMENTARY FEATURES

Micro-Laminations. Many Spraberry cores have finely laminated or apparently *varved* sections. The alternately light and dark layers range from under 1 to over 3 millimeters in thickness. Plate 8 at the top shows the appearance of these laminations on a section cut perpendicular to the bedding. The appearance is that of alternating silt and shale. Microscopic examination shows that dark layers are actually mostly silt with shaly partings and fillings. The photomicrograph shown at the bottom of Plate 8 shows a layer free from shaly material followed above by a darker layer containing dark shaly material and organic matter. The deposition of silt seems to continue uninterrupted regardless of whether finer particles are also being deposited. This could be brought about by deposition in quiet waters with lateral transport of particles restricted to the upper layers of water.

Concretions. Concretions of calcareous material have been found in the Spraberry at irregular intervals. These are generally about 1 to 2 inches long and often contain small shells sometimes partially replaced by pyrite (see Plate 9). A concretion of silt was found in a finely laminated



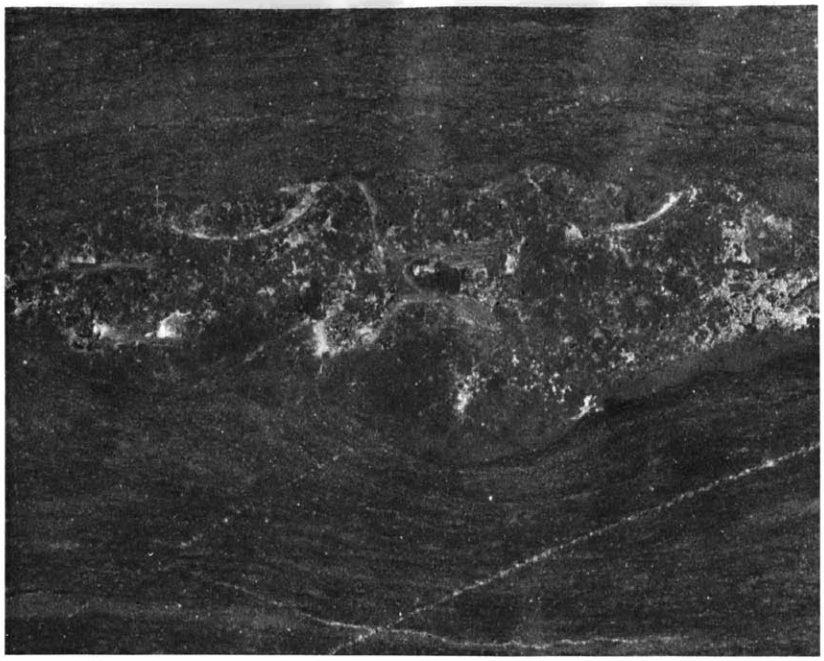


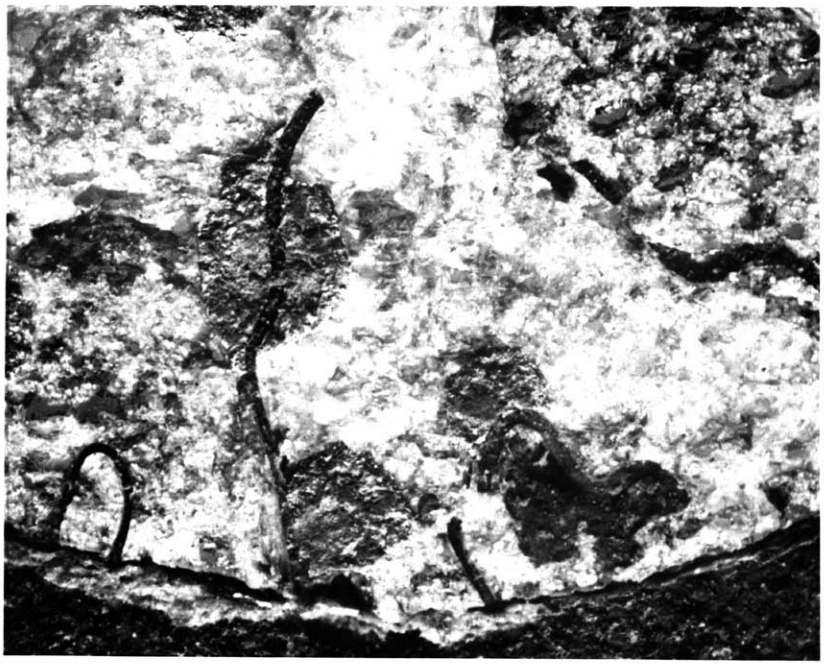
Upper Picture: Divisions are tenths of an inch. Sample cut across bedding.

Lower Picture: Thin sections cut across bedding. Plain light X 65.

PHOTOGRAPH AND PHOTOMICROGRAPH OF MICROLAMINATIONS

PLATE 8





Upper Picture: Plain light X 3
Lower Picture: Plain light X 18

PHOTOGRAPHS OF CONCRETIONS

PLATE 9

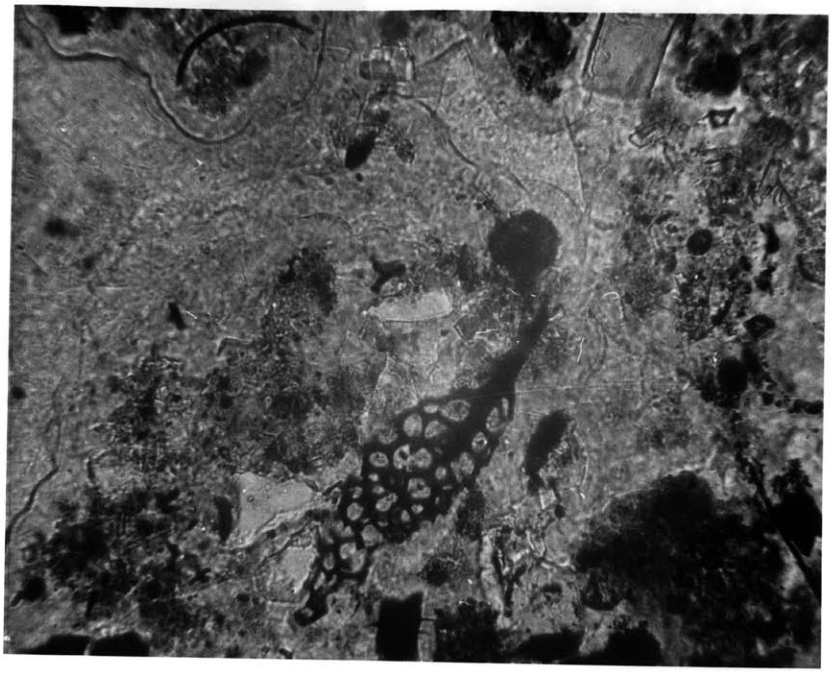
section and did not appear to vary in grain size from the silt in the matrix. This concretion was about 3/4 of an inch in diameter and was somewhat ellipsoidal. The nodule was a little darker than the matrix and apparently had a higher iron content.

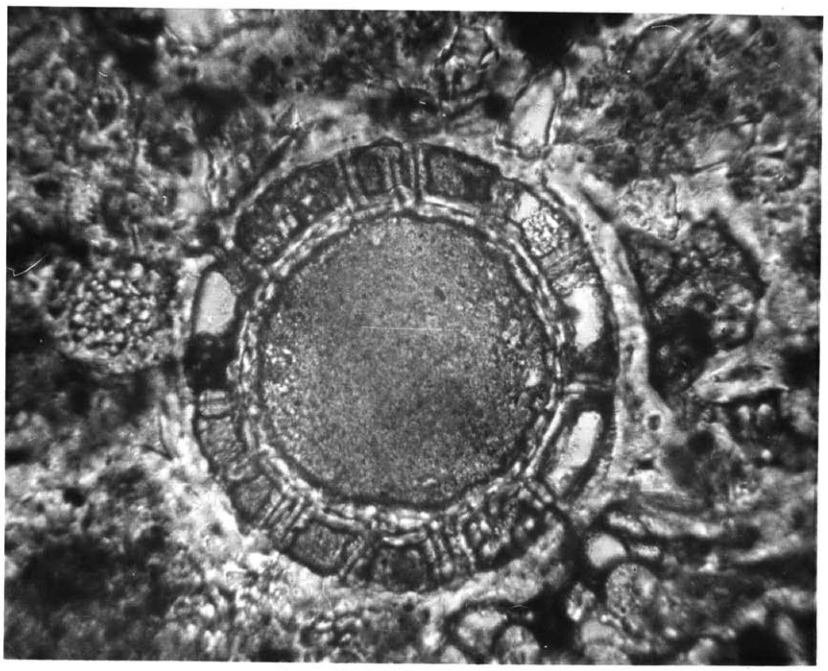
4. PALEONTOLOGY

A few unidentifiable brachiopod or pelicipod shells were found in concretions. The only fossils seen in the matrix of the rock were Radiolaria. These occurred in great abundance on some horizons but were completely absent on most. Thirty-one of the thin sections examined were cut parallel to the bedding. Of these only 6 contained Radiolaria with only 2 slides on which they could be considered abundant.

Identification of the Radiolaria is very difficult since so little information is available. Many genera of Radiolaria extend over such a long span of time that their use as index fossils is precluded. Some of the forms found are shown on Plates 10 and 11, and the tests are seen to be in good state of preservation.

The fossil assemblages in the Spraberry are undoubtedly a thanatocoenose and are not the normal associations of living types. The indications are that the bottom conditions during Spraberry deposition were not conducive to the

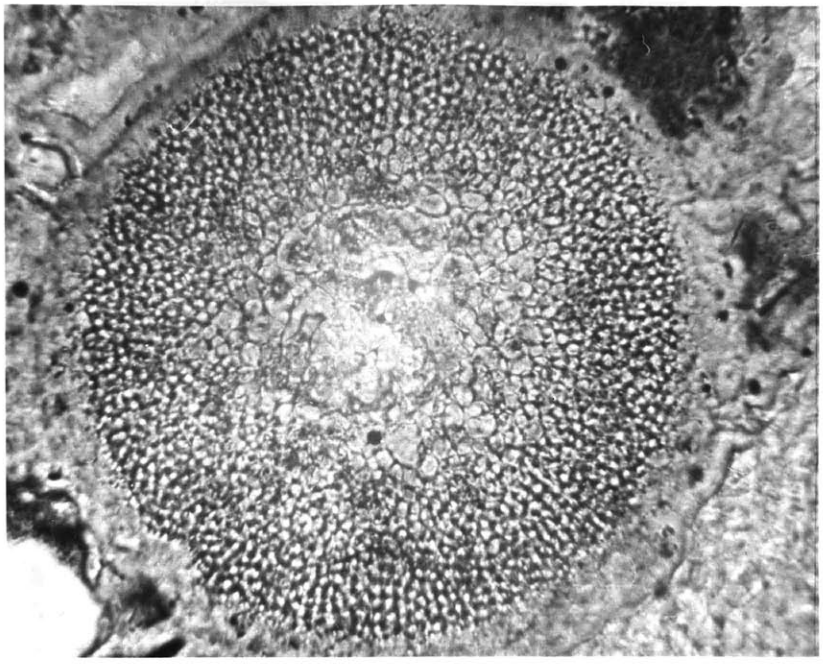


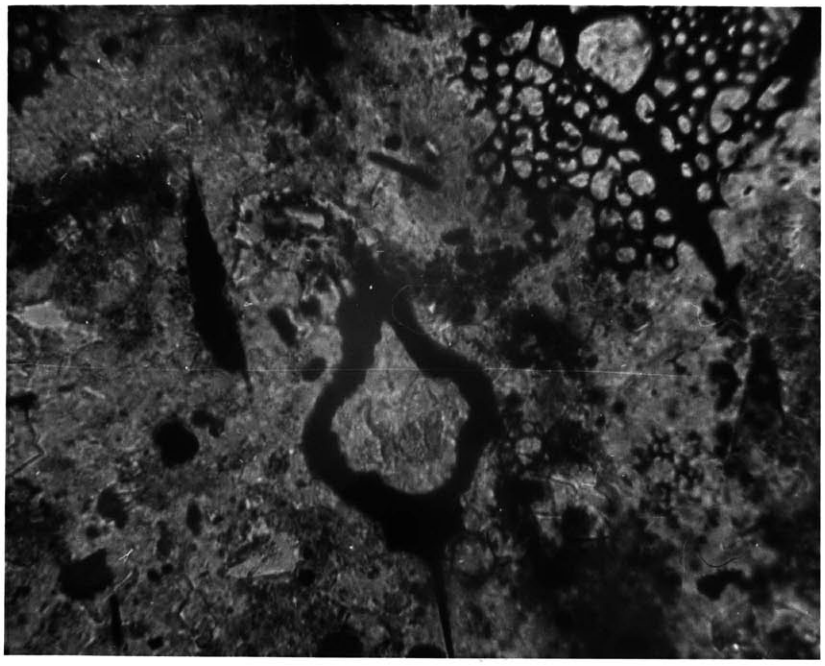


Both thin sections cut parallel to bedding. Plain light X 293.

PHOTOMICROGRAPHS OF RADIOLARIA

PLATE 10





Both thin sections cut parallel to bedding. Plain light X 293.

PHOTOMICROGRAPHS OF RADIOLARIA

PLATE 11

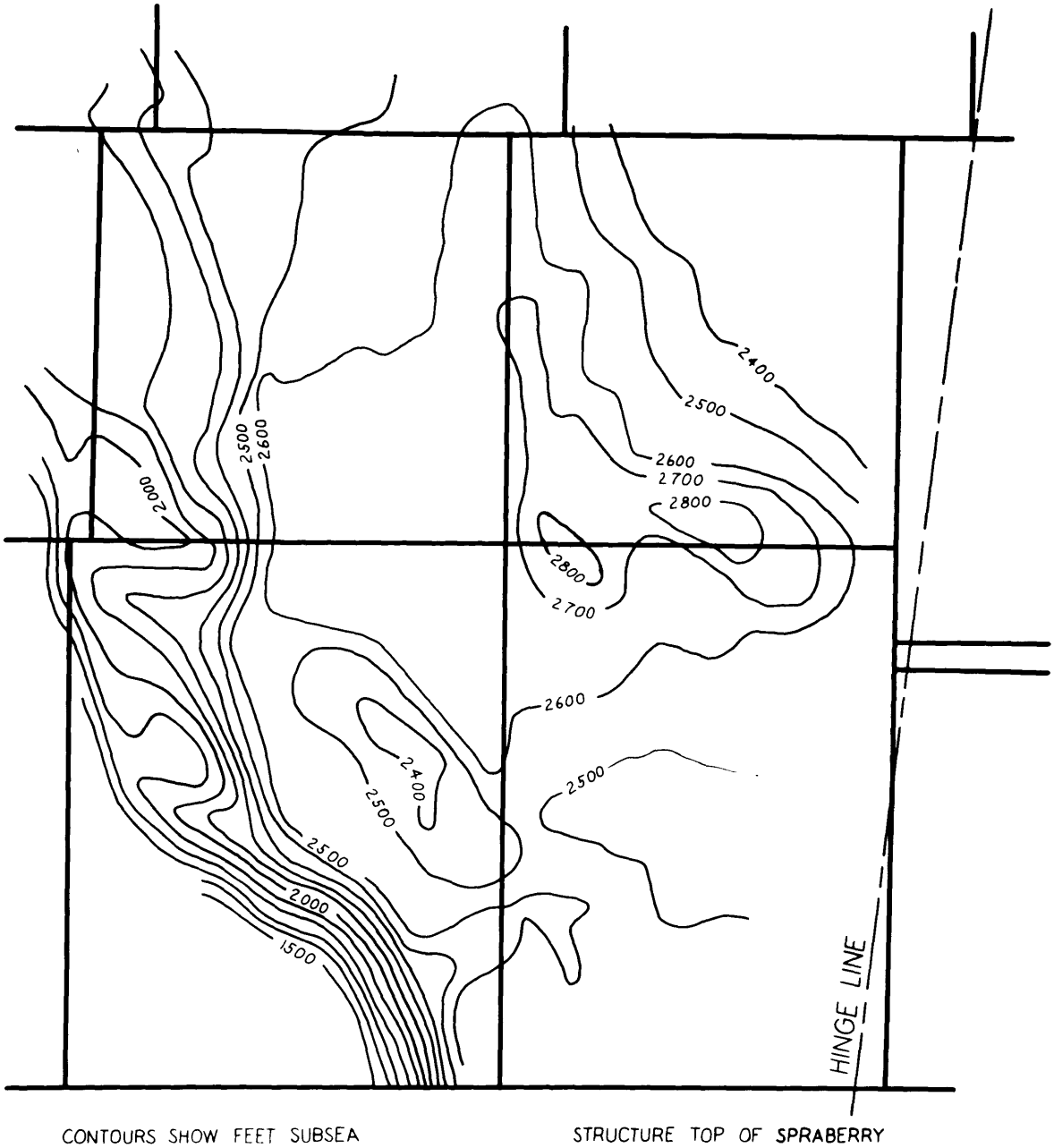
existence of a benthonic fauna. At infrequent intervals a few more adaptable forms may have existed on the bottom, but most fossils now found were probably transported from another environment such as the shelf areas. Radiolaria are pelagic and live in the waters near the surface. After death their tests fall to the bottom but are usually destroyed by the bottom fauna, particularly the burrowing forms, unless conditions are unfavorable for the existence of bottom life.

5. PALEOGEOGRAPHY

A. CONSTRUCTION OF PALEOGELOGIC MAPS

Geographic maps constructed to represent topography at some specific time in the geologic past are useful tools in the interpretation of past environmental conditions. They are of special use in studying the hydrology at the time represented and give information about the probable areal extent of bodies of water, the depths of these bodies, and the heights of neighboring land masses. Where whole regions appear to have been tilted without appreciable warping paleogeographic maps can be made by rotating the structure map of the desired horizon until the regional dip caused by the tilting is eliminated.

In the construction of a paleogeologic map a hinge line must be chosen on the structure map. This is generally parallel to the average strike of the present structure map. An average regional dip is selected and used to determine the amount of rotation. The hinge line is usually selected on or past the edge of the map so that the whole area is either raised or lowered. The amount by which any point on the structure map is changed is dependent only on the distance from the hinge line once the amount of rotation has been decided. The new elevations can then be transferred to the paleogeographic map point by point. A more rapid and more accurate system was used for the paleogeographic maps presented below. On a piece of tracing paper were ruled evenly spaced parallel lines to represent the loci of points on the structure map to be raised successive even multiples of 100 feet. This was placed over the structure map so that the first line (marked 0) was coincident with the hinge line on the structure map, and another piece of tracing paper was placed over this for the paleogeographic map. Since the contour lines on the structure map were at 100 foot intervals, lines of constant elevation on the new map occurred at successive opposite corners of the parallelogram shaped areas formed by the intersections of the lines on the map with those on the overlaid grid. The paleogeographic map was sketched quite rapidly with a maximum of control points.

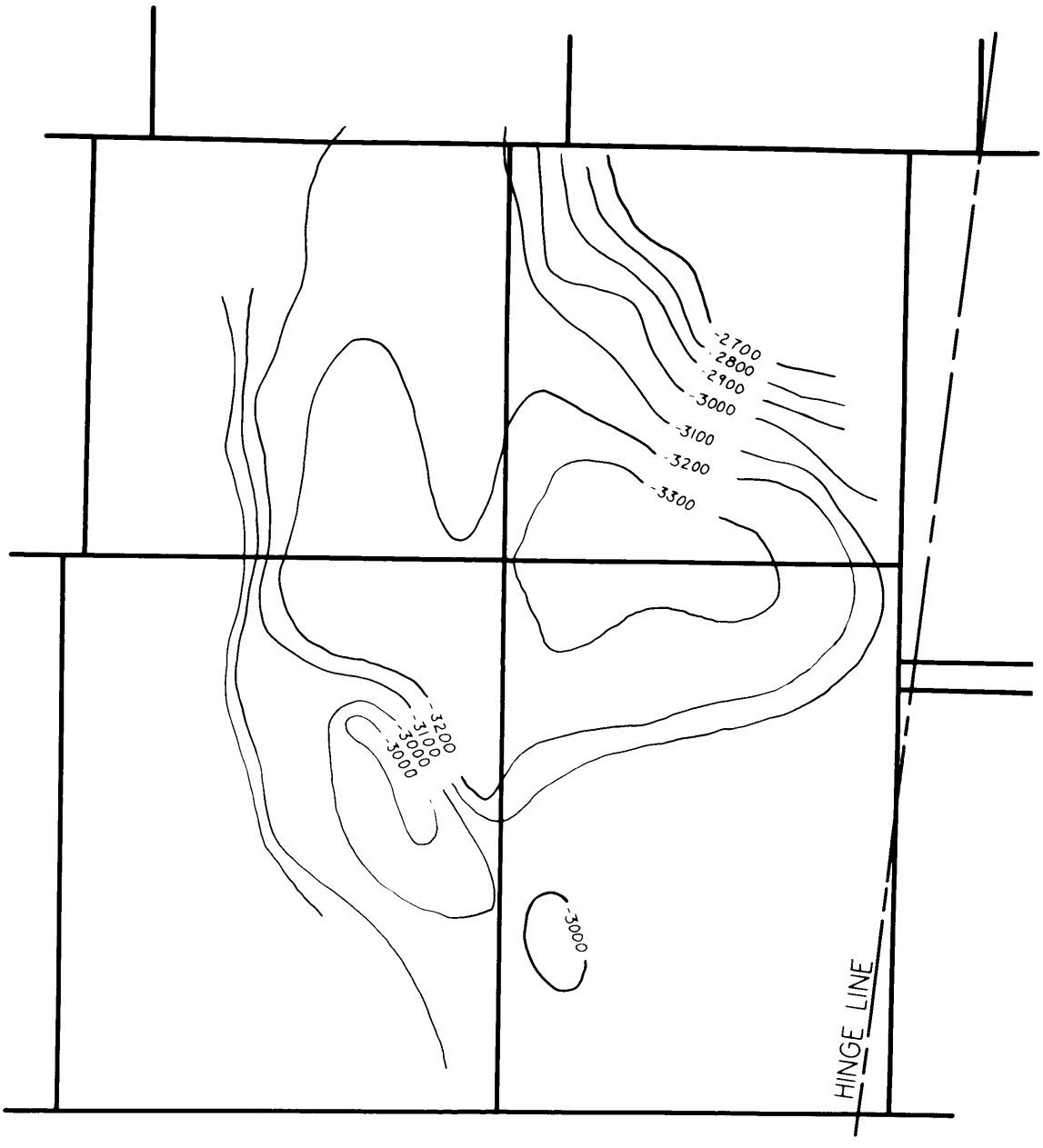


CONTOURS SHOW FEET SUBSEA

STRUCTURE TOP OF SPRABERRY

PALEOGEOGRAPHIC MAP

FIGURE 20



CONTOURS SHOW FEET SUBSEA

STRUCTURE BASE OF DEAN

PALEOGEOGRAPHIC MAP

FIGURE 21

B. DISCUSSION OF PALEOGEOGRAPHIC MAPS OF SPRABERRY

Figure 20 is a paleogeographic map of the four county area at the end of Spraberry time while Figure 21 is a paleogeographic map on the base of the Dean sandstone, which is somewhat before the start of Spraberry deposition. These maps were constructed using the hinge lines shown and a rotation amounting to 50 feet per mile which is the present average regional dip to the westward at right angles to the hinge line. These two maps are separated by the interval shown on the isopachous map which is Figure 11. At the base of the Dean the deepest part of the basin was a fairly broad area near the center of the four county area. After Spraberry deposition the conditions were almost the same except that the deepest part of the basin had shifted a few miles to the east. The evidence presented here confirms that of the isopachous maps (Figures 11 and 12) and the lithofacies map (Figure 19).

The deepest parts of the basin occurred where the present oil fields are now located. This correlation is very good for the paleogeographic map drawn on the top of the Spraberry (Figure 20) since most of the oil fields shown (Figure 5) are producing from the Upper Spraberry.

6. CONCLUSIONS ABOUT BASIN CHARACTERISTICS

The Midland Basin during Spraberry deposition appears to conform to the conditions in stagnant basins as outlined by Pettijohn (1949, pp. 456 to 460 and Fig. 120 after Fleming and Revelle). The characteristics of the sediments in such basins are given as follows:

1. Fine grained
2. Highly reducing
3. H_2S present
4. $CaCO_3$ high
5. Laminated
6. No bottom fauna
7. Mixed fossil assemblage
8. Organic matter high
9. Fossils only in certain layers

The Spraberry sediments appear to conform to these characteristics which are outlined below according to the numbering of the characteristics above.

1. The average grain size of the Upper Spraberry is 0.0056 mm based on thin section analyses of 12 samples.

2. The reducing conditions are indicated by the high organic content and the lack of bottom fauna as well as the formation of pyrite.

3. H_2S is indicated by the presence of pyrite and marcasite.

4. Many of the samples are almost completely cemented by $CaCO_3$, and no core samples examined were entirely free of such cementation.

5. Alternating light and dark laminations about 2 mm thick are seen in many Spraberry cores.

6. The bottom dwelling fauna in the Spraberry cores occurs only at infrequent intervals, usually in calcareous concretions and has probably been transported from another environment.

7. The fossil assemblages which are found represent a thanatocoenose or death assemblage. The only fossils found were either pelagic forms from the surface waters or bottom types probably transported from another environment.

8. Organic matter is high in the Spraberry giving a dark color to many of the cores, particularly those which are laminated.

9. The bottom types found occurred only in a few of the cores examined while Radiolaria were found in only 6 of the 31 bedding plane thin sections examined, indicating that the fossils occur only in certain layers.

While the evidence is not conclusive, the paleogeologic maps seem to indicate the long shallow sill which is characteristic of stagnant basins. In view of the data given above and the fact that there is no conflicting evidence, it seems safe to assume that the Midland basin during Spraberry time was a stagnant basin.

CHAPTER IV

FRACTURE STUDY

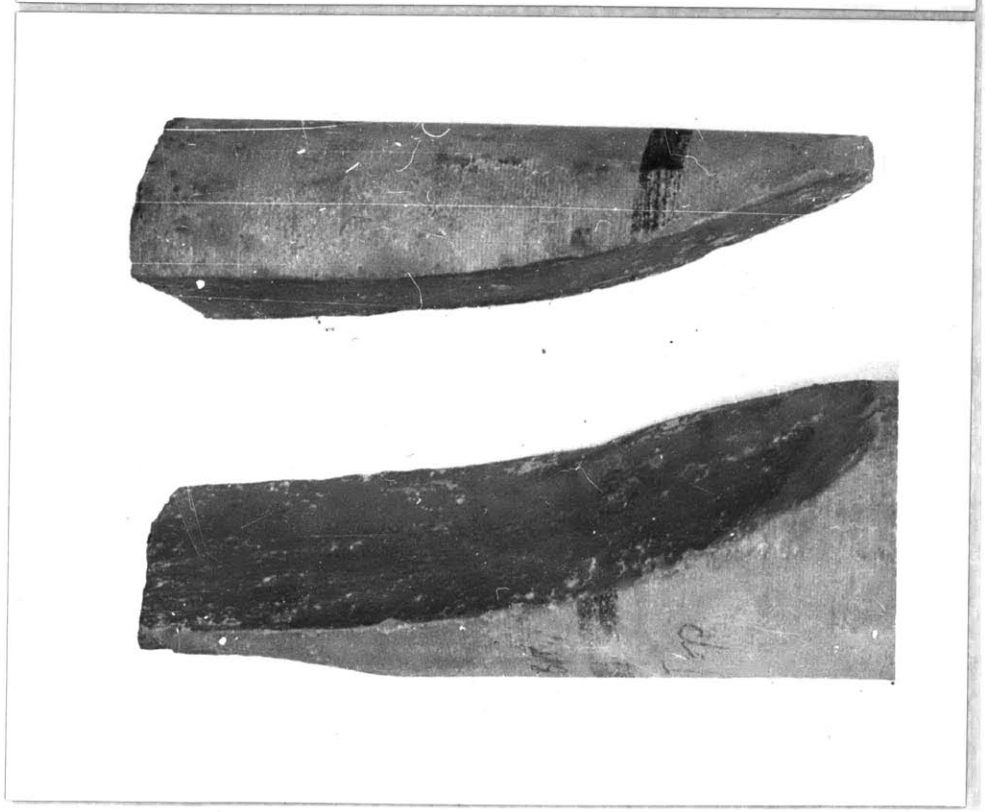
1. RELATION OF FRACTURES TO CENTERS OF CORES

A. METHOD OF STUDY

One of the most striking things about the cores from the Spraberry is the number of clean fractures which occur along the center of the length of the core. Plate 12 shows a few cores which are fractured. Individual fractures in the wells studied sometimes ran over 20 feet (Sunray, 1952). The fractures usually occurred very close to the centers of the cores and were clean and straight with only one fracture in each core. Sometimes the fractures would terminate within the core sample and sometimes would curve out through the side of the core (Plate 12). Cores have been found which contained many parallel fractures ("Is World's Largest Oil Field, etc." O. & G. J., Fig. 1, 1951). No cores were examined containing more than two fractures and one of these was always near the center.

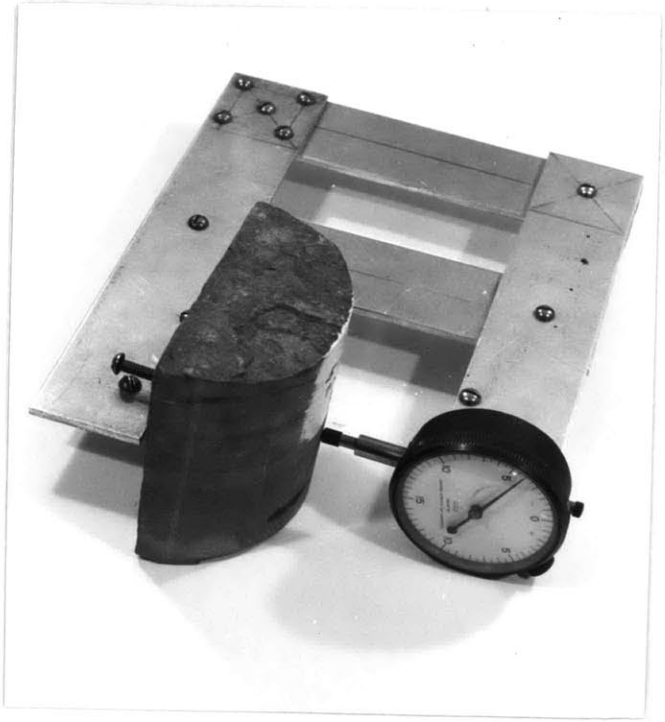
A study was made to determine the distance of the fractures from the core centers. The writer mounted a dial gage as shown at the top of Plate 13. The thickness of each half of each fractured core was measured to 0.001 inches. The distance of the fractures from the core center was half

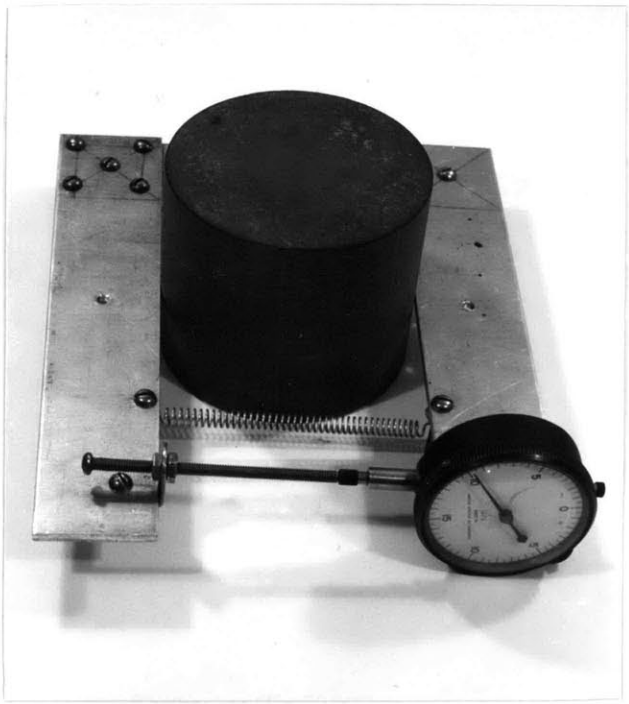




TYPICAL SPRABERRY CORES

PLATE 12





CORE MEASURING EQUIPMENT

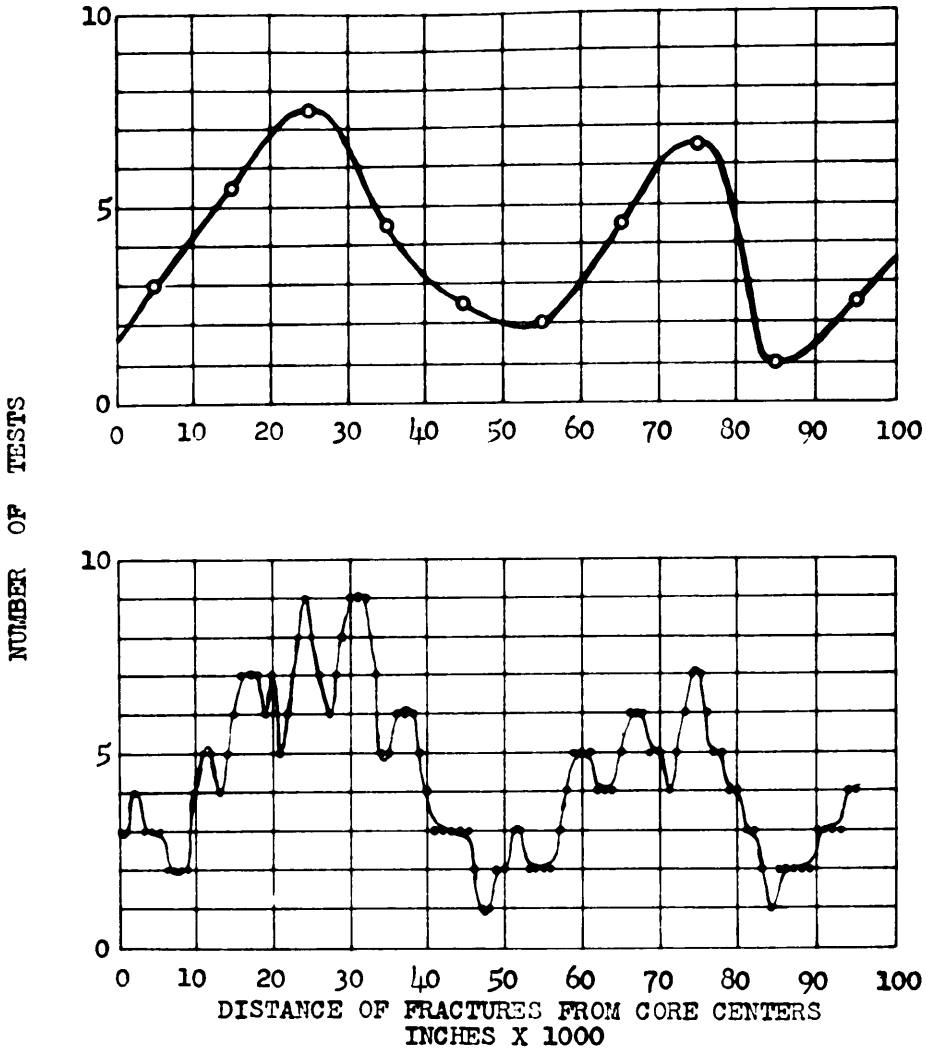
PLATE 13

the difference in the thickness of the two halves. Each thickness was measured two or three times to be sure of a representative reading.

B. RESULTS OF STUDY

Measurements were made on all of the fractured cores selected by the writer in Tulsa. It was found that long core pieces gave quite different readings at each end. Thus two readings were made on core samples 7 inches or more in length. The readings obtained on 51 measurements are listed in Table X. There were 3 more cores with fractures more than 0.180 inches from the center but were beyond the scale of the instrument. The valves below 0.100 inches on Table X are plotted on Figure 22. The upper curve was plotted by taking the sum of the number of points occurring in each successive 10/1000ths inch interval. The lower curve results from plotting the sum of the points within a moving 10/1000ths inch span. Each curve shows two definite maxima, one at about 0.025 and one at 0.075 inches.

Because of the fact that there were two maxima and a general broad spread of points outside these maxima, it was decided that any determination of standard deviation would not be significant. The average distance of the fractures from the core centers for the readings taken was 0.065 inches. The inclusion of the 3 readings which could not be made would make the average a little higher.



UPPER CURVE - TOTAL TESTS IN EACH 10 MIL INTERVAL
LOWER CURVE - TOTAL TESTS IN MOVING 10 MIL SPAN

RELATION OF FRACTURES TO CORE CENTERS

FIGURE 22

C. SIGNIFICANCE OF RESULTS

The average fractured core has its fracture about 1/16 of an inch from the center line of the core. It would appear that the fractures are either made artificially during or after coring, or that the drill or core bit tended to follow an existing fracture in the formation. Each of these possibilities is examined in some detail later in this chapter along with others. There is evidence that the drill or core bit is not influenced to follow the Spraberry fractures. If this is true, it would be very fortuitous if the cores should all happen to be made so that the fractures were so close to the centers. The only conclusion is that there are forces involved which determine the position of the fracture after the position of the core has been fixed. If these forces acted on a completely homogeneous core in such a way as to influence fractures to form near the center, the maximum number of fractures would occur at the center with decreasing frequency away from the center. If instead of being homogeneous the cores had incipient planes of weakness spaced at definite intervals, the fractures in each core would occur along the nearest one of these weakness planes. Under these conditions the fracture distribution would be expected to be uniform over the range from zero to a half the interval between the planes of weakness. If the interval between the incipient planes of weakness were not constant

Table X

Deviation of Fractures from Core Centers

1000ths of an inch

51 readings

0	27	47	77	120
3	27	54	78	131
7	28	56	79	139
13	28	62	90	150
15	29	63	90	158
15	33	64	95	158
16	34	65	99	180
19	35	70	105	
20	36	71	105	
21	40	73	113	
25	41	75	114	

Average = 0.065 inches

the distribution would be constant to half the minimum interval and then decline in frequency ending abruptly at a center-to-fracture distance equal to half the maximum interval.

The measurements shown in Table X and plotted on the graphs of Figure 22 seem to indicate close spaced incipient fractures rather than homogeneous cores based on the reasoning above. No explanation for the two maxima is readily apparent.

2. FRACTURE DIMENSIONS

There is considerable evidence that many of the fractures were not actually open in the formation. However, it was decided to study the fractures to learn what proportion were open in the ground and to what extent.

A. DIRECT MEASUREMENT OF WIDTHS

Theory. If a fracture with measurable opening existed in the formation and were cored it could be expected that the core diameter perpendicular to the fracture would be less than the core diameter parallel to the fracture. The closure of the fracture during the measurement would result in a decreased diameter across the fracture but would not affect the diameter along the fracture. Any lack of roundness

in the cores would merely give a statistical spread to a large number of readings.

Method of Study. The instrument used to measure the core diameters is shown at the bottom of Plate 13. The actual core illustrated is not fractured since the instrument was also used for another purpose in Chapter V. The smallest divisions on the dial gage were 0.0005 inches but the arm of the device acting against the core provided an amplification of any variation of core diameter of 2 1/2 times so that each division on the gage was really 0.0002 inches of change in core diameter. The reading could be estimated to 1/4 of these divisions. The spring shown applied a constant contact pressure of instrument against core for all readings. Short cores were measured at only one place. Two measurements were made on cores over 6 inches in length and three measurements were made on those over 9 inches in length. It was felt that this procedure was permissible because of the fact that the two or more readings on any core were seldom the same, and because of the fact that the data plotted for single measurements on each core (39 measurements) gives results similar to that obtained by using all the measurements (83 measurements).

Results. Table XI gives the results of the study. The fracture widths as given are the diameters across fractures subtracted from diameters along fractures. This gave

some negative values. These are included in the table and the statistical treatment because it is felt that these are due to experimental error and lack of core roundness which caused the scatter of points around the mean. The table gives the number of points occurring within half a thousandth (0.0005") of each even thousandth of an inch of width. The average opening width by this method is 0.00193 inches and the standard deviation, σ, and probable error of the mean, $r_{\bar{m}}$, can be computed as outlined in Chapter II.

$$\sigma = \left(\frac{1198.5}{82}\right)^{1/2} = 3.82 \text{ thousandths}$$

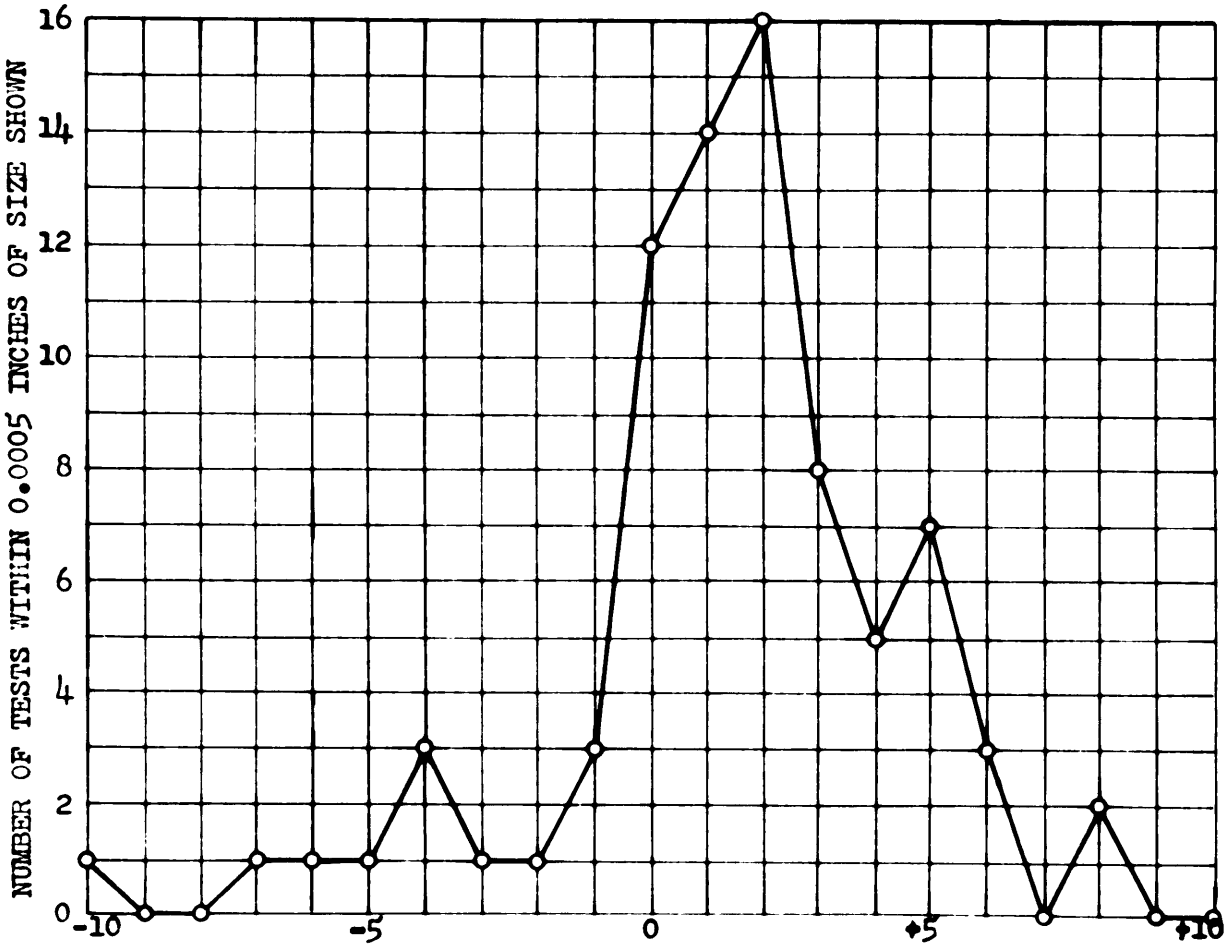
$$= 0.00382 \text{ inches}$$

$$r_{\bar{m}} = 0.6745 \left(\frac{1}{83}\right)^{1/2} \times 3.82 = 0.28 \text{ thousandths}$$

$$= 0.00028 \text{ inches.}$$

The measurements listed in Table XI which are between $\pm$ 0.010 are plotted on the graph which is Figure 23.

Conclusions. These results would seem to indicate that the fractures are open about 2 thousandths of an inch on the average. But the conclusions drawn in the previous section and the experiments with the pressure vessel described later in this chapter indicate that the fractures are not open in the ground but are present only as incipient planes of weakness. Therefore another explanation is offered for the results found.



FREQUENCY DISTRIBUTION OF FRACTURE SIZES

FIGURE 23

Table XI

Distribution of Fracture Widths

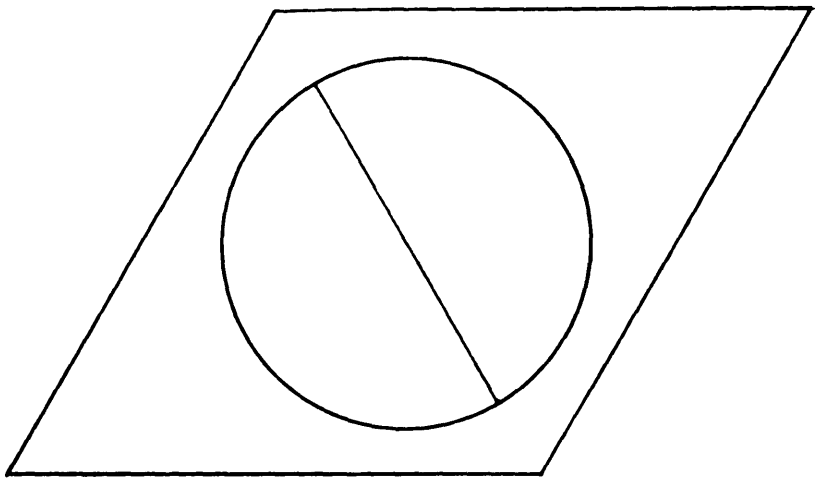
Number of measurements within ± 0.0005" of width shown

Width in 1/1000"	Number	e	e^2	ne^2
13	2	+ 11.07	122.55	245.1
12	1	+ 10.07	101.40	101.4
11	1	+ 9.07	82.26	82.3
8	2	+ 6.07	36.85	73.7
6	3	+ 4.07	16.56	49.7
5	7	+ 3.07	9.42	65.9
4	5	+ 2.07	4.28	21.4
3	8	+ 1.07	1.15	9.2
2	16	+ .07	.01	.1
1	14	- .93	.86	1.2
0	12	- 1.93	3.72	44.6
- 1	3	- 2.93	8.58	25.7
- 2	1	- 3.93	15.45	15.5
- 3	1	- 4.93	24.30	24.3
- 4	3	- 5.93	35.12	105.4
- 5	1	- 6.93	48.02	48.0
- 6	1	- 7.93	62.88	62.9
- 7	1	- 8.93	79.75	79.8
-10	1	- 11.93	142.33	142.3
	83			1198.5

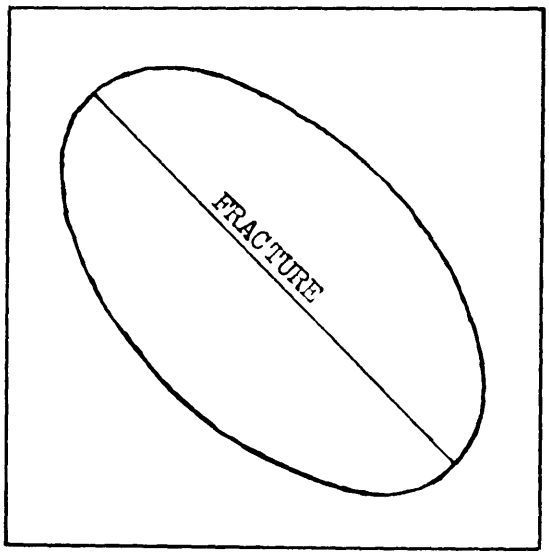
Average opening width (1/1000 ths) = 1.93

If the formation were under a slight horizontal stress at the time it was cored, the originally round core would rebound to an elliptical cross section after coring. Figure 24 at the top shows in plan a strained block of rock into which a circular core is cut. When the core is examined at the surface, it will be free from the differential stress to which it was subjected at depth and part or all of the rock's strain will be relieved. Some of the original strain in the formation at depth might be due to creep and thus would not recover on release of stress. Regardless of the amount of creep there will always be some recoverable strain in the rock if it is under stress. The magnitude of the recoverable strain is dependent on the stress and on Young's modulus for the rock under existing conditions. The diagram at the bottom of Figure 24 shows the shape of the core after release of stress.

From a knowledge of Young's modulus, E, and the deformation of the core found above it is possible to determine the magnitude of the differential stress. Unlike metals, the modulus of elasticity, E, of most rocks is dependent on stress to a considerable degree. Physical tests on the Spraberry are presented in Chapter V and the relation of E to stress is shown on Figure 35. If it is assumed that the average horizontal compressive stress is 1500 p.s.i. as determined from Hydrafrac data (Figure 10) the value of E



CORE CUT INTO FORMATION WHICH IS UNDER
A DIFFERENTIAL HORIZONTAL STRESS



UNSTRESSED CORE UNDER SURFACE CONDITIONS
WOULD NO LONGER BE ROUND.

EFFECT OF STRESS ON APPARENT FRACTURE OPENING

FIGURE 24

is found to be 1.2×10^6 p.s.i. The stress required to give a distortion of 0.00193 inches in a 3 1/2 inch core can now be found.

Stress = $1.2 \times 10^6 \times 0.00193/3.5 = 605$ p.s.i.

This means that one horizontal axis would have to have a compressive stress of 605 pounds per square inch more than the other horizontal axis.

The stress obtained above is the minimum stress to cause the deformation and assumes that the direction of incipient fracturing is parallel to the short diagonal of the parallelogram shown at the top of Figure 24. Other orientations would require a greater stress to produce the difference in length of the diamters along axes oriented with the fractures. In such cases the maximum differences would be found by measuring diameters along two mutually perpendicular axes at some intermediate angle with the fracture direction. The maximum differences on the cores tested seemed to be in the directions in which the recorded measurements were made.

The validity of this stress theory could be checked by measuring various diameters on unfractured cores. Unfortunately this could not be done with the cores available since all of the whole cores had been tested in the pressure vessel (see below) before these measurements were made.

B. CALCULATION OF LATERAL EXTENT

The lateral extent of fracturing was estimated in Chapter II by means of volume of gel used in completion. The result was found to be in the neighborhood of 1300 feet if the fracture was considered to extend in both directions with no loss of fluid into the matrix or intersecting fractures. This problem can be approached from the standpoint of fluid flow during production. The hydraulic equation for laminar flow between two parallel plates as adapted from Taylor (1948, p. 107) is

$$Q = 1/12 \; x(w^3/u)x \; i$$

where

Q = flow in cc/sec. for 1 cm height of fracture

w = width of fracture in cm.

u = viscosity of oil in poises

i = hydraulic gradient along fracture in degrees/cm^2 per cm. of length.

For this calculation a large flow per foot of producing horizon will be chosen. After Strata-frac treatments a well in the Driver field tested 795 B.O.P.D. from a 35 foot section of perforated casing (Moore and McCormick, 1951, p. 104). The width of the fracture is known to be 0.020 inches due to the separation maintained by the sand injected with the Strata-frac gel. The viscosity of oil in the Upper Spraberry averages about 0.70 centipoise (Brack, 1951). The hydraulic

gradient will be determined to learn how far the oil must travel to drop 500 p.s.i.g.

After converting to the proper units the following values are found,

Q = 1.37 cc/cm per 1 cm. height of fracture

w = 0.051 cm.

u = 0.007 poises.

The head loss for this flow along the fracture is computed to be 864 dynes per square centimeter per centimeter of length. The presence of sand grains in the fracture would increase the loss of head by a factor of about 5. The effective area available for flow if the grains were arranged on a checkerboard pattern would be about half that of the open channel so that the given flow, Q, would have to travel at double the velocity and, with laminar flow, would suffer twice the loss of head. Also under these conditions the wetted perimeter of the area of travel would be about twice as great so that the friction and head loss from this would increase by a factor of two. This means that the total head loss would be 3456 dynes/cm^2/cm. This is equivalent to a loss of 500 p.s.i.g. in 327 feet. Since oil is entering the fracture along its entire length, the maximum loss of head used in the computation would occur only close to the well bore, meaning that the actual loss of head would be less and the fracture length probably greater. The choice of 500 p.s.i.g. as the loss of head within the fracture

during the potential test was arbitrary, but it gives some idea at least of the extent of the fracture.

There is visible evidence also that single fractures can extend for 90 feet (Bartley, 1951, a). Well core photographs showing the complete cores of one of the wells from which the writer selected residue cores also showed individual fractures extending for many tens of feet.

The lower value for the lateral extent of the fractures is probably more nearly correct than the value of about 1300 feet found in Chapter II from the displacement of the gel treatment. The low loss of head of the gel in the fracture, as indicated by the very small increase of pressure during injection (see Figure 10), indicates that the fracture is probably open several times as wide as the sand diameter during injection. Cement lost during the cementing of casing has been found in cores below the bottom of the casing in fractures. In some cases the fractures were found to be separated by as much as 1/4 inch of cement. Thus if the fracture is opened several times wider than the diameter of injected sand with the gel, then the length of the fracture opened by 3000 gallons of gel must be several times less than calculated.

3. DISCUSSION OF FRACTURE FORMATION

The first section of this chapter indicated that the core fractures occurred along planes of weakness existing in the formation in its natural state. The second section discussed reasons for believing that the fractures were closed even if present. There is reason to believe that the drill is not caused to follow a pre-existing fracture or plane of weakness since fractures have been observed crossing the axes of cores at varying angles. In some cases this angle is quite small and the deviation necessary for the drill or core bit to follow the fracture would be small. The fractures which cross the core axes do not generally extend for great distances but terminate in a bedding plane break at the end of the core piece, with the fracture in the adjoining piece starting nearer the core axis. Sometimes the fracture curves abruptly and passes out through the side of the core (see Plate 12). This would seem to indicate a break not controlled by the incipient fractures.

The evidence presented shows that most of the fractures are not open in the ground. The question then arises as to the forces producing them in the cores. The drilling alone does not provide an adequate answer. Torsion along the length of a core would be more likely to cause bedding plane failures rather than to open vertical fractures.

Torsion failure of bars of brittle homogeneous material can theoretically cause a fracture pattern consisting of a plane radial surface extending from the bar's axis and an adjoining helical surface. (Whitehead, 1952) Since the Spraberry formation is not homogeneous even horizontally, it is felt that the breaks in the formation are not due to torque produced during drilling. Several small pieces of Spraberry core were subjected to torsion. The finely laminated samples broke along bedding planes while more massive samples gave an irregular break. The fractures found in cores are equally well developed in the finely laminated sections and in the more massive sections of siltstone. The core is generally enough smaller than the inside of the core barrel so that there will not be much friction developed to produce a torque. Moreover, it would be very remarkable for all types of coring bits to form equally well-developed fractures.

The release of pressure during and after coring is the next cause of fracturing to be examined. This must be studied both from the standpoints of release of rock pressure and of release of pore pressure. The stresses presently acting on the rock mass are not enough to cause failure of the rock in any direction, either vertical or horizontal. This is true regardless of whether the horizontal stresses (discussed above) and the vertical stresses acted alone or together. This is discussed quantitatively in the next

section of this chapter. In addition any strains or stresses developed on release of these presently acting stresses would act throughout the whole body of the rock and would not act preferentially to cause fractures at the core centers.

On the other hand, it is possible for a release of pore pressure to cause a maximum stress at the center of the core. In the formation the pore spaces are filled with liquid and gas under high pressure. As the core is withdrawn from the well the reduction of pressure causes some of the oil and gas to ooze or "bleed" from the core. The pore spaces near the sides of the core will drop in pressure quite rapidly while those near the center will remain longer near reservoir pressure. This causes the central part of the rock mass to be subjected to an intergranular tension which is a maximum at the core's center. In order to test this it was decided to re-pressurize cores in a pressure vessel and then release the pressure quickly. This work is described in the next section.

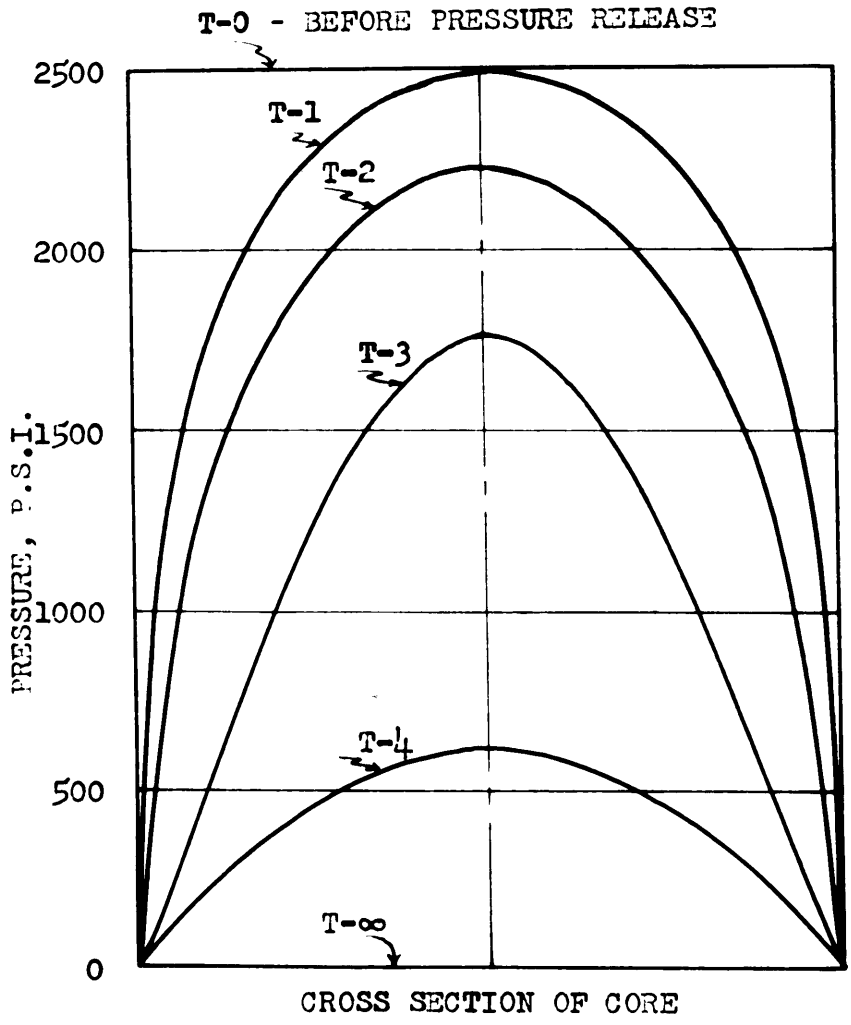
4. PRESSURE VESSEL WORK

A. GENERAL THEORY

In the reservoir the total weight of overburden is supported not only by the solid framework of grains in the rock but also by the pore fluids which are under pressure.

If the overburden amounts to 8000 p.s.i. and the pore pressure is 2000 p.s.i., then the grains carry 6000 pounds of load over each square inch. This is true even though the pore space may be only a few percent. This can be explained by considering an essentially horizontal surface in the formation which undulates so as to pass between grain contacts and not transect any grains. The actual contact areas of the grains are very small and represent a negligible portion of this surface's area. It is evident that the force of the fluid on one square inch of this surface is equal to the fluid pressure and that the intergranular force acting on the small grain contacts would increase if the fluid pressure were to decrease.

If a core is suddenly removed from the formation the applied intergranular pressure drops to zero at once while the pore pressure continues to act. This effectively causes an intergranular tension. Another viewpoint, using the example above, is to consider that relief of the 8000 p.s.i. of overburden which is supported by 2000 p.s.i.g. of fluid and 6000 p.s.i. effectively by the grains causes no change in the pore pressure but only in the intergranular force. The pore pressure cannot change rapidly in a tight formation like the Spraberry. The gas and oil under pressure must escape to a considerable extent to cause a pressure change, particularly when there are large amounts of gas. Thus the



CHANGE OF PRESSURE DISTRIBUTION WITH TIME

FIGURE 25

counter action to the relief of 8000 p.s.i. takes place entirely in the intergranular forces which change from a 6000 p.s.i. compression to a 2000 p.s.i. tension.

If all external forces acting on the core, including fluid pressure, were removed suddenly as in the example above, the intergranular tension would instantly act throughout the whole mass of the core. After some time the pressure would drop near the side of the core and be a maximum at the center (see Figure 25). In actual practice the intergranular pressure is removed before the pore fluid can effect an intergranular tension. After the core has been cut the fluids at the bottom of the well still act to maintain the pore pressure. During the time the cores are raised from the bottom of the well the pore fluids start to cause an intergranular tension and also start to drain near the sides. Thus the maximum pressure acts only in the center as shown on Figure 25. The maximum intergranular tension also acts only at the center.

Since these tensile stresses are radial no plane fractures would form if there were not planes of weakness. The fracture would be expected to form on the plane of weakness nearest to the center. The formation of this fracture immediately starts a reduction of pressure in the pores near the fracture and new maximums develop in each half core.

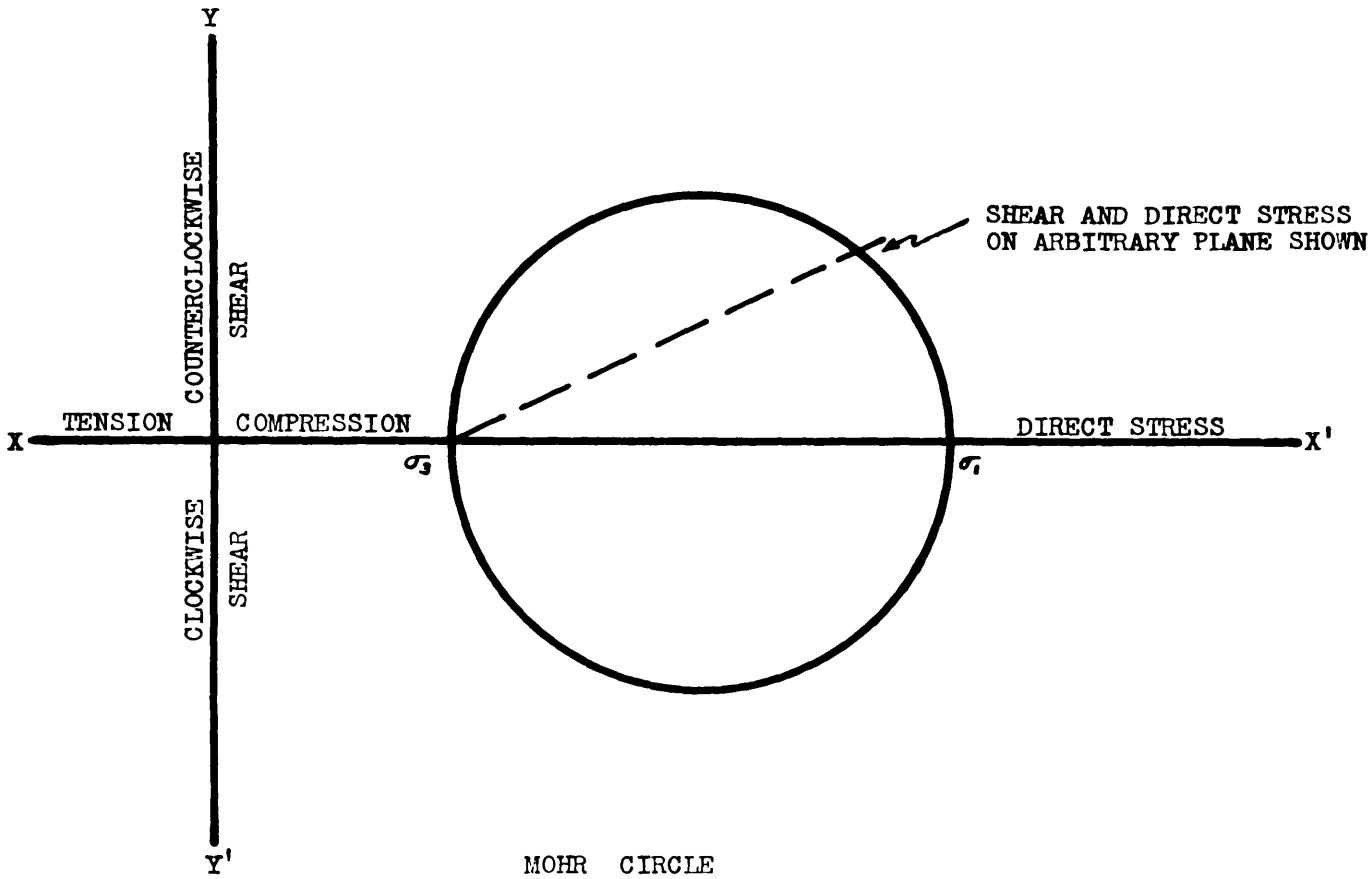
B. ANALYSIS OF STRESSES

The general changes of stress distribution with time are shown on Figure 25 and have been discussed above. It should be pointed out that in an infinitely long core all surfaces of equal pressure, or equipotential surfaces, are cylindrical surfaces which are coaxial with the core axis. In a finite piece of core the equipotential surfaces would form closed surfaces more or less cylindrical with rounded ends. A visualization of the form and changes of form of the equipotential surfaces during release of pore pressure aids in understanding the stresses acting on the rock's intergranular structure.

The presence of a non-radial filled fracture in the core would cause a distortion of the normal cylindrical shape of the equipotential surfaces. There would be a flattening of the surfaces near the fracture on the side nearest the center of the core and successive surfaces would become more closely crowded together. The maximum pressure would occur at some point between the center and the fracture, and the area enclosed by the equipotential surfaces near the maximum would be extended in the direction parallel to the fracture. Such a mechanism could account for fractures in unusual locations. In a similar manner impervious shaly partings parallel to the bedding could distort the normal equipotential surfaces and the stress distribution.

The Mohr Diagram. The Mohr Diagram has not been widely used in the interpretation of geologic phenomena and it is felt that its use would serve to analyze stresses in rocks and calculate failure conditions. Bucher (1921) used the Mohr diagram to explain some aspects of rock failure and explained its use. Because of its use in analyzing the conditions in the pressure vessel and in the reservoir, the use of the Mohr diagram and Mohr envelope will be described here in some detail.

It is possible to analyze the stresses acting on any point in a body under stress. It has been found both experimentally and analytically that the stresses acting on any plane can be resolved into a shearing component and a direct component and that under any system of applied stresses there are always three mutually perpendicular planes on which there is only direct stress (i.e. pure tension or compression) and no shear. These planes are called principal planes. In the most general case the stresses acting on the three planes will all be unequal and the planes are designated major, intermediate, and minor according to the relative magnitudes of the three stresses. The intermediate principal plane contains the lines of action of stresses on the other two planes, which stresses are called major and minor principal stresses. Also any one of the principal planes contains the lines of action of the stresses acting on the other two planes. If on Figure 26 shearing stresses

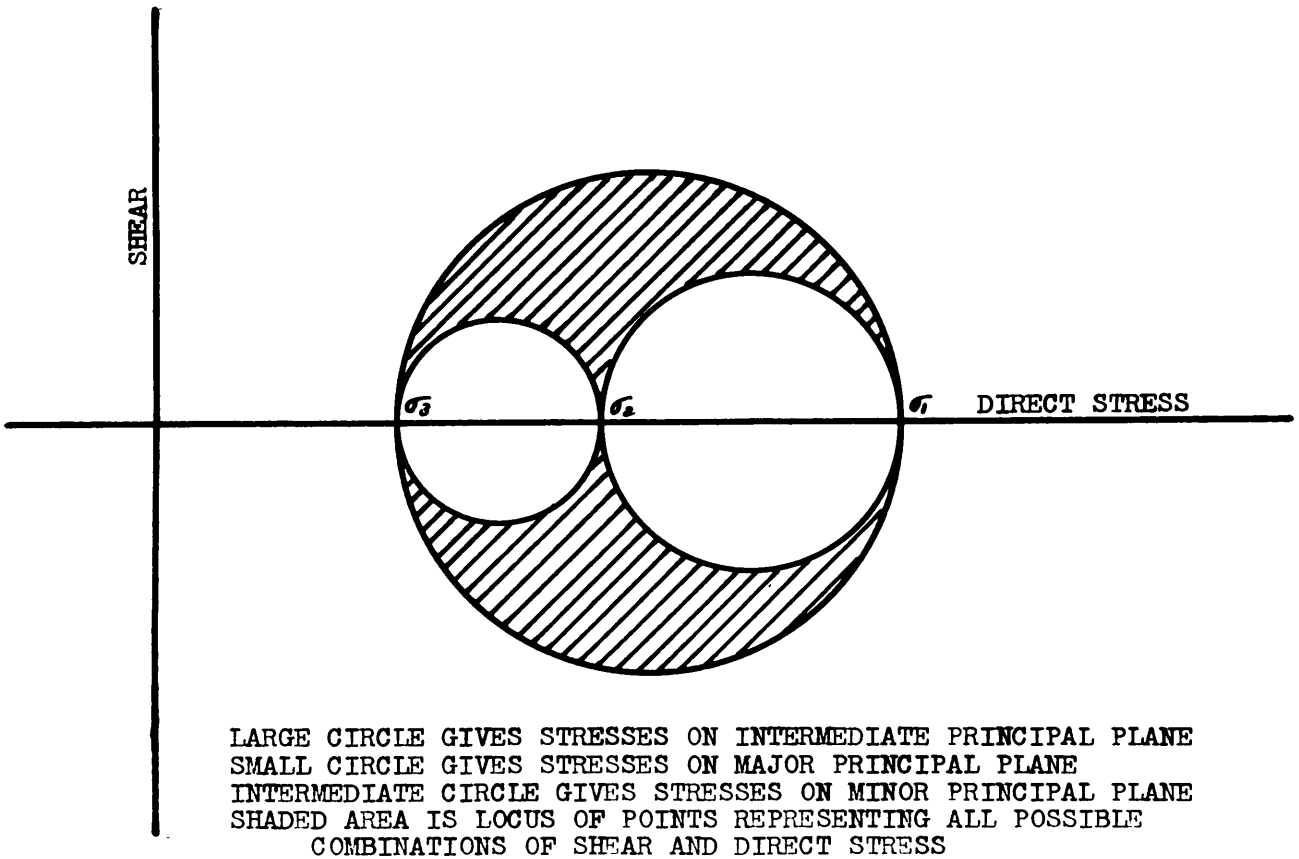


MOHR CIRCLE

FIGURE 26

acting on all planes perpendicular to the drawing are plotted as ordinates and the direct stresses on these planes are plotted as abscissas, the locus of the coordinates of all combinations of direct stress and shear is a circle. The drawing is made in the plane of the major and minor or principal stresses (σ_3 and σ_1, respectively). These are shown plotted on the diagram. The stresses acting on any plane can be found by passing a line parallel to this plane through σ_1 on the "x" axis as shown on the drawing. The intersection of this line with the circle gives the values of shear and direct stress acting on the plane. Lines drawn through σ_1 perpendicular and parallel to the "x" axis represent pure direct stress acting on the minor and major principal planes, respectively, while all intermediate angles indicate some combination of shear and direct stress. In this discussion the positive direction on the "x" axis is used to indicate compression while counterclockwise shear is positive on the "y" axis.

The most useful diagram and the one most generally used is that drawn parallel to the intermediate principal plane as shown by the largest circle of Figure 27. It is instructive to study the stress distribution on the planes perpendicular to the other principal planes. On Figure 27 the smaller circle represents the locus of stresses acting on all possible planes which are perpendicular to the major



LARGE CIRCLE GIVES STRESSES ON INTERMEDIATE PRINCIPAL PLANE
SMALL CIRCLE GIVES STRESSES ON MAJOR PRINCIPAL PLANE
INTERMEDIATE CIRCLE GIVES STRESSES ON MINOR PRINCIPAL PLANE
SHADED AREA IS LOCUS OF POINTS REPRESENTING ALL POSSIBLE COMBINATIONS OF SHEAR AND DIRECT STRESS

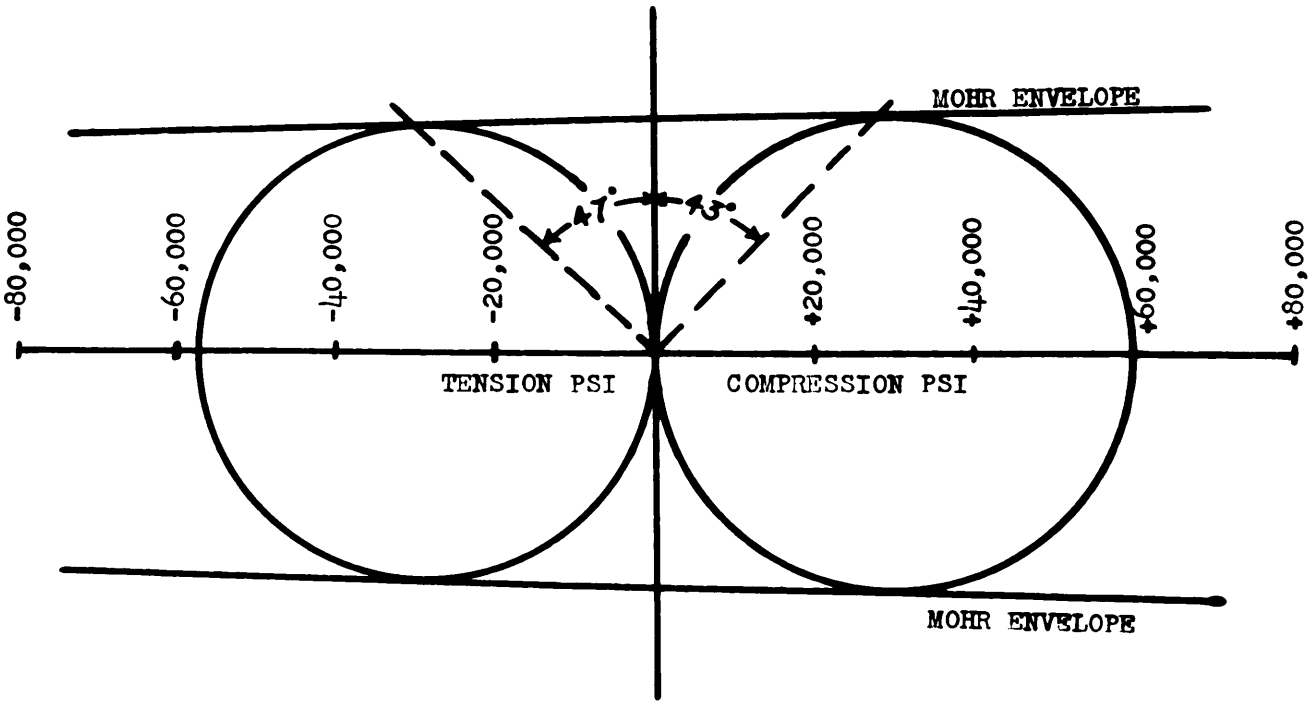
MOHR CIRCLES FOR THE THREE PRINCIPAL PLANES

FIGURE 27

principal plane. The relative sizes of these two circles depends on the value of the intermediate principal stresses.

All stress combinations on planes perpendicular to any of the principal planes lie on the circles. All combinations of stress acting on planes at any angle through a point subjected to the principal stresses shown lie within the shaded area of Figure 27. It should be noted that all possible combinations lie on a single circle if any two principal stresses are equal. If all three are equal the circle becomes a single point.

Considering now only the intermediate principal plane (as in Figure 26), the Mohr circle becomes larger as the difference between the major and minor principal stresses becomes larger. At some point dependent on the characteristics of the material there will be failure by shearing. For any material there can be drawn limiting lines within which can be drawn all possible non-failure circles. These lines are known as the Mohr envelope and are shown for steel in Figure 28. Any circle touching or crossing the envelope represents a failure condition. Actually in any material being subjected to stress it is impossible for the circle to exist outside the envelope and failure occurs when the circle touches the envelope. The failure plane is given by the first point of contact of the circle with the envelope. In the case of steel shown in Figure 28 the failure



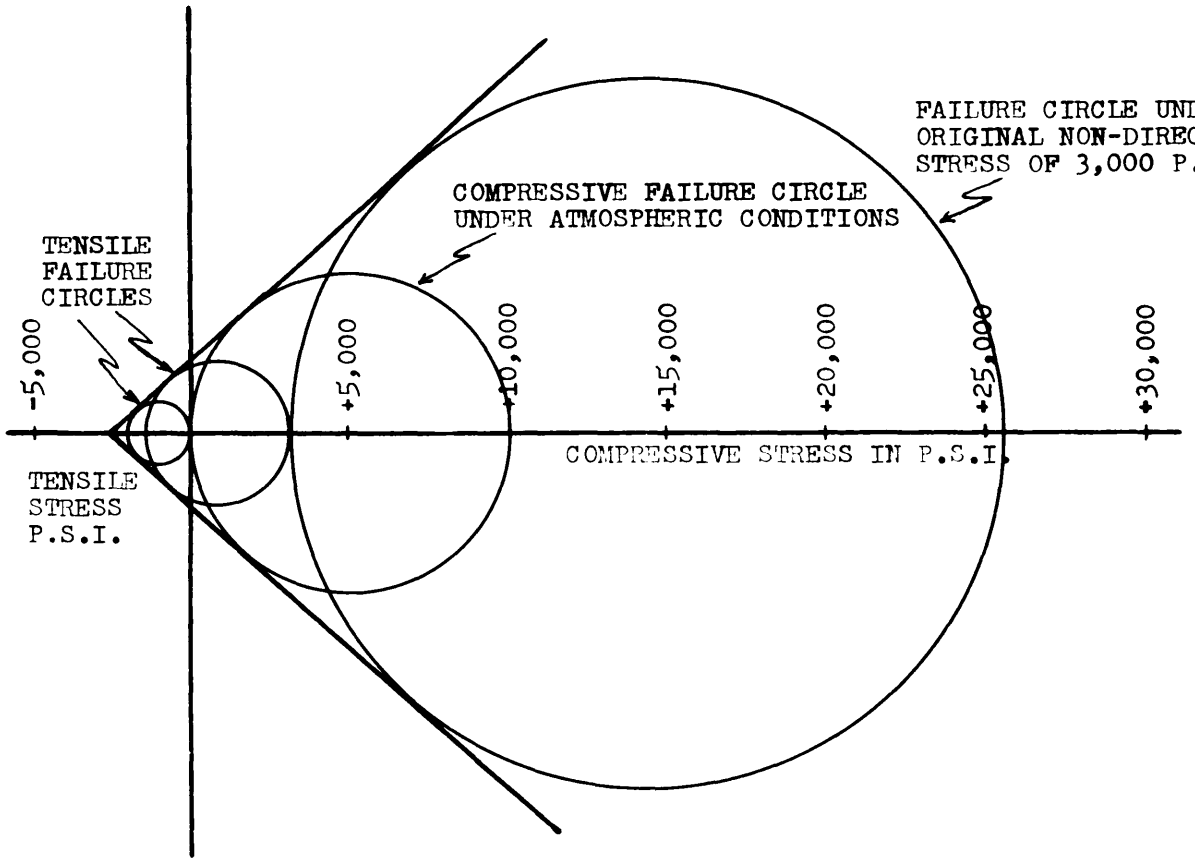
MOHR ENVELOPE AND FAILURE CIRCLES FOR STEEL

FIGURE 28

plane makes an angle of about 47° with the major principal plane or 43° with the major principal stress acting on this plane for a compression failure. Thus a system of two shears would form an acute angle toward the compression. For steel and other ductile materials the direct stress for failure in tension is only slightly less than that for compression.

Most rocks are brittle and fail in tension at a considerably lower direct stress than that required for compression. Figure 29 shows the Mohr envelope for the Spraberry resulting from several tests which are described in Chapter V. The envelope is drawn tangent to the known failure circles for tension and compression. Additional control for the envelope could be obtained only by conducting failure tests with stress on three axes as, for instance by a combination of non-directional pressure and differential stress. Tests of this sort are described for several types of rock by Bucher (1921).

Examination of Figure 29 shows that when the rock is initially subjected to a non-directional pressure, then a much larger differential stress is required in addition on one axis to cause failure than the axial stress required for failure when no pressure acts initially. The diagram shows that when the rock is initially subjected to a non-directional or confining pressure of 3000 p.s.i. the additional axial



MOHR ENVELOPE AND FAILURE CIRCLES FOR UPPER SPRABERRY

FIGURE 29

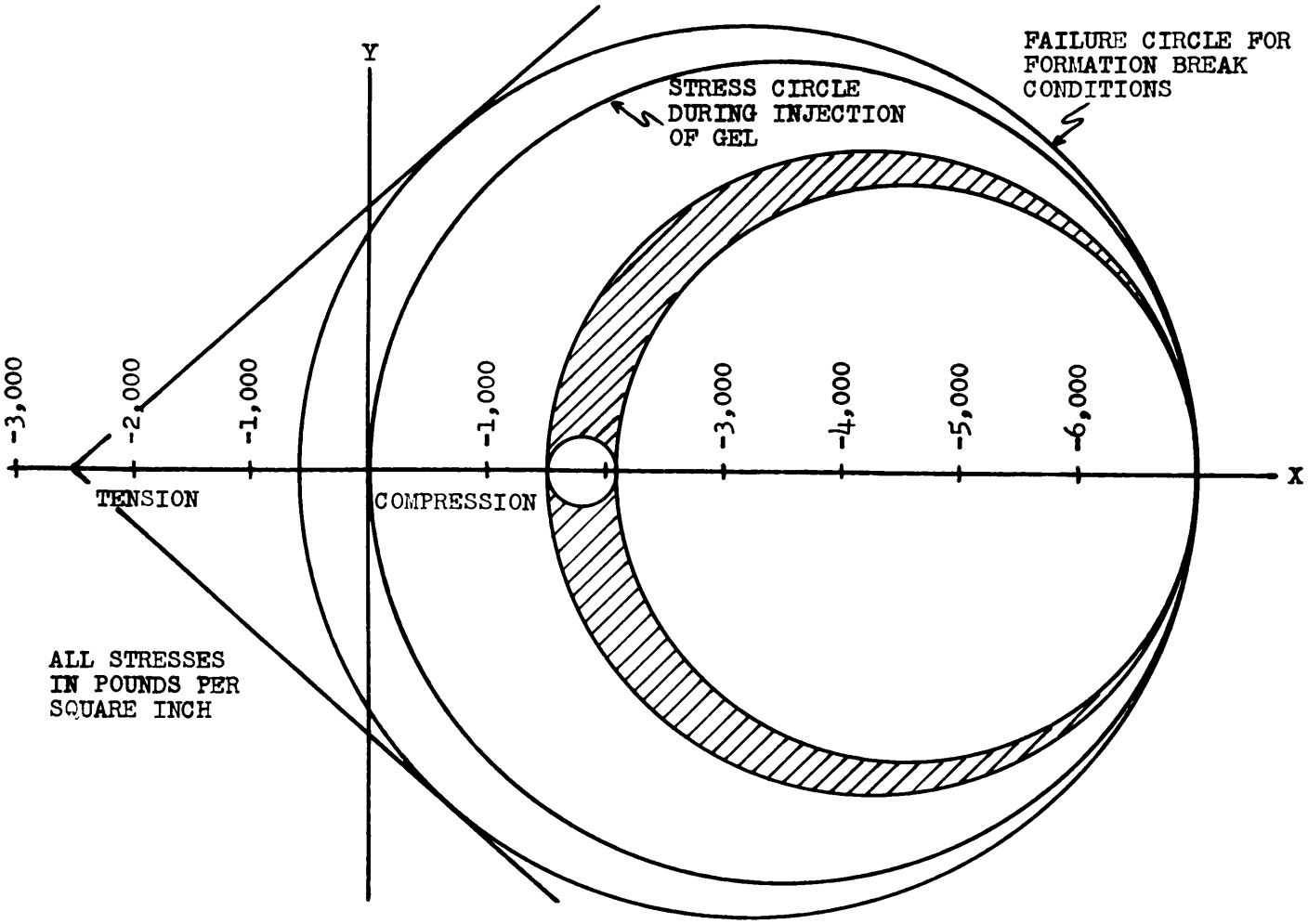
stress required to cause failure by compression is 22,600 p.s.i. instead of the 10,000 p.s.i. which was required with no confining pressure. The total stress on the loaded axis is the differential stress plus the confining pressure, or 25,600 p.s.i. The diagram also shows that a differential stress of 4,200 p.s.i. would be required for a tension break rather than the 2000 p.s.i. required under room conditions. The net tension on the loaded axis is 1200 p.s.i. It can be seen that for confining pressures greater than 10,000 p.s.i. the net stress during tension failure is actually a compression.

At this point another example may help to demonstrate this phenomenon. Assume that a test bar of pure aluminum breaks under a tension of 9000 p.s.i. under surface conditions. If a second identical test piece is subjected to a hydrostatic pressure of 20,000 p.si.g., as in a pressure vessel, the differential tensile stress required to break it would be a little in excess of 9000 p.s.i.g. The reason for the small increase is that the Mohr envelope for ductile materials is similar in shape to that shown in Figure 28, and there is little increase of ultimate strength with increase of confining pressure. However, under these conditions the test specimen would not separate into two pieces at the break because a net compression of 11,000 p.s.i. would still be holding the pieces together.

It should be remembered that the Mohr envelope is a characteristic of the rock while the Mohr circles are dependent on the imposed conditions of stress. The actual conditions existing in the Spraberry at the present time may be somewhat as indicated in Figure 30. The major principal stress is that due to overburden and equals about 7000 p.s.i. The minor and intermediate principal stresses act horizontally and equal about 1500 and 2100 p.s.i. respectively. The reasoning on which the 600 p.s.i. difference is based has been set forth in the second section of this chapter. With this stress condition the additional stress required to cause fracturing would be between 2200 and 2800 p.s.i. while the stress required to relieve net compression for the purpose of opening a fracture would lie between 1500 and 2100 p.s.i.

If the rock contains incipient vertical planes of weakness, the ultimate tensile strength in one horizontal direction should be different from that in the other. Thus the Mohr envelope would be different on the two axes. The difficulty of cutting good specimens for tests perpendicular to fractures precluded the possibility of investigation along these lines.

On release of pressure in the pressure vessel an intergranular tension develops as explained above. This tensile stress acts almost equally in all directions so that the stress



MOHR DIAGRAM FOR EXISTING CONDITIONS

FIGURE 30

conditions on the diagram are indicated by a point or very small circle on the tension side of the "x" axis. Thus failure would occur at the point of the envelope which can be called the limit of hydrostatic tension. In this connection it should be noted that a condition of incipient failure caused by tension on only one axis should be relieved by tension on the other two axes since this would reduce the size of the Mohr circle.

C. GENERAL DESCRIPTION OF EQUIPMENT

Full details of the design and construction of the pressure vessel as well as difficulties encountered during construction and operation are discussed in Appendix B. Also discussed are suggestions for future designs. A brief description will be given here of only those details pertinent to an understanding of the test conditions. The vessel itself is steel and weighs about 486 pounds and has a pressurized space 4.890 inches in diameter and 35 1/2 inches in length. The design pressure is 5000 p.s.i.g. and the vessel has been used up to pressures of 5000 p.s.i.g. Pressures up to about 2200 p.s.i.g. are obtained from a cylinder of nitrogen and can be applied quite rapidly. Pressures above this are obtained by means of a small booster which requires about a half hour to get the vessel up to 4000 p.s.i.g. and about twice as long to get to

5000 p.s.i.g. High pressure valves are provided to release the pressure at the end of a test. The problem of finding an ideal gasket or gasket cement has not been completely solved, and trouble from this source often necessitated several trials before achieving a successful run.

The size of the vessel allows several core samples to be tested at one time increasing the efficiency of the tests for which no trouble developed. The vessel was provided with an inner liner so that fluids could be used which would normally dissolve the gasket cement.

D. CHOICE OF PORE FLUIDS

The first tests were tried using water but were not successful. The water used was fresh and probably caused a swelling of clay minerals with the result that very little of the water could have entered the pore space of the rock. In order to achieve the desired results the applied hydrostatic pressure must act throughout the pore space of the rock matrix leaving the intergranular structure unstressed. If the fluid cannot flow into the core there will be a compression on the rock structure which will merely be relieved when the pressure in the vessel is released.

Even if salt water were used the experiments might not be successful. Based on the lowest permeability of the cores, the pore pressure at the center of the core should reach 99% of the hydrostatic pressure applied to the vessel in

about ten minutes. However, because of the fact that the cores originally contained oil which may have become viscous during storage of the cores, the actual time for the inflow of salt water might have been many times longer. This situation would be aggravated by the concentration of oil in the outer part of the core by the "bleeding" and evaporation of water shortly after coring. This could effectively form an impervious layer near the surface and prevent passage of water to the interior.

The next fluid tested and the one finally selected as the best was kerosine. Since the molecular polarization with kerosine would be very small, it was felt that there would be no trouble with swelling of clay minerals. Also it was felt that kerosine could soften any hardened or tarry hydrocarbons. Some success was obtained using kerosine when the pressures were maintained for a considerable length of time before pressure release.

Since the viscosity of acetone is about 1/3 that of kerosine and its ability to dissolve the hardened hydrocarbons should be much better it was decided to make a test run using this fluid. The run was not successful because acetone escaped from around the flexible diaphragm of the liner and mixed with the small volume of water in the space between the liner and the vessel wall. This dissolved the gasket cement and caused a leak. The same trouble developed

even more quickly on a second attempt. However, in each case the pressure was maintained long enough so that if the acetone had been markedly superior to kerosine there should have been some positive results.

An attempt was made to clean the cores with acetone prior to the test in the pressure vessel using kerosine. It was thought that the acetone could be made to flow through the core by applying a partial vacuum to one end of the core. The problem of sealing a gasket to the core so that acetone would not flow directly past the gasket and into the evacuated space was solved for a time by cementing a rubber membrane to the sides of the core. A partial vacuum of 13 to 14 p.s.i.g. was maintained by means of a hydroaspirator. The flow of acetone could be measured in drops per day for a six inch core and there was no assurance that even this was not leaking along the membrane. A major leak occurred because the acetone dissolved the cement before the test had progressed for a sufficient time.

Next a 1/4 inch hole 2 inches long was drilled toward the center of a 6 inch long core along the axis. A piece of 1/4 inch copper tubing was cemented into the hole using litharge and glycerin. To be sure that the cementing mixture had not plugged the tube or rock pores an 1/8 inch steel rod was used to extend the hole about 2 inches further into the rock past the end of the copper casing. The whole core

was immersed in acetone and the partial vacuum applied to the end of the copper tube through an intermediate collecting vessel. The flow was very slow at first and amounted to only about 12 cc. per day. This was determined by measuring the interval between the drops which dropped into the collecting bottle. No direct measure of volume was possible because of the rapid evaporation of the acetone. Using the value of flow given above and the equation for radial permeability given by Pierson (1950, p. 56), the value of permeability is found to be less than 0.01 microdarcys or 0.00001 millidarcys. While some of the conditions of the experiment do not exactly fit those for which the equation was set up, the value of permeability found is still in the right order of magnitude and indicates that the flow of acetone was impeded by heavier hydrocarbons. After this cleaning operation had continued almost continuously for a week the flow was about 25 times greater, and a deposit of dark hydrocarbons was found in the collecting vessel. No further cores were cleaned in this way because of the effect of the hole on the operation and results of the pressure vessel. The cores were placed directly into the pressure vessel with kerosine for a pore fluid.

E. TIME REQUIRED FOR TEST

Calculations of the time required for the fluid pressure to act throughout the core are very difficult to make. As stated above, the time should be only a few minutes based on permeabilities determined on sealed cores by the Sunray technicians. The results found by means of the flow of acetone would indicate a time of about 16 hours to reach 99% of the vessel pressure. Since the kerosine cannot dissolve the existing oils as well as the acetone the time required might be even longer.

To check the penetration of the kerosine several cores were cut and examined. In such a fine grained material it was difficult to be sure of kerosine penetration near the center especially since the residual oil and gas, and the air in the outer pores would all be pushed to the center ahead of the kerosine. It seemed that even on some cores on which pressure had been maintained overnight, the kerosine did not penetrate adequately.

There is a good method to test the average pore pressure of the core while in the vessel which will be outlined here for possible use on future tests. The method could not be used during the present tests because of the time and expense which would have been required. When the fluid pressure is first applied to any core, the core will suffer a volume decrease because of the intergranular compressive

stresses developed. As the fluid flows into the pores and the fluid comes to act on all sides of all the grains this intergranular stress reduces gradually to zero. If an electrical strain gage such as the Baldwin SR-4 gages were cemented to the rock and connected to indicators outside the vessel, the strain associated with the stress could be observed. Such strain gages cemented to the rock in three mutually perpendicular directions could give information about the physical properties of the rock such as the bulk modulus.

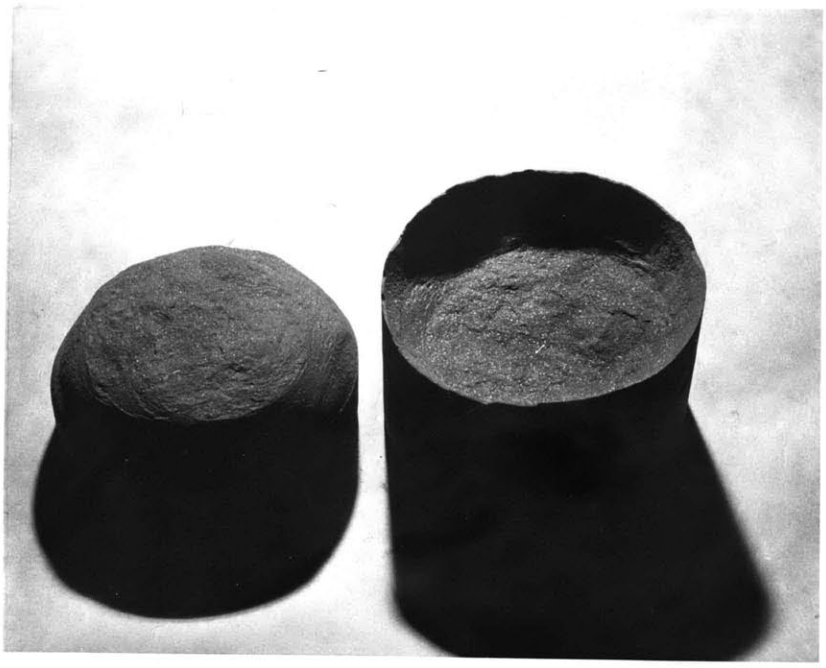
F. RESULTS

Fourteen pieces of whole core were tested in the pressure vessel and nineteen pieces of half core or fractured core were tested. Three specimens broke along bedding planes and exhibited no other fractures. The summary of those cores in which fractures developed is given below.

Whole cores.

1) Complete longitudinal fracture in core 4" long with the fracture about 1/16" from core center. This is the only core which had complete fractures almost identical to those which come from the core barrel already fractured. Fracture from release of 1800 p.s.i.g. after about two days.

2) Complete longitudinal fracture in core about 12" long with the fracture about 1/2" from the core center.





UNUSUAL FRACTURES FROM PRESSURE VESSEL

PLATE 14

In this case the fracture was more irregular than usual. Pressure released from 2250 p.s.i.g. after 15 hours.

3) Break parallel to bedding but turning upward toward the edge of the core to form a radially symmetrical "cup and cone" type of break. (See Plate 14) Pressure released from 2250 p.s.i.g. after 15 hours.

4) Two planar breaks forming an acute angle bisected by the core axis. The traces of these planes on the end of the core were parallel. Pressure released from 2250 after one day. (See Plate 14)

5) Two partial or incomplete fractures close to the core axis and intersecting each other at about 80°. Each partial fracture passed out through the sides of the core but at points separated by about 3 inches. This core was 14inches long. These partial fractures might have been overlooked if the vessel had not been opened quickly after the test since the fractures could be seen only by a slight flow of kerosine out of the fracture after the whole core had been cleaned in acetone. The fractures were almost invisible after the whole core had dried. Pressure release from 4700 p.s.i.g. after 3 hours. The specimen had been released from 4500 p.s.i.g. after 5 hours on the previous day but the vessel was not opened for examination.

6) One whole core showed bedding plane failure in three places on release of pressure from 2250 p.s.i.g.

This sample was finely laminated and would probably have separated along the shaly partings at a much lower pressure.

Previously Fractured Cores. Of the half cores tested only 4 showed any change, two by incomplete longitudinal fractures and two by separation along bedding planes. The longitudinal fractures were not complete but were quite easy to see. They were both about 3/4 of an inch from the existing fracture to which they were generally parallel, but one was slightly curved with the concave side away from the previously existing center fracture.

All of the cores were tested at the lower pressure in the neighborhood of 2200 p.s.i.g. Those which showed no change were subjected to release of pressure from 4500 p.s.i.g. or higher. In some cases tests were made at intermediate pressures because of leaks at the gaskets which could be stopped at the intermediate pressure but would not allow the full pressure. It is to be noted that only two samples showed any change at the higher pressure after being subjected to the lower pressure release. One of these was a bedding plane failure in a half core while the other was the 14 inch core with two incomplete fractures.

There may have been more incomplete or partial fractures which were missed because the vessel was not opened quickly enough after the release of pressure. The time required for one man to dismantle the vessel and remove the

cores is almost an hour. Two or three assistants can reduce the time to about ten minutes. On the one occasion when the vessel was opened rapidly a faintly bleeding fracture was found. This core was subjected to the release of 4600 p.s.i g. again to try to complete the two fractures but with no success. On removal from the pressure vessel after being cleaned in acetone the core was examined in ultraviolet light to learn whether the fractures could be seen more clearly by means of the fluorescence of the exuding kerosine, but they could not because of the general presence of other hydrocarbons not cleaned off and the extreme thinness of the film of kerosine near the fractures.

There was one thin section which happened to have been made across the place where a partial fracture developed later, but no sign of fracturing nor of any lineation parallel to the fracture could be found.

G. CONCLUSIONS

The fact that even a few fairly smooth fractures could be produced attests the presence of a preferred direction of weakness in the rock. The cup and core type break seems to indicate a break in a core free from any such characteristic. The cone intersects the side of the core at an angle less than 45° indicating either axial compression or radial tension. Since the former is impossible under the given conditions, the latter, as would be expected, is the stress

condition at failure. The two shears indicate tension which is greater along one radial direction than at right angles. This difference need not be great; in fact it is a wonder that the stresses and material could ever be uniform enough to give the cup and cone break.

5. ORIENTATION OF FRACTURES

A. MAGNETIC CORE ORIENTATION

Theory. Any particle which possesses a residual magnetism when it is deposited in quiet water will be acted upon during sedimentation by the earth's magnetic field. The tendency is to align the magnetic poles of the particles with the earth's field. Since fine particles are generally deposited in quieter water than coarse particles, and because they are longer in suspension, there is more likelihood of their having a good magnetic alignment. On this basis the Spraberry sediments should show good polarity.

The direction of preferred orientation depends on the direction of the earth's field at the locality and the particular time. Historic records show that the direction of the magnetic field can change as much as 35° in 400 years. If sedimentation were sufficiently slow as in the shaly parts of the formation a single test sample might

include one or more cycles of variation of the earth's field and a sort of mean value would result. It has been estimated that siltstone deposition may be a foot in perhaps 60 or 70 years (Pettijohn, 1949, p. 474). Thus the orientations from a 4 inch length of core from the siltstone could differ from the average by almost 20° on the basis of shift of earth's field alone.

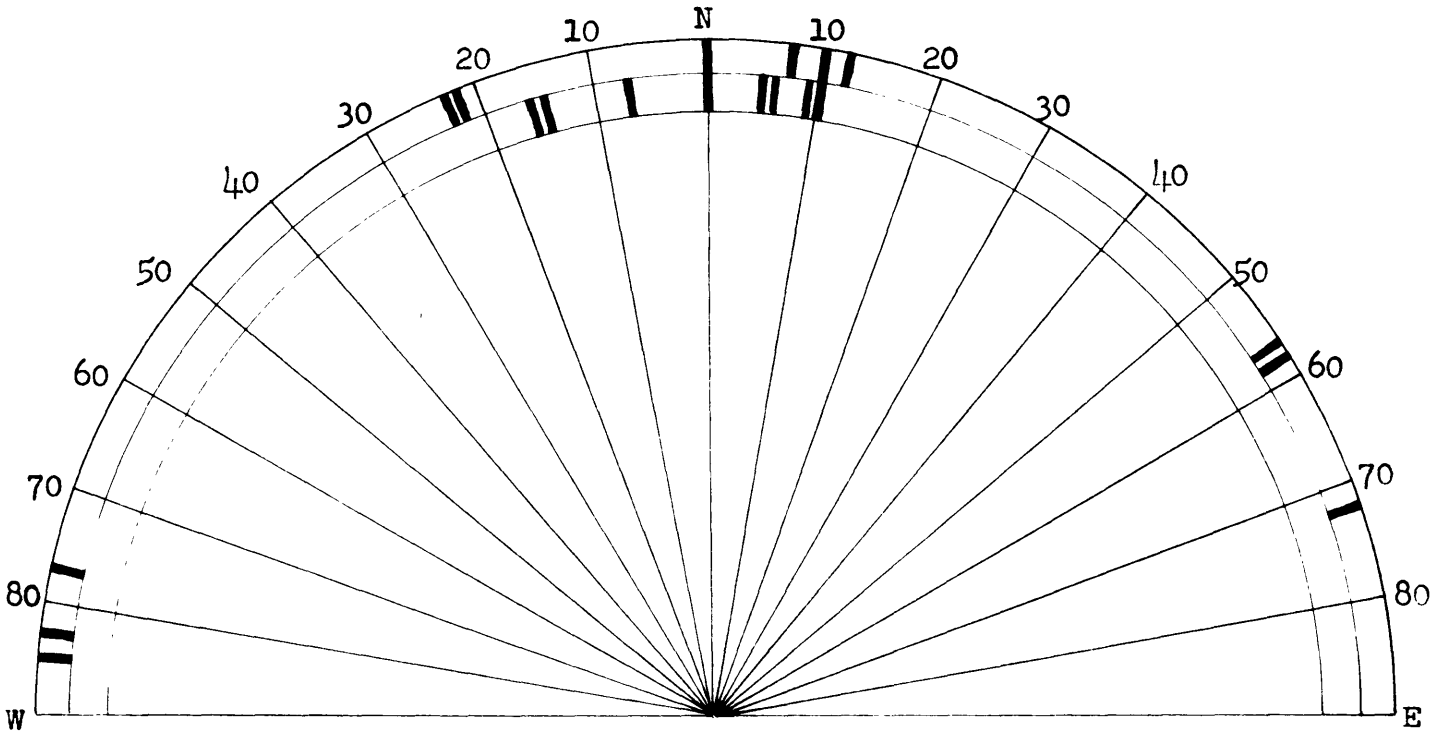
Elongated grains have a tendency to become aligned parallel to the depositing current. Thus the final resting place of a grain may well depend on the vectoral sum of the forces due to current and those due to magnetic effect. It is conceivable that constant conditions over a long period could give a polarity not aligned with the earth's field. In an extreme case large elongated grains with magnetic poles near the ends could develop a sediment with a strong polarity aligned only with the current direction.

Lengths of cores from 3 to 4 inches are generally used for magnetic orientations. A fracture in a core makes no difference but both halves of the core must be used. In one type of equipment the core is rotated close to a special electronic tube so that the core's magnetic field can deflect an electron beam in the tube. The magnitude and direction of the deflection of the electron beam is recorded automatically with respect to the fracture direction or other reference mark on the core. The whole equipment is shielded heavily against the influence of the earth's magnetic field (California Research Corporation, 1952).

Results. The results of determinations of fracture direction from magnetic core analysis were obtained from Sohio and Sunray for 20 tests. Four of these were made on each of the two most northwesterly Sunray wells while 12 were made on the Sohio well indicated on the map (Figure 2). Figure 31 shows the results of these tests with the orientations from the Sohio well plotted on the outer circle. The results from the two Sunray wells are plotted together since these two wells are quite close together. Since it is believed that the fractures are similar in origin to joints, it could be expected that the fractures would show uniform direction over considerable distances (Parker, 1942). There is a concentration of fractures around the magnetic north. This magnetic north is, of course, not the present one but that of the section of core used for each separate test. The corrected fracture direction is about north northeast- south southwest. The general opinion seems to be that the main set of fractures trends about N 25 E with minor sets at about right angles (Fisk 1952, Wilkinson, 1952).

B. ORIENTATION OF FRACTURES FROM PRODUCTION DATA

During the visit to Midland the writer was given a copy of a map which contoured the Tex Harvey field in terms of potential production of the wells (Skrabanek, 1952). This map outlined areas with wells whose potentials were 600,400, and



OUTER CIRCLE FOR SOHIO WELL INNER CIRCIE FOR SUNRAY WELLS

ORIENTATION OF FRACTURES FROM MAGNETIC POLES OF CORES

FIGURE 31

200 barrels per day. There were many small areas separated from each other which had potentials in the highest category. These areas were generally elliptical in plan with the longest direction generally north or east of north. The areas delineated by lower potentials had a tendency to trend more nearly north-south following the productive trend. Fisk (1951) has also shown this to be true.

The range lines run about N 16 W so that the major fractures make an angle of about 41 degrees with the north-south lines of the coordinate system on which the wells are laid out. Wells which are diagonal from each other and almost parallel to the major fracture system would be expected to influence each other's production. Tests have been made showing that when one well on a lease is shut in for a while, those which are N.N.W. and S.S.E. (i.e. diagonal almost parallel to major fracture pattern) showed increased production. Wells in other directions were almost unaffected (Sohio, 1952).

These data show that a major fracture set exists and trends N.N.W. over wide areas. The magnetic fracture orientations indicate fractures crossing the major set which are not so consistent in direction or so numerous.

6. MECHANICS OF FRACTURE FORMATION

A. EVIDENCE THAT FRACTURES ARE JOINTS

The fractures seen in cores are generally fairly well developed plane surfaces and show no signs of lateral motion. The fracture direction appears to be uniform over wide areas. The characteristics are those of joints. Tension joints are not indicated by the fact that the surfaces are not curved, but in fine grained sediments tension joints may have smooth plane surfaces (Nevin, 1949, p. 150). The joints cut through concretions without apparent change of direction; this would not be expected of tension joints. These joints seem to be perpendicular to the bedding and thus are not exactly vertical (Sohio, 1952). This would indicate formation of fractures before the development of a regional dip to the west.

The fractures have been attributed to other causes than jointing. Gibson (1951) proposed an origin related to a change of volume of the sediments, which "was probably due to a change in the constituent minerals which is a form of metamorphism." The writer has photographs taken of shaly cores which had been washed with gasoline (Atlantic Refining Co., 1952). The drying gasoline showed a fracture pattern on a bedding surface similar to the pattern of mud cracks except that the pattern distorted near the edges to

conform to the circular core. This last feature indicates that these cracks may be due to volume change but are formed after coring. Another photograph showed a core with three longitudinal fractures each making an angle of about 60° with the others. The Mohr diagram for the Spraberry (Figures 29 and 30) shows that a combination of two shears in compression with one tension failure could give such an arrangement. The evidence presented by the uniformity of the fracture system does not support the idea of formation from change of volume.

B. RELATION OF JOINTS IN SURROUNDING AREAS

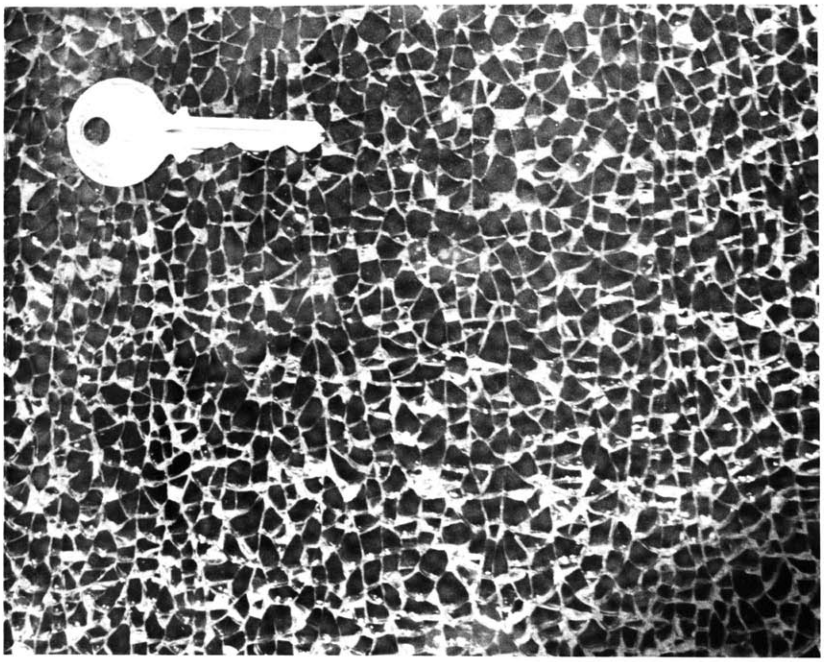
Joint patterns on outcrops on the west have been done by King (1948) in the Delaware Mountains and Carlsbad Caverns. The major joint set in the Delaware Mountains is about N 30 W with the other set at right angles. In the caverns the major set is almost east-west with the other set almost at right angles such that the acute angle is toward the southeast. Both sets are well developed and have nearly equal numbers of joints. On the Eastern Platform major joints trend W.N.W. with a minor set at right angles (Melton, 1934). The overall regional pattern appears to be a gradual swing of the joint system to form a fan-like pattern radiating from the south.

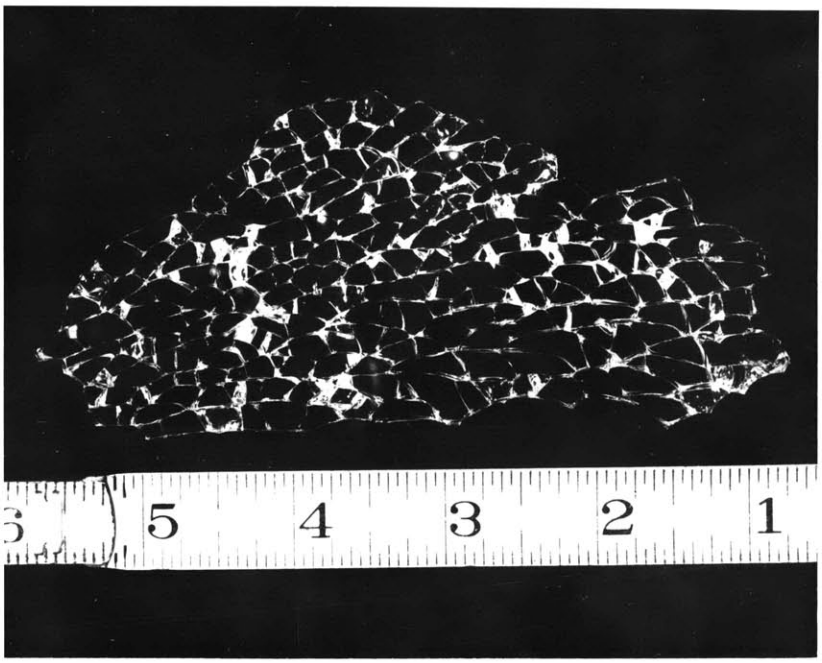
The relation of the joints to other tectonic features is not clear on the basis of this information. The Coahnilla System, which is south of the Marathon System, was being deformed in late Permian time (Eardley, 1951) and is the only apparent source for the uniform compressive stresses acting on the rocks to the north.

C. MECHANICAL REPRODUCTION OF FRACTURES

The writer was able to reproduce a fracture system similar to that believed to exist in the Spraberry. The material used was plate glass about 1/4 inch thick and slightly curved initially. The glass was from an automobile rear window and was not laminated. The fragment used was about 16 inches long and 10 inches wide. The radius of curvature was less across the short dimension. Uniform stresses were applied in two directions by pulling heavy pieces of wood against the edges of the glass. The greatest stress was applied to the long direction, but stress was applied gradually to each axis. The fractures were not all formed exactly simultaneously but developed over several seconds. However, no additional force was applied to the glass once the fracturing started. The results of this are shown on Plate 15.

Wilkinson (1952) showed the writer a diagram showing a theoretical Spraberry fracture pattern. The main fractures





ARTIFICIALLY PRODUCED FRACTURES IN GLASS

PLATE 15

were parallel and continuous and trended N 25° E. The cross fractures were discontinuous and did not cross more than three or four of the major fractures. The fractures shown reproduce these conditions very closely. In the upper photograph of Plate 15 the major pattern is across the length of the key. Some of these fractures extend the whole width of the picture. The cross fractures seldom cross more than one or two of the major fractures. The major fractures are parallel to the long direction of the glass which is also parallel to the axis of greatest curvature. The fracture direction appears to be controlled by the warping rather than by the applied stresses alone. Without the warping the two fracture sets should have formed acute angles toward the major compressive stress. The warping caused failure dependent on each compressive stress and the direction of easiest relief which was upward. The glass was probably under greatest compressive stress along the direction of greatest curvature on the inside of the curve and perhaps a net tension on the outside. The long fractures apparently formed first relieving this stress. The short cross fractures then formed as a result of stress on the other axis. The writer believes that either the whole thickness of glass was under compression before fracturing or that at most only a small part of the top of the curved glass was in tension. If this were not true, the pieces of

glass would have become displaced immediately upon breaking and no further fractures would have occurred. Since the glass was curved upward the pieces remained in place after the fracturing.

The fractures produced by this experiment have a different relation to the applied stresses than what the writer believes to be the actual case for the Spraberry fractures. However, the results point the way to a possible method of producing a fracture pattern in a warped sheet of brittle sediments. Further work along this line might yield quantitative results of value.

CHAPTER V

PHYSICAL TESTS OF SPRABERRY CORES

1. DESIRED INFORMATION

Some of the data contained in this chapter has already been used in the development of ideas and in computations of previous chapters. A knowledge of the physical behavior of the rock under surface conditions can be used to give a fair idea of the rock's behavior at depth. The most exact results would, of course, obtain from tests performed under various confining pressures, but these require quite elaborate equipment.

The breaking strength of the formation in tension and compression was needed to construct the Mohr envelope shown in Figures 29 and 30. The relations of stress and strain were found and used in Chapter IV to determine the stress required to produce the difference of core diameter which was found. From this was found Young's modulus at different applied stresses; this depended on the applied stress to a greater extent than was expected. Poisson's ratio was found and used in Chapter II. Other uses for the physical data are presented later in this chapter.

2. METHODS OF TESTING AND RESULTS

A. SR - 4 GAGES

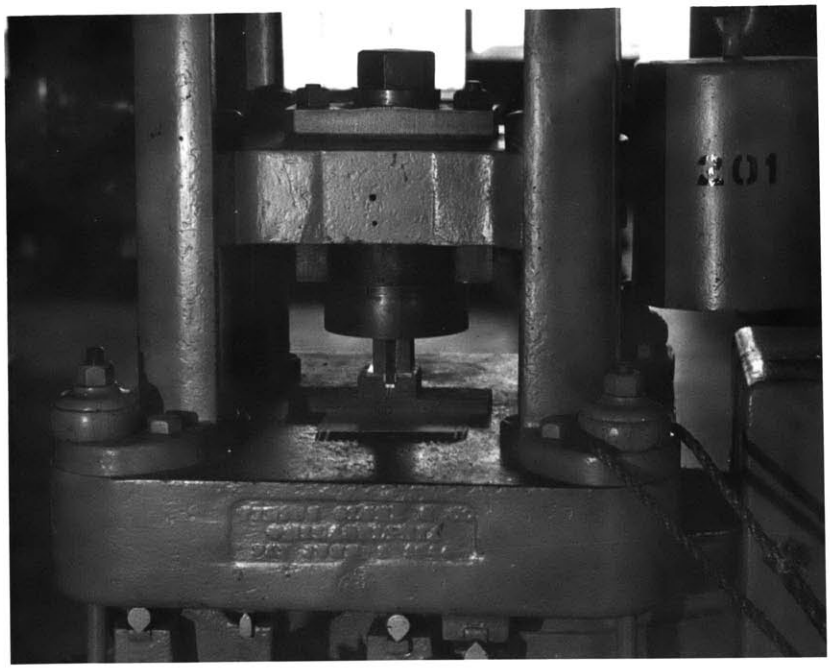
Baldwin SR-4 strain gages are manufactured by the Baldwin-Lima-Hamilton Corporation. There are almost 90 different types of gages for use under different conditions of operation and different limits of strain (Baldwin, 1950). The principle of operation of these gages is quite simple. They consist of a length of wire arranged in various patterns on a special paper backing. The gage is firmly cemented to the material to be tested. Any elongation or compression of the material being tested causes a corresponding change in the length of the gage wire and some change in the wire's diameter. These dimensional changes in the wire cause a change in the wire's electrical resistance which can be measured. The bridge circuit in which the gages are used has provision for connection of a dummy gage to compensate for temperature variations.

The strain gages were used with a Baldwin SR-4 type "L" portable strain indicator which measures strain directly in micro-inches per inch. The gages used in the experiment were Type A-1 which are 13/16 of an inch long and about 3/8 of an inch wide. The small gage size enabled the use of small test specimens. These gages are wired so that the strain measured is in the long direction of the gage, and the strain reading is practically unaffected by strain at right angles.

From a single half of a fractured core were cut three rectangular blocks each about an inch on each side. One gage was attached to each block so as to measure strain in each of three directions, namely, perpendicular to bedding, parallel to bedding and fracture, parallel to bedding and perpendicular to fracture.

The test pieces were each mounted in turn in a compression testing machine so that the strain measurements were parallel to the direction of application of stress. The test pieces were mounted between pieces of soft lead at each end so that no friction would develop between the loading plates and the specimen and to insure a uniform distribution of stress. Plate 16 at the top shows a test specimen in the testing machine.

The results obtained were somewhat erratic. The readings at high stress did not continue the trend of those of lower stress, and for one of the specimens loaded parallel to the bedding the strain readings decreased for an increase in compressive stress and finally passed the initial gage reading and showed tension. These anomalous results are explained by the fact that brittle substances tend to break in tension with breaks parallel to the direction of application of stress. See Plate 16, bottom. The outer elements of the test piece tend to bow outward toward the end of the test like the staves of a barrel. Thus the strain gage was measuring the strain of the extreme outer fiber of the test





USE OF SR-4 GAGES
BROKEN TEST PIECES

PLATE 16

specimen and not that of the rock as a whole. The stress-strain relations at lower stresses checked fairly well with the value of the modulus of elasticity (Young's modulus) found by another method, but these values are not used in a quantitative way nor are they presented here because of the changes of error from the same causes as those producing the very erratic results at higher stresses. The test made perpendicular to the bedding did not show the doubling back mentioned above, but the strain at high stresses dropped off considerably from the trend started by the lower values. This may have been due to a poor bonding of the gage to the specimen.

From a qualitative standpoint the tests showed two things. The modulus of elasticity perpendicular to the bedding was less than that found for the tests perpendicular to the bedding. Also there was no marked difference in the modulus of the two samples loaded parallel to bedding but at different relations to the fracture direction.

B. DESTRUCTIVE TENSION AND COMPRESSION TESTS

Compression. The three specimens used for the tests with the electrical strain gages were later tested to the rupture point along with three other specimens. The results of these compression tests are shown in Table XII. Two tests were made in each direction, but no marked differences appeared

Table XII

Test of Ultimate Compressive Stresses

Piece No. and Load	Dimensions in inches	Test Area Sq. inches	Load Pounds	Stress p.s.i.
1 Perp. to Bedding	L: 1.37 W: 1.28 H: 1.25	1.75	14,000	7,990
5 Perp. to Bedding	L: 1.34 W: 1.25 H: ---	1.67	16,850	10,060
2 Parallel Fracture	L: 1.34 W: 1.25 H: 1.34	1.67	14,000	8,360
6 Parallel Fracture	L: 1.44 W: 1.00 H: 1.33	1.44	17,500	12,150
3 Perp. to Fracture	L: 1.41 W: 1.40 H: 1.28	1.98	18,000	9,130
4 Perp. to Fracture	L: 1.37 W: 1.09 H: 1.25	1.49	12,750	8,550
Average				9,380

in any direction. The average value for the ultimate compressive stress is 9,380 p.s.i. with a computed value of probable error of 438 p.s.i., found by the method described in Chapter II. In all of these tests sheets of soft lead were used to transmit the load to the test specimen to help give a uniform stress distribution. Five of the six test specimens are shown in the photograph at the bottom of Plate 16.

Tension. The tension tests described here were all made parallel to bedding and parallel to the fracture direction. Value for ultimate tensile strength perpendicular to bedding is found by the beam tests of the next section. It was not possible to cut a tension specimen perpendicular to the fracture direction because of the smallness of the half core and limitations on minimum size imposed by the testing machine.

The core samples were cut into the shape of a bone to fit the standard testing machine used for concrete tension tests. The test pieces were roughed out on the lapidary's saw and then filed to a smooth contour by hand. The results of these tests are given in Table XIII.

The average of the four tests as shown on the table is 1544 p.s.i. with a calculated probable error of 134 p.s.i. It should be pointed out that with only 4 samples there is a probability of about 0.3 that the probable error is wrong by 50%. The probability of error in the probable error decreases rapidly with increase of the number of tests.

Table XIII

Test of Ultimate Tensile Stresses

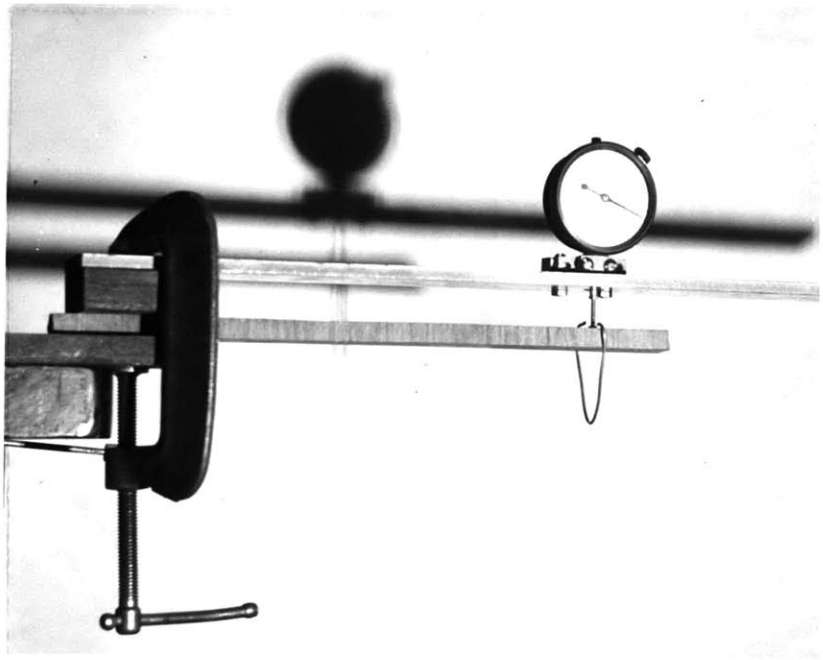
Piece Number	Area at break sq. inches	Load Pounds	Stress p.s.i.
1	0.303	470	1550
2	0.197	295	1497
3	0.383	415	1082
4	0.217	445	2050
	Average		1544

Tension applied parallel to fracture direction in all pieces.

In both tension tests and compression tests it is felt that the maximum readings obtained are probably nearer the best correct value than the average readings. The reason for this is that the slightest flaw or crack in a specimen causes a large concentration of stress. This would cause particular trouble in the tension tests. Since the rock samples used have been considerably disturbed from their natural conditions in the formation, by coring, sawing and filing, there is considerable chance of having small flaws to reduce the rock's ultimate strength. It is known that small scratches or surface imperfections can greatly reduce the strength of a tensile specimen. For these reasons the values chosen for the determination of the Mohr envelope (Figure 29) are 10,000 p.s.i. for tension and 2000 p.s.i. in tension.

C. CANTILEVER TESTS

A section of Upper Spraberry core was cut into the shape of a rectangular prism and then mounted as a cantilever. This was fixed so that deflections could be read as the beam was loaded. The sample was cut with length perpendicular to the bedding which was the only possible orientation. Two tests were made using different lengths of cantilever. The test arrangements are shown on Plate 17.



ARRANGEMENT OF EQUIPMENT FOR CANTILEVER TEST

PLATE 17

The tests were run by placing the weights shown on the beams at the distances shown in each test and noting the deflections in thousandths of an inch. In the first test five runs were made in rapid succession. After the loads were removed the gage did not return to zero. The discrepancy was recorded, and the gage dial then reset to zero. After the fifth test the maximum load was left on to find the change of deflection with time. The data from these tests is shown on Table XIV. After one hour the load was removed, and the rebound from the creep recorded over a period of an hour. Then four more runs were made in the same manner as the first ones.

It is of interest to note that the modulus of elasticity does not change greatly even after a considerable amount of creep. The immediate elastic rebound after the release of load was, in 1/1000ths, 22.0 (49.0 less 27.0) even though the specimen had just finished a creep of 23.6. This value is almost identical to the average deflection for the reapplication of this load after the specimen had recovered for an hour. The second test was run with a shorter cantilever, the successive applications of load being made in rapid sequence. See Table XV.

From this data the modulus of elasticity can be determined by the formula

$$E = Pl^3 / 3 d I$$

Table XIV

First Cantilever Test

Dimensions: Depth 0.383 inches
Width 1.43 inches
Length 8.15 inches

Deflections in inches x 1000. Gage reset each run.

Load, lbs.	1	2	3	4	5	Ave.
0	0	0	0	0	0	0
0.211	5.3	4.7	3.9	4.2	4.5	4.5
0.370	8.2	8.5	8.2	8.3	8.3	8.3
0.610	15.3	14.3	14.3	14.4	14.7	14.6
0.799	20.9	21.4	20.4	20.5	20.2	20.6
0.971	--	27.2	26.0	25.0	25.4	25.9
0	5.0	--	3.0	2.5		

After 5th test load of 0.971 pounds left to note creep. Gage not reset.

Mins.	Defl.	Mins.	Defl.	Mins.	Defl.
0	25.4	25	39.4	50	47.0
5	30.5	30	40.8	55	48.2
10	33.8	35	41.5	60	49.0
15	35.5	40	44.5		
20	37.2	45	46.0		

After one hour the load was removed to note recovery. Gage not reset.

Mins.	Defl.	Mins.	Defl.
0	27.0	5	21.0
2	22.5	50	18.6

Table XIV Continued

Four more tests were run after creep test and one hour for recovery. Gage reset each run.

Load, lbs.	6	7	8	9	Ave.
0	0	0	0	0	0
0.211	4.0	3.9	3.8	3.7	3.8
0.370	7.4	7.4	7.3	7.1	7.3
0.610	12.9	12.6	12.5	12.5	12.6
0.799	17.8	17.4	17.2	17.2	17.4
0.971	23.0	21.6	21.3	21.4	21.8
0	2.0	.7	.4	1.4	

Table XV

Second Cantilever Test

Dimensions: Depth 0.383 inches
Width 1.43 inches
Length 2.55 inches

Dimensions in inches x 1000. Gage reset after each run.

Test No. 1		Test No. 2		Test No. 3	
Load, lbs.	Defl.	Load, lbs	Defl.	Load, lbs.	Defl.
0	0	0	0	0	0
.971	.8	.798	.7	1.2	1.0
1.523	1.3	1.586	1.4	4.78	5.0
2.494	2.2	6.534	7.1	6.81	8.0
3.242	3.1	7.322	8.0	8.15	11.0 (1)
4.213	4.1	8.120	9.6	8.45	15.0 (2)
4.765	4.7				
5.736	6.0				

(1) Rapid creep after this load.

(2) Specimen broke immediately after this reading.

where

E is the modulus of elasticity in p.s.i.

P is the applied load in pounds

l is the length of cantilever in inches

d is the deflection in inches

I is the moment of inertia, m^4 ($I = 1/12\ wd^3$)

Substituting the values indicated the following values of E are obtained.

First cantilever before creep test, average value of 5 runs using maximum load value - 988,000 p.s.i.

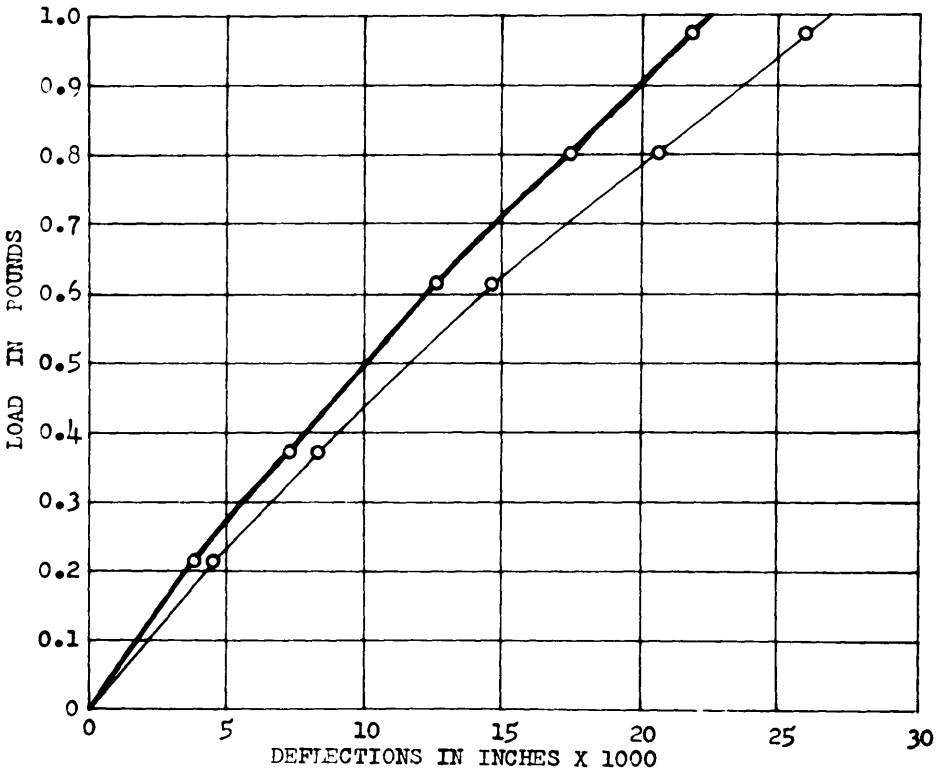
First cantilever after creep test, average value of 4 runs using maximum load value - 1,118,000 p.s.i.

Second cantilever: since the first two runs when plotted follow a single curve, the deflection for an eight pound load was picked from the plot - 710,000 p.s.i.

After the one hour creep the modulus of elasticity increased. It would be interesting to conduct a series of tests over a considerable time to find out the ultimate value. It would also be of interest to measure the values on core samples soon after release from the core barrel and then on the same samples again after a period of time. This could lead to a better understanding of the relations of horizontal to vertical stresses in the formation.

Since E, the modulus of elasticity, is defined as the ratio of stress to strain, it can be seen that the slope of

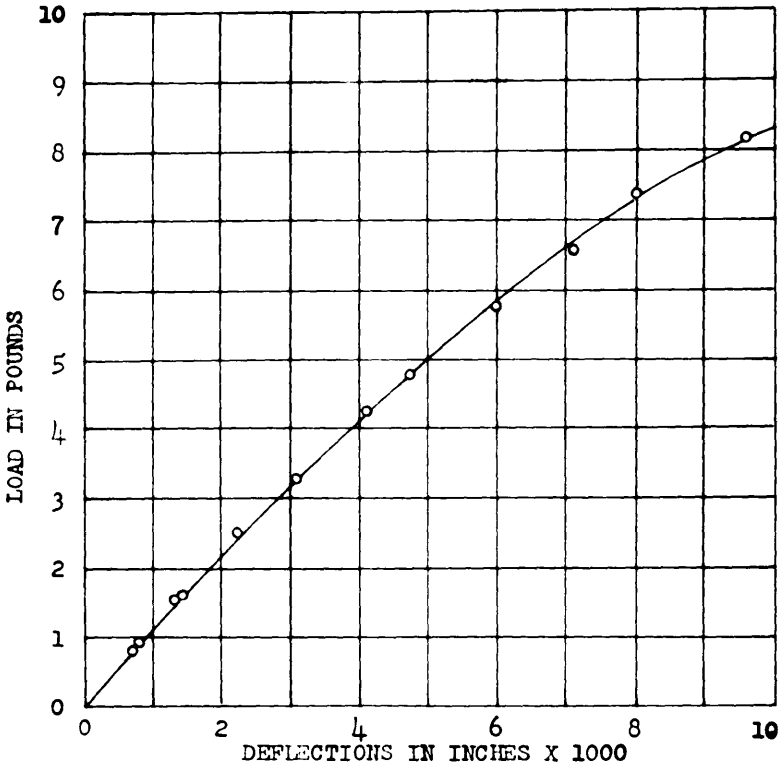
LIGHT LINE GIVES RESULTS ON PREVIOUSLY UNTESTED SAMPLE
HEAVY LINE GIVES RESULTS AFTER HOLDING MAXIMUM LOAD ON CANTILEVER FOR ONE HOUR



LOAD VS. DEFLECTIONS FOR FIRST CANTILEVER TEST

FIGURE 32

POINTS PLOTTED ARE FROM FIRST TWO RUNS



LOAD VS. DEFLECTIONS FOR SECOND CANTILEVER TEST

FIGURE 33

the curves of Figures 32 and 33 is proportional to E. In each case the slope decreases for an increase of load. Also the extreme fiber stress in the cantilever can be computed from the equation

$$f = \frac{P\,l\,d}{2\,I}$$

where f = stress in outermost fiber in p.s.i.

P,l,d, and I are load, length, depth and moment of inertia as before.

From these can be plotted E in terms of extreme fiber stress in the cantilever. The data of Table XIV and Figure 32 yield the following results.

Stress in outer fiber	E before creep	E after creep
23.4 p.s.i.	1,270,000	1,420,000
70.0 p.s.i.	1,100,000	1,265,000
117.0 p.s.i.	1,040,000	1,187,000
164.0 p.s.i.	830,000	1,070,000
210.0 p.s.i.	830,000	1,070,000

When the cantilever is loaded with weights, its upper side is in tension while its lower side is in compression. The stress values just found indicate the magnitude of compression at the extreme bottom and the magnitude of tension at the top. It is shown below that E increases with compressive stress. If this increase of E on the compressive side were counterbalanced by a decrease of E on the tension

side, the changes would not be so large as those found. Thus the data indicate that E decreases with increase of tensile stress to a greater extent than the counteracting increase on the compression side. A strict quantitative analysis of a cantilever test would have to use the average stress which would be about half the extreme stress but would also be dependent on the variation of E throughout the cross section. In addition allowance should be made for the downward shift of the neutral plane away from the center because of the lower value of E in the tensile or upper half. This would be a complicated mathematical problem.

The extreme fiber stress computed for the rupture point in the second test is 618 p.s.i. This ultimate tensile stress across bedding is considerably lower than any of the values found parallel to bedding in the tension tests discussed previously.

D. TESTS WITH MECHANICAL GAGES

Because of the difficulty experienced with the electrical strain gages another compression test was made using mechanical gages. The tests were run using a dense, apparently homogeneous, section of unfractured core. The diameter of the core sample was 3.50 inches and the length was 3.05 inches. The ends of the core were ground plane and parallel as accurately as possible. A sheet of soft lead was used over

each end during the tests. The testing machine used had a capacity of 50,000 pounds which produced a stress of 5,200 p.s.i. over the test surface. The use of a large specimen reduced any error caused by a bowing out or barrelling of the outer fibers.

Measurements were taken in two ways during the tests. One dial gage measured the change of length of the specimen, while the arrangement shown on Plate 13 at the bottom was used to measure change of diameter. A compressive stress on the axis of the core will shorten its length by an amount dependent on the modulus of elasticity and will increase its width by an amount dependent on Poisson's ratio.

Unlike metals which are ductile, the values of the modulus of elasticity, E, and Poisson's ratio, σ, for a brittle rock are dependent on the applied stress. Thus an average slope on the stress vs. strain curve would not give a representative value of E. The test and computations are made so that the values for E and σ can be found at any stress within the range tested. The full load was applied in steps of 4000 pounds and released in steps of 10,000 pounds with readings taken at these increments. This cycle was repeated several times. During the first application of stress the modulus of elasticity was somewhat lower than on subsequent applications. Three more applications and releases of stress were made and each followed the

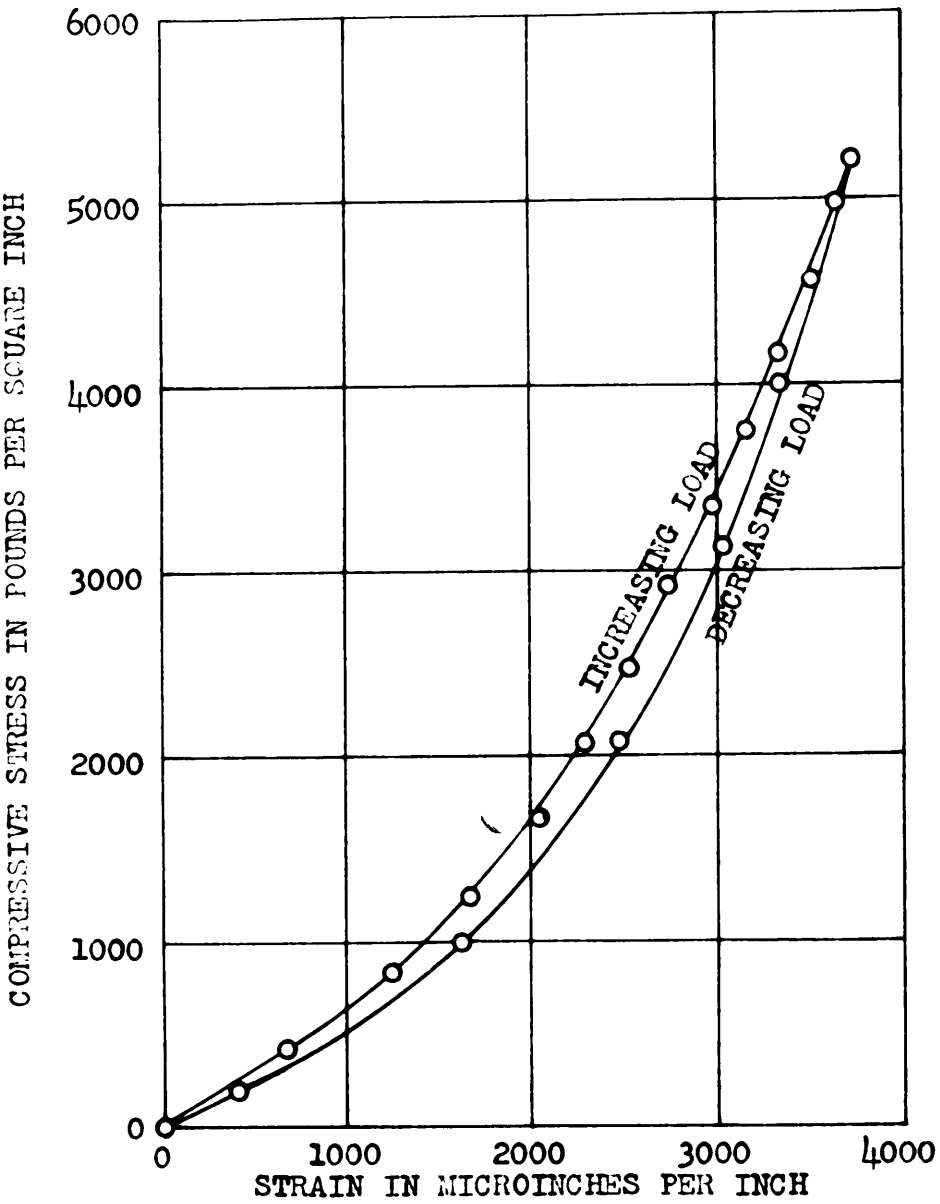
same stress vs. strain curves on each cycle as closely as the points could be plotted. The averages of these last three cycles are used for the data of Table XVI.

The first column gives the applied stress found by dividing the applied load by the cross sectional area of the core (9.63 sq. in.). The second column gives the strain in micro-inches per inch found by dividing the shortening of the core's length as read on the dial gage by the length of the core sample (3.05 m.). The next column gives the differences between the successive length strain readings. The fourth column gives the increase in the core's diameter in micro-inches per inch. This increase in the width of the rock mass is found by dividing the increase of diameter, after allowing for gage factor (see Chapter IV and Plate 13), by the diameter of the core (3.50 inches). The fifth column gives the successive differences in the lateral strain readings. Since E is the ratio of stress to strain, the values of E for the successive steps can be found by dividing the stress increments (415 p.s.i. except the last) by the longitudinal strain occurring in the step. Since the strain is in micro-inches per inch the division indicated gives E in millions of p.s.i. Since Poisson's ratio is the ratio of lateral unit deformation to longitudinal unit deformation, it can be found by dividing column 5 by column 3, and the values are, of course, dimensionless.

Table XVI

Compression Test Perpendicular to Bedding with Dial Gages
All strains in micro-inches per inch. E x 10^6.

Stress	$\frac{\Delta l}{l}$	$\Delta\frac{\Delta l}{l}$	$\frac{\Delta w}{w}$	$\Delta\frac{\Delta w}{w}$	E	σ
0	0		0			
208		- 680		12	0.61	.0177
415	- 680		12			
624		- 562		11	0.74	.0195
831	- 1242		23			
1039		- 429		11	0.97	.0254
1247	- 1671		34			
1452		- 354		10	1.17	.0282
1661	- 2025		44			
1870		- 270		9	1.54	.0333
2079	- 2295		53			
2280		- 235		9	1.77	.0383
2490	- 2530		62			
2700		- 218		8	1.90	.0368
2908	- 2748		70			
3116		- 212		7	1.96	.0330
3321	- 2960		77			
3530		- 195		7	2.13	.0358
3740	- 3155		84			
3940		- 175		7	2.37	.0400
4150	- 3330		91			
4360		- 170		7	2.44	.0412
4570	- 3500		98			
4780		- 155		7	2.68	.0452
4990	- 3645		105			
5200	- 3715	- 70	109	(4)	2.96	(.0572)



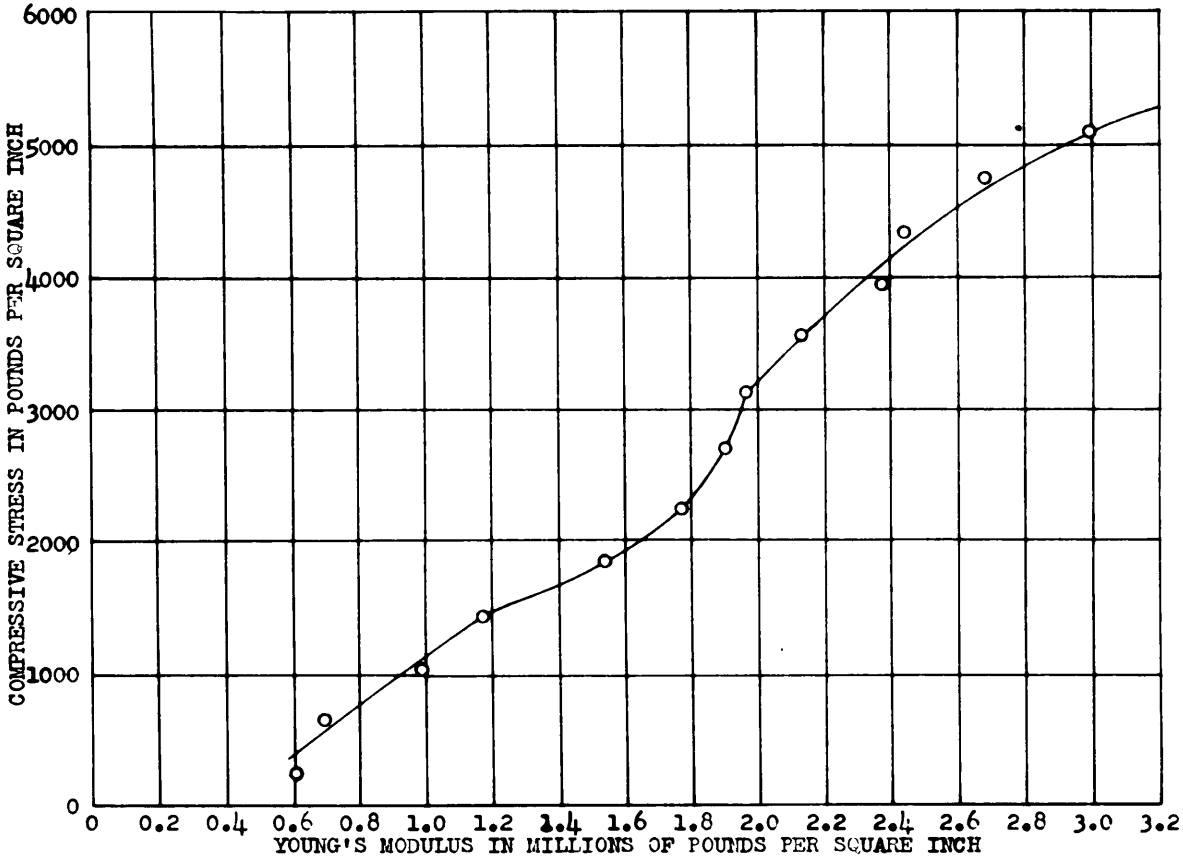
STRESS VS. STRAIN FOR UPPER SPRABERRY CORE LOADED PERPENDICULAR TO BEDDING

FIGURE 34

The stress strain relation for increasing loads as shown on the table are plotted on the graph which is Figure 34. Also plotted are the strains for reducing loads. The displacement of the decreasing curve from the increasing curve is toward the direction of greater strain by these amounts measured in micro-inches per inch.

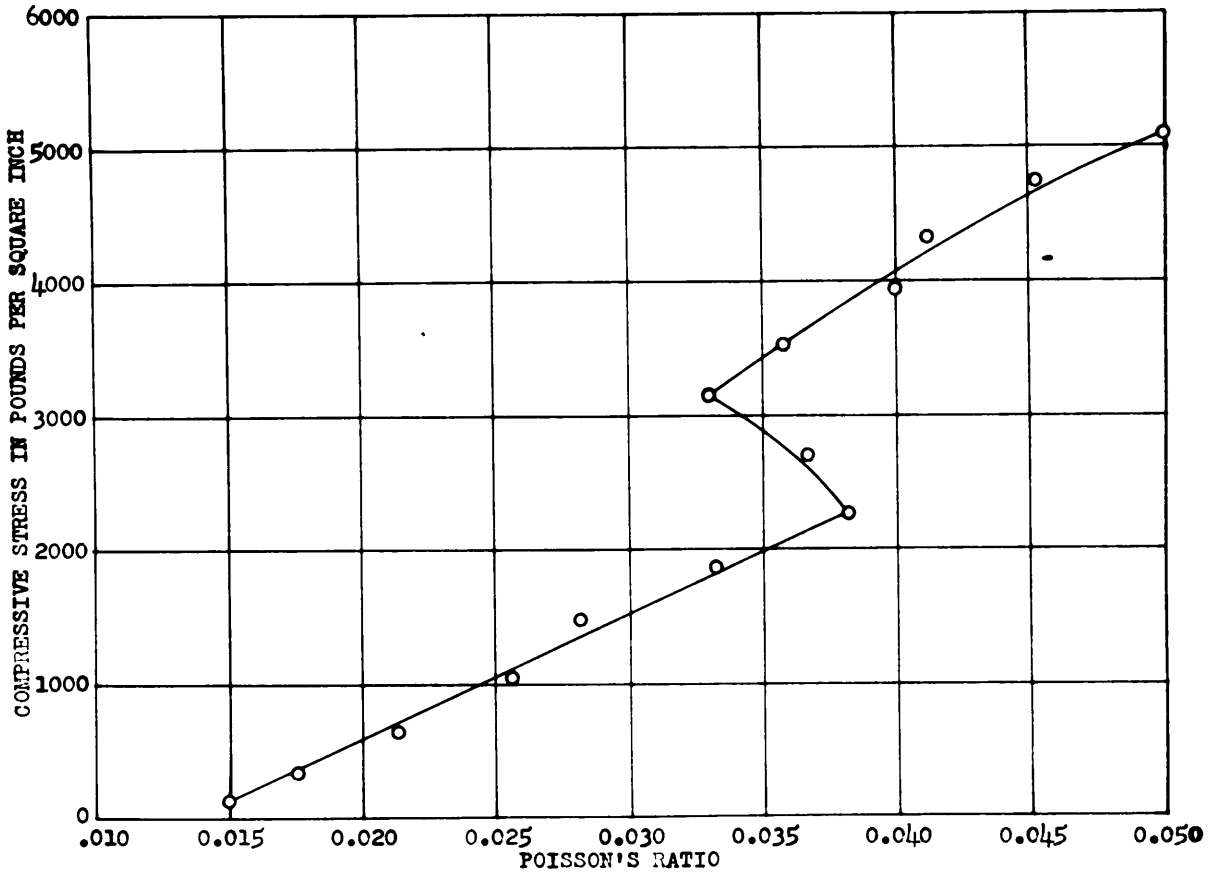
50,000 p.s.i. - 0
40,000 p.s.i. - 74
30,000 p.s.i. - 186
20,000 p.s.i. - 180
10,000 p.s.i. - 191
2,000 p.s.i. - 63
0 - 0

The values of the modulus of elasticity and of Poisson's ratio are plotted in Figures 35 and 36, respectively. Figure 35 is essentially a plot of the slope of the stress strain curve shown in Figure 34, i.e. is its first derivative. The irregularity in the E curve is represented only as a slight change in the rate of change of slope on the stress-strain curve and is hardly noticeable. The irregularity is also reflected in the plot of Poisson's ratio (Figure 36). The cause of the irregularity is not known, but the sample repeated the phenomenon during three successive series of measurements within very close limits indicating that it is not an observational error or an instrumentational quirk. Besides this the several anomalous points seem to form a smooth curve.



STRESS VS. YOUNG'S MODULUS FOR UPPER SPRABERRY CORE LOADED PERPENDICULAR TO BEDDING

FIGURE 35



STRESS VS. POISSON'S RATIO FOR UPPER SPRABERRY CORE LOADED PERPENDICULAR TO BEDDING

FIGURE 36

To be sure that the lateral strain measurements were not being affected by the barrelling effect mentioned previously, several more test runs were made using different diameters and different positions along the length of the core for measurement. Even with the gage measurements only 1/4 inch from the end bearing plates (lead) the strain measurements were unchanged.

The maximum applied stress was sufficiently low so that creep was negligible. The residual strains were very small after each complete release of load and even these strains recovered in a minute or two. After the last test the rock was subjected to the maximum stress of 5200 p.s.i. for 45 minutes, and close observation by the writer and an assistant revealed no creep.

E. TORSION TESTS

An attempt was made to learn whether the incipient fracture planes could be opened by torsion such as might occur during coring. No attempt was made to obtain quantitative data because of the difficulty of fashioning test pieces of a suitable shape. The pieces used were prisms with a square cross section about an inch on a side and long dimension parallel to the length of the core. Two massive siltstone samples produced an irregular break while two finely laminated samples broke more or less along bedding planes.

3. SIGNIFICANCE OF PHYSICAL TESTS

Poisson's ratio and the modulus of elasticity both increase with an increase of stress. These changes are very marked even though the range tested accurately was not more than half the rock's ultimate strength. The changes indicate a shift toward less brittleness with increase of compressive stress. Thus the angle between a pair of conjugate shears should be nearer to 90 degrees. Thus the Mohr envelope would not diverge indefinitely, but the limbs would curve toward parallelism and eventually even converge. It is evident that under the great confining pressures and plastic conditions existing at great depth the Mohr envelope must return again to the "x" axis. However, within the range tested at the present depth of the Spraberry formation no large change in the Mohr envelope is indicated from that shown in Figures 29 and 30.

A question is sometimes raised about the quantity of energy involved in rock deformation in terms of heat. Referring to the Mohr diagram on Figure 29 it is shown that to fracture the Spraberry under a 3000 p.s.i. confining pressure would require a differential compressive stress of 22,600 p.s.i. The curve for the value of E does not extend nearly far enough and could not unless confined tests were made, but the value would probably be in the order of $4\ 1/2 \times 10^6$ p.s.i. The energy required to fracture a cubic inch of the formation is the product of total strain and

average force. (The rock can be assumed elastic to the breaking point because of its brittleness.)

$$\frac{22,600}{2} \times \frac{22,600}{4\ 1/2 \times 10^6} \times \frac{1}{12} = 4.83 \text{ foot pounds.}$$

Assuming a specific heat of 0.170 for the sample this energy would raise the temperature of the rock by 0.21 C^{o}. Under the same confining pressure the energy for a tension break would be about 0.75 foot pounds and the temperature increase only about 0.03 C^{o}. A large number of fractures does not necessarily mean a greater energy expenditure. Work is done compressing a rock to the point of incipiant rupture and involves the whole rock mass. The formation of one or more fractures does little to change the stress throughout the rest of the rock mass.

A repeated number of stress applications and stress releases will generate heat because the elastic rebound curve does not exactly retrace the curve of increasing stress. This is shown on Figure 34. Although the two curves each start and end at the same points, the energy given out by the rock following the return path is not quite as much as the energy which was put into the rock. This phenomenon is known as hysteresis, and the energy consumed during a single cycle is given by the area between the two curves. Thus, considering a cubic inch of sample, the energy consumed in one cycle of stress as shown on Figure 34 would be about

$$5200 \times 150 \times 10^{-6} \times 1/12 = .065 \text{ foot pounds.}$$

Again using the value of specific heat of 0.170, it can be shown that the rock would have to be subjected to over 350 cycles to raise the temperature 1 C^{o}. These simple calculations show that within the elastic limit the generation of heat by deformation is small.

CHAPTER VI

SUMMARY OF CONCLUSIONS

The Spraberry formation of Permian Leonard age consists, in the southern Midland basin, of about 1000 feet of siltstone and shale. The oil producing horizons have a very low permeability and owe their producing ability to closely spaced vertical fractures. The productive trend is a very large stratigraphic trap on the flank of a westward dipping monocline.

The variation of thickness of the formation and the areal changes of lithology indicate the east or southeast as the source of Spraberry sediments. During Spraberry deposition the Midland Basin appears to have had the characteristics of a stagnant basin. The sediments in the Upper Spraberry have a median diameter of 0.0056 mm which is in the coarse silt range of the Wentworth scale. The sorting is good. The fossils are almost entirely pelagic and occur only at infrequent intervals. The calcium carbonate and organic content of the sediments is high and reducing conditions are indicated.

About half of the well cores made in the Spraberry contain fractures down their length which divide them into two almost equal parts. Measurement of core diameters across and parallel to fractures shows an apparent fracture opening of about 0.002". A differential horizontal stress of 600 p.s.i.

could also produce the effect of an apparent fracture opening. Of the cores with single fractures which were studied, over 75% had the fracture within 1/10 inch of the centerline of the core. Calculations from production and Hydrofrac treatment data show that the lateral extent of the fractures opened artificially must be several hundred feet. Release of hydrostatic pressure applied in a pressure vessel produced a few "artificial" fractures showing that a direction of incipient weakness exists in some of the specimens and that some of the fractures are not open in the formation. The major fracture set trends N 25° E with a more poorly developed set of fractures crossing the main set. This fracture pattern was duplicated in warped plate glass by means of compressive stress in two directions.

Physical tests on the siltstone show that the value of Young's modulus is strongly dependent on the applied stress. Poisson's ratio is similarly dependent on stress and has a very low value indicative of a very brittle material. Samples were found to creep under prolonged high stress. The Mohr diagram construction was used to analyze rupture conditions under confining pressures. The rupture stress required is much larger when confining pressure acts.

REFERENCES

"Air Drilling Tried." The Oil and Gas Journal, Vol. 50, p. 152, June 21, 1951.

Atlantic Refining Co., Personal communication June 17, 1952.

Baldwin-Lima-Hamilton Technical Bulletins Nos. 279, 279A, 279B, and 316 (not dated).

--- "SR-4 Strain Gages Instruments and Accessories." April 15, 1950.

Bartley, J. M., "Spraberry Drilling Activity Exceeds all Previous Plays in West Texas Area." Oil and Gas Journal, Vol. 50, p. 126, Aug. 16, 1951 (a).

--- "Stratigraphy and Structure of the Spraberry Trend." Oil and Gas Journal, Vol. 50, p. 101, Dec. 6, 1951 (b).

--- "Geology of the Spraberry Trend of the Permain Basin of West Texas." Paper presented at A.P.I. meeting in Shreveport, La. March 5, 6, and 7, 1952.

Berry, O. H., "Air Drilling the Spraberry Sand." World Oil, p. 169, Sept. 1951 (a).

--- and Bill Queensbury, Jr., "Air Drilling Operations." Oil and Gas Journal, pp. 80-82, Nov. 22, 1951 (b).

Brace, Wm., Personal communication, Feb. 9, 1953.

Brack, Ray, "Reservoir Performance." Oil and Gas Journal, pp. 97-99, Dec. 6, 1951.

Bridgeman, P. W., "Studies in Large Plastic Flow and Fracture." 1st ed. McGraw-Hill Book Co., New York, 1952.

Bristol, B., Jr. and Cy Helm, "Acid Flushing Fractures in Spraberry Sand." Oil and Gas Journal, p. 94, Dec. 6, 1951.

Bucher, Walter H., "The Mechanical Interpretation of Joints." The Journal of Geology, Vol. XXIX, No. 1, p. 1, Jan.-Feb. 1921.

Buckley, Stuart E. et al., "Petroleum Conservation." Am. Inst. of Mining and Met. Engrs., 1951.

California Research Corp., Personal communication, June 24, 1952.

Calson, Ray F., "Dozen Rigs Now Running in Tex Harvey Field." The Oil and Gas Journal, Vol. 49, no. 10, p. 97, June 13, 1950.

--- "West Texas' Spraberry Fields." The Oil and Gas Journal, p. 197, Feb. 22, 1951 (a).

--- "Active Area." The Oil and Gas Journal, Vol. 50, p. 149, June 21, 1951 (b).

--- "Spraberry Puzzle." The Oil and Gas Journal, Vol. 50, pp. 150-152, Oct. 4, 1951 (c).

--- "Spraberry Fractures." The Oil and Gas Journal, Vol. 50, pp. 76-77, Oct. 25, 1951 (d).

--- "Spraberry Study." The Oil and Gas Journal, Vol. 50, P. 85, Oct. 11, 1951 (e)

--- "Spraberry Grows Up." The Oil and Gas Journal, Vol. 50, p. 173, Dec. 20, 1951 (f)

--- "Spraberry Innovations." The Oil and Gas Journal, Vol. 51, p. 37, Feb. 4, 1952 (a).

--- "Youthful Oil Area." The Oil and Gas Journal, Vol. 51, p. 74, Mar. 31, 1952 (b).

--- "Spraberry Operators Eye Gas as Revenue Source as Declining Oil Production Looms." The Oil and Gas Journal, Vol. 51, pp. 234-236, June 2, 1952 (c).

--- and Philip C. Ingalls, "Progress Report: Midland County." The Oil and Gas Journal, Vol. 49, Oct. to Dec. 1950.

Carlsten, Kirk, "Oriented Cores." in Subsurface Geologic Methods compiled by L. W. LeRoy, p. 591, 1951.

Carter Research Laboratories, Personal communication, June 6, 1952.

Casey, R. S. and J. W. Perry, "Punched Cards." Reinhold Publishing Corp., New York, 1951.

Christie, R. S., and J. C. Blackwood, "Production performance in Spraberry." The Oil and Gas Journal, Vol. 51, p. 107, April 7, 1952.

Clark, J. B., "Hydrofrac Process for Increasing the Productivity of Wells." Paper presented at meeting of Am. Inst. of Mining and Met. Engrs., Oct. 4, 5, and 6, 1948.

Cox, John L. "Drilling and Casing Procedures." The Oil and Gas Journal, pp. 74-76, Nov. 29, 1951.

Den Hartog, J. P. "Advanced Strength of Materials." 1st ed. McGraw-Hill Book Co., New York, 1952.

Dickey, Park A., Personal communication, June 6, 1952.

"Drilling Hot Spot." The Oil and Gas Journal, Vol. 50, p. 179, July 26, 1951.

Eardley, A. J., "Structural Geology of North America." Harper Brothers Publishers, New York, 1951.

Eshbach, O. W., "Handbook of Engineering Fundamentals." John Wiley and Sons, Inc., New York, 1949.

Fairbairn, H. W., "Structural Petrology of Deformed Rocks." Addison-Wesley Press Inc., Cambridge, Mass., 1949.

Fisk, Harold N., "Jointing in the Spraberry." Paper presented at the Third Oil Recovery Conference in Midland, Oct. 19-20, 1951.

--- Personal communication, Nov. 14, 1952.

Franklin, Leonard O., "Drilling and Completing in the Spraberry Trend." The Oil and Gas Journal, pp. 86-95, Mar. 31, 1952.

Gibson, George R., "Relation of Fractures to the Accumulation of Oil." The Oil and Gas Journal, p. 107, Nov. 29,1951.

--- "The Controversial Spraberry." World Petroleum, pp. 63-66, Mar. 1952 (a).

--- Personal communication, June 11, 1952 (b).

Glaessner, Martin F. "Principles of Micropaleontology." Melbourn University Press, Victoria, 1945.

Griggs, David and J. B. Bell, "Experiments Bearing on the Orientation of Quartz." Bull. Geol. Soc. of Am., No. 49, pp. 1723-1746, 1938.

Grossman, Waldo L., "Hydrofrac Operations." The Oil and Gas Journal, pp. 77-81, Nov. 22, 1951.

Hassebrock, W. E., "Hydrofrac Treatment." In Subsurface Geological Methods compiled by L. W. LeRoy, 1951.

Honolulu Oil Corp., Personal communication, June 10, 1952.

Hedden, A. H., "Developments in West Texas and Southeast New Mexico in 1951." Bull. Am. Assoc. of Pet. Geol., Vol. 36, No. 6, pp. 1128-1146, June 1952.

Howe, W. S., "Mud Programs." The Oil and Gas Journal, pp. 82-83, Nov. 22, 1951.

Humble Petroleum Co. "Cracking the Rock Curtain." in The Humble Way, Vol. VII, No. 5, pp. 1-3, Jan-Feb. 1952 (a).

--- Personal communication, June 16, 1952 (b).

Hetenyi, M., "Handbook of Experimental Stress Analysis." John Wiley and Sons, Inc., New York, 1950.

Ingalls, Phillip C., "Up-An'-Comin' Upton." The Oil and Gas Journal, Vol. 50, p. 163, Mar. 29, 1951 (a).

--- "Midland Basin's Spraberry." The Oil and Gas Journal, Vol. 49, p. 163, May 17, 1951 (b).

"Is World's Largest Oil Field Looming Up in West Texas?" The Oil and Gas Journal, Vol. 50, p. 98, Oct. 11, 1951.

King, P. B., "Geology of the Glass Mountains, Texas." Part I, University of Texas Bull. 3038, Oct. 8, 1930.

--- "Geology of the Southern Guadaloup Mountains, Texas." U. S. Geol. Survey Prof. Paper 215, 1948.

--- "The Tectonics of Middle North America." Princeton University Press, Princeton, N. J., 1951.

King, R. E. "The Geology of the Glass Mountains, Texas." Part II, University of Texas Bull. 3042, Nov. 8, 1930.

Krumbein, W. C., and F. J. Pettijohn, "Manual of Sedimentary Petrography." Appleton-Century Co., Inc., New York, 1938.

--- and L. L. Sloss, "Stratigraphy and Sedimentation." W. H. Freeman and Company, San Francisco, Cal. 1951.

Legendre, Harry E., "Completion Practices in the Spraberry." World Oil, p. 230, Sept. 1951.

Lloyd, E. Russel, "Correlation Chart, Permian of West Texas and Southeastern New Mexico." West Texas Geological Society, April 1952 (a).

--- Personal communication, June 10, 1952 (b).

Lytle, W. J. and R. R. Rieke, "Well Logging in the Spraberry." The Oil and Gas Journal, Vol. 50, Dec. 13, 1951.

Mardock, E. S. and Jack P. Myers, "Radioactivity Logs Define Lithology in the Spraberry Formation." The Oil and Gas Journal, pp. 96-101, Nov. 29, 1951.

Marsh, Joseph W., "Spraberry Reservoir of West Texas." Bull. Am. Assoc. of Pet. Geol., Vol. 36, No. 11, p. 2189, Nov. 1952.

McLennan, Lamar, Jr. and Waring H. Bradley, "Spraberry and Dean Sandstones of West Texas." Bull. Am. Assoc. of Pet. Geol., Vol. 35, pp. 899-908, April 1951.

Melton, F. A., "Fracture Systems in Central Texas." in Geology of Texas by E. H. Sellards and C. L. Baker, University of Texas Bull. 3401, 1934.

Midland Reporter-Telegram map, "The Permian Basin's 509 Oil Pools." Feb. 25, 1951.

Milner, Henry B., "Sedimentary Petrography." Thomas Murby and Co., London, 1952.

Moore, Jack M. and J. C. McCormick, "A New Stimulation Technique." The Oil and Gas Journal, pp. 102-107, Nov. 29,1951.

Moore Jack M. and Ray S. Ousterhout, "Stra-frac Completions." Petroleum Engineer, Feb. 1952.

Moore, R. C., C. G. Lalicker, and A. G. Fisher, "Invertebrate Fossils." McGraw-Hill Book Co., New York, 1952.

Nevin, C. M., "The Principles of Structural Geology." John Wiley and Sons, Inc., New York, 1949.

Ogden, Victor, and Jack Locke, "What are the Facts and Figures for 'Spraberry Trend' Core Analyses?" The Oil and Gas Journal, p. 94, Jan. 14, 1952 (a).

--- Personal communication, June 11 and 13, 1952 (b).

Osborn, W. M., "History and Development of the Spraberry Trend." The Oil and Gas Journal, p. 100, Dec. 4, 1951.

Parker, J. M., "Systematic Jointing in Slightly Deformed Sedimentary Rocks." Bull. of Geol. Soc. of Am., Vol. 53, pp. 381-408, 1942.

Pettijohn, F. J., "Sedimentary Rocks." Harper Brothers, New York, 1949.

Phillips Petroleum Co., Personal communication, June 12, 1952.

Pierson, S. J., "Elements of Oil Reservoir Engineering." 1st ed., McGraw-Hill Book Co., Inc., New York 1950.

Senning, R. C., "The Spraberry Play in West Texas." World Oil, p. 125, Sept. 1951.

Shrock, R. R., and W. H. Twenhofel, "Principles of Invertebrate Paleontology." McGraw-Hill Book Co., Inc., 1953.

Skrabanek, J. W., Personal communication, June 10, 1952.

Sohio Petroleum Company, Personal communication, June 12,1952.

"Steel Construction Manual." Am. Inst. for Steel Constr." New York, 1947.

Sunray Oil Corporation, Personal communication, June 4,5,6 1952.

Taylor,D.W., "Fundamentals of Soil Mechanics." John Wiley and Sons, Inc., New York, 1948.

Timoshenko, S., "Theory of Plates and Shells." 1st ed., McGraw-Hill Book Company, Inc., New York, 1940.

Trask, P. D., "The Origin and Environment of Source Sediments of Petroleum." Gulf Publishing Co., Houston, Texas, 1932.

Twenhofel, W. H. "Principles of Sedimentation." McGraw-Hill Book Co., Inc., New York, 1939.

Waldschmidt, William A., Personal communication, June 9, 1952.

Warn, Fredrick G., "Spraberry Structural Conditions, Part I." World Oil, p. 83, Mar. 1953.

Whitehead, W. H., Personal communication, 1952.

Wilkinson, W. M., Personal communication, June 13, 1952.

APPENDIX "A"

DESCRIPTION OF PHOTOELECTRIC ORIENTATION MEASURING INSTRUMENT

It has been mentioned in the text that quartz grains often have their long dimensions parallel to the crystallographic optic axis. If these grains were deposited in flowing water they would have a preferred orientation, and their optic axes would also have a preferred orientation. If all of this were true the light transmission of a bedding plane thin section on a petrographic microscope should vary depending on the relation of the preferred direction to polarizer and analyzer. The total light transmission through the thin section with low power magnification would represent the total transmission of light by many grains, and observation of variations in this total transmission of light during rotation of the microscope stage could give information about a preferred orientation which might otherwise require a count of hundreds of individual grains. The method would be particularly useful for very weak orientations which ordinarily require a count of a prohibitive number of individual grains.

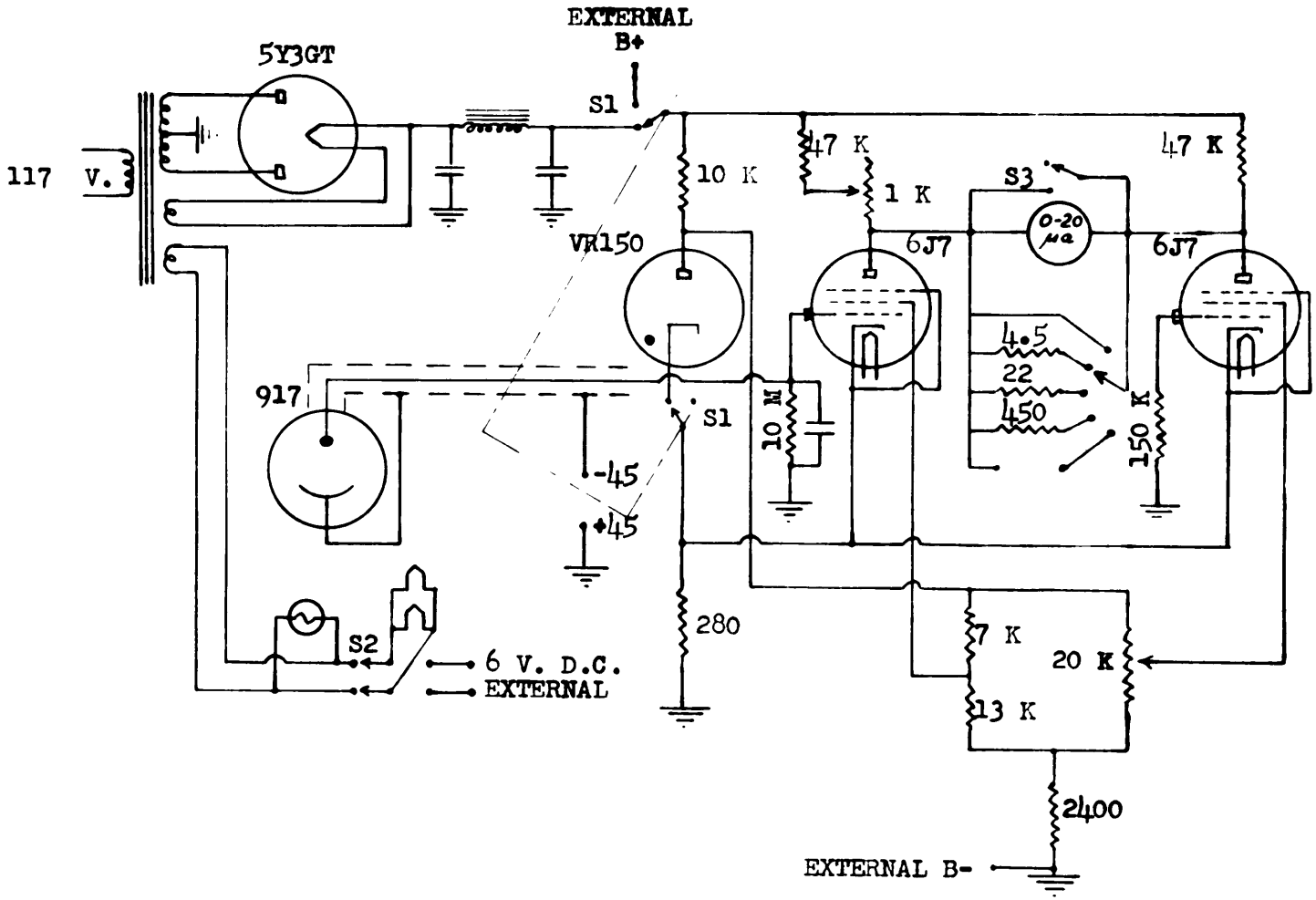
In order to test this a photoelectric tube and bridge circuit amplifier were constructed. It is felt that the device has a wide enough application to other problems to warrant a fairly detailed description of design considerations

here. The design considerations and methods of satisfying these will be considered together.

1) The instrument must have high sensitivity. The mere ability to make a reading of light transmission over the microscope is not enough. Some photographic light meters can do this. The required instrument must be able to give readings on the variation of the light transmission which may amount to only 1% of the total light. To do this the instrument should be able to read 0.1% of the total light. This sensitivity can be achieved while still maintaining fairly good stability by using two matched high gain pentodes in a bridge circuit as shown on Figure 37.

2) To measure such small variations of light it is necessary to have several scales with different sensitivity arranged so that the more sensitive scales read only the variation and not the total light. The circuit used (Figure 37) had three scales which gave sensitivities in the ratios of 1, 10, and 100. The 20,000 ohm coarse adjustment gave a range sufficient so that the bridge circuit could be balanced on all scales even with a full peak light reading.

As an actual example of the use of the instrument consider a thin section which has a weak orientation such that light variation with stage rotation amounts to about 2%. With the microscope light turned off and the instrument on the coarsest scale, the instrument's meter is adjusted to



PHOTOELECTRIC AMPLIFIER CIRCUIT

FIGURE 37

zero. The light is switched on, and the stage rotated to note any variation; 2% would be so small a change as to be hardly discernable, but if variation is seen the maximum reading is recorded. Say that the reading on this coarsest scale is 15 divisions on the meter. Now with the light still on, the meter is adjusted to zero by means of the coarse adjustment. The instrument is switched to the medium scale and should still read zero; if not, it can be adjusted with the coarse or fine adjustment. The instrument is turned to the fine scale, and the fine adjustment set so that the extreme variations of reading with rotation of the stage are on the scale. The total variation of scale reading is noted; say this is 33 divisions. The percentage variation of light is

$$33/(15 \times 100) = 2.2\ \%.$$

More strongly oriented sections might have a variation too great for the fine scale and would then be read on the medium scale. Metamorphic rocks were tested which gave variations so great that only one scale was needed. For these no cancelling of the initial reading was necessary, and the whole variation was read on the first scale.

3) The instrument must be stable. Very small changes in tube characteristics or circuit constants can cause a large change in meter reading on the fine scale. The screen voltage of the circuit was voltage regulated, and precision resistors were used in the grid circuits. The bridge arrangement

automatically helps eliminate trouble from variations which are the same on each side. Provision is made for the use of batteries for either plate voltage or heater voltage or both. Batteries were found useful for fine readings with weakly oriented sections. The instrument as constructed required about a half hour to warm up and reach an equilibrium condition of good stability.

4) The light source must be stable. A bulb connected directly to commercial power is generally not at all satisfactory. The power dissipated in a resistance is given by

$$W = E^2 / R.$$

Thus a change of voltage of 2% means a change of power consumed of over 4%. With an incandescent bulb the variation will be even greater since change of power and hence of filament temperature causes an opposite change of filament resistance. To maintain a light output which is steady to 0.1% the voltage regulation must be somewhat better than 0.05%. A "Sola" voltage regulating transformer was used to give a constant voltage, but it did not give regulation within the required limits. However, its regulation was sufficiently good so as to be useful for most of the thin sections analyzed. The whole assembly of equipment is shown in Plate 18 in readiness for use.

5) The phototube must have a current output which is proportional to light input. This result is best achieved



GRAIN ORIENTATION EQUIPMENT

PLATE 18

with a high vacuum type phototube. Also the phototube should be operated at a low voltage so as not to ionize any small quantity of residual gas in the envelope. The tube used for work with the microscope for the set-up shown on Plate 18 was a type 917.

6) There must be no variations from sources other than grain orientation. This is a very difficult specification to meet, but was harder for whole-thin-section analyzer described below than for the microscope set-up. This trouble arises from uneven sensitivity of the photosensitive surface and from the selective reception of light from different parts of the field of view. This problem is discussed in greater detail below. On the microscope a small piece of doubly ground glass was placed over the exit pupil of the eyepiece to diffuse light over the whole sensitive surface of the phototube. In this way the light from each part of the field of view was distributed to all parts of the emissive surface and variations of sensitivity of the surface were of no consequence.

It is evident that coarse grained samples would not contain enough grains in a single field of view even on low power to give a reliable estimate of any orientation. Some of the Spraberry thin sections showed slight variations in the orientation of the minimum light readings. For these reasons the use of the microscope was abandoned, and a device

was built which would measure the light transmission of a whole thin section. The completed instrument is shown on Plate 19. The design considerations for such a device will be considered in turn.

To illuminate a whole thin section with polarized light or to analyze the light therefrom requires polarizing areas larger than those of most prisms. The obvious choice was polaroid. It was found that the difference of meter reading between crossed and parallel polaroids with no thin section was only about 30% even though the change of light intensity by visual examination appeared to be in the order of magnitude of 50 to 1. Several hours search revealed the trouble to be that ordinary polaroid does not polarize infra-red light. An incandescent light has a large part of its radiant energy in the infra-red while the peak sensitivity of the 917 phototube is in the infra-red. The trouble could be remedied at the light, the polarizer or analyzer or the phototube. Changing the light source was impractical since other light sources such as fluorescent lights have a light output which varies to a greater extent than incandescent lights. This output varies with temperature and has an appreciable 120 c.p.s. modulation which might cause trouble in the amplifier. An attempt was made to filter the incandescent light but it was found that none of the easily mounted gelatine filters absorb infra-red. It is known that a cell containing water or a solution of copper chloride





WHOLE THIN SECTION ANALYZER

PLATE 19

will not transmit infra-red, but these cells are hard to construct and to keep from leaking. The Polaroid Corporation loaned the writer two of their newly developed "HR" polarizers which polarize light effectively to a wave length of about 30,000 angstroms. These had two disadvantages. Their light transmission was quite low and the loss by transmission through the pair of filters reduced the sensitivity of the instrument. Also, the transmission in the visual range was only 2% so that a pair had a transmission of visible light of only 0.04% making visual observation of the thin section impossible. The final solution of the problem, and undoubtedly the easiest, was to use regular polaroid and a type 929 phototube which has no sensitivity in the infra-red. The change of meter reading was then in the order of 80 to 1 between parallel and crossed polaroids.

Since the voltage regulating transformer was not entirely satisfactory, a new light source was used with the whole-thin-section instrument. This was a six volt storage battery and a two filament automobile headlight bulb. The switches were arranged so that either filament or both could be used.

Some thin sections are far from round and may even be very elongate in area. It is very difficult to keep such an odd shape from producing an elongate illuminated area on the phototube. Since the phototube is elongate, has a

curved emissive surface, and loses light because of the shadow cast by the anode, rotation of an elongate thin section causes a pronounced variation even though there is no grain orientation. The problem is to sufficiently diffuse the light. A phototube mounted over a microscope does not present this problem because the field of view of the microscope is found. Neither six plates of ground glass nor a cell one inch thick with pulverized glass gave sufficient diffusion of light. The final solution was to face the phototube away from the light source and line its chamber with white blotting paper to reflect light uniformly and non-directionally. To test the effectiveness of this method a thin copper sheet containing a very thin elongate slit was rotated on the stage; the light variation from even this extreme shape caused only a small variation on the finest scale.

Plate 19 shows the instrument with front covers removed and photographs of the instrument in use. The phototube chamber can be rotated to enable visual observation of the thin section. The components of the instrument are listed below in their correct order from bottom to top.

1. Light bulb which can be adjusted horizontally and vertically.

2. Piece of plate glass about 1" thick and ground on both sides. This diffuses the light and is necessary to prevent formation of an image of the filament.

3. Two plano convex condensing lenses with convex sides facing each other and almost in contact.

4. The lower polaroid or polarizer. This is in a fixed position and cannot be rotated except by disassembling the instrument.

5. Platform containing light switches and pointer for rotatable scale on turntable or stage.

6. Stage for thin section with hole 1 1/4" in diameter.

7. Upper polaroid or analyzer which is in the cover which can be raised. See Plate 19. This polaroid can be rotated or even removed entirely by swinging the phototube chamber to one side.

8. In the lower part of the phototube chamber are two collecting lenses.

9. The phototube is mounted at the top of the phototube chamber. An additional socket is mounted on the other wall of the chamber and connected into the circuit so that the type 917 phototube can be substituted easily if desired.

10. There is a removable connection to the bridge circuit at the back of the phototube chamber.

Except for the light and the phototube all components are larger in diameter than the 1 1/4" hole in the stage.

It may be in order to mention some of the uses and limitations of such an instrument. It is especially useful for measuring orientations in bedding plane thin sections of sedimentary rocks. Any current derived orientation is most likely

to exist only in this plane, especially for fine grained material in which an imbricate structure is unlikely. It is easy to test whether the quartz grains (or others) are optic axis long and give selective extinction if acted on by current. This can be done by measuring the selective extinction of a section cut perpendicular to bedding. Grains are generally deposited with the shortest dimensions vertical so that such a thin section should have all of the long axes in the bedding plane, and, if the grains are optic axis long, the traces of the optic axes on the thin section would have a constant direction. Spraberry thin sections cut across bedding showed marked orientation.

One major disadvantage is that each complete rotation of the stage gives four minima. There is no way to tell which pair of these represents the correct grain orientation. The reason for the four minima is that each grain extinguishes each time the trace of its optic axis is parallel to the plane of polarization of either the polarizer or the analyzer. An individual grain analysis to determine dimensional orientation would give a single line as the direction of preferred orientation.

The device could not be used to analyze a tectonite without making several oriented thin sections unless the tectonic axes were already known. A universal stage could accomplish the same results with a single thin section.

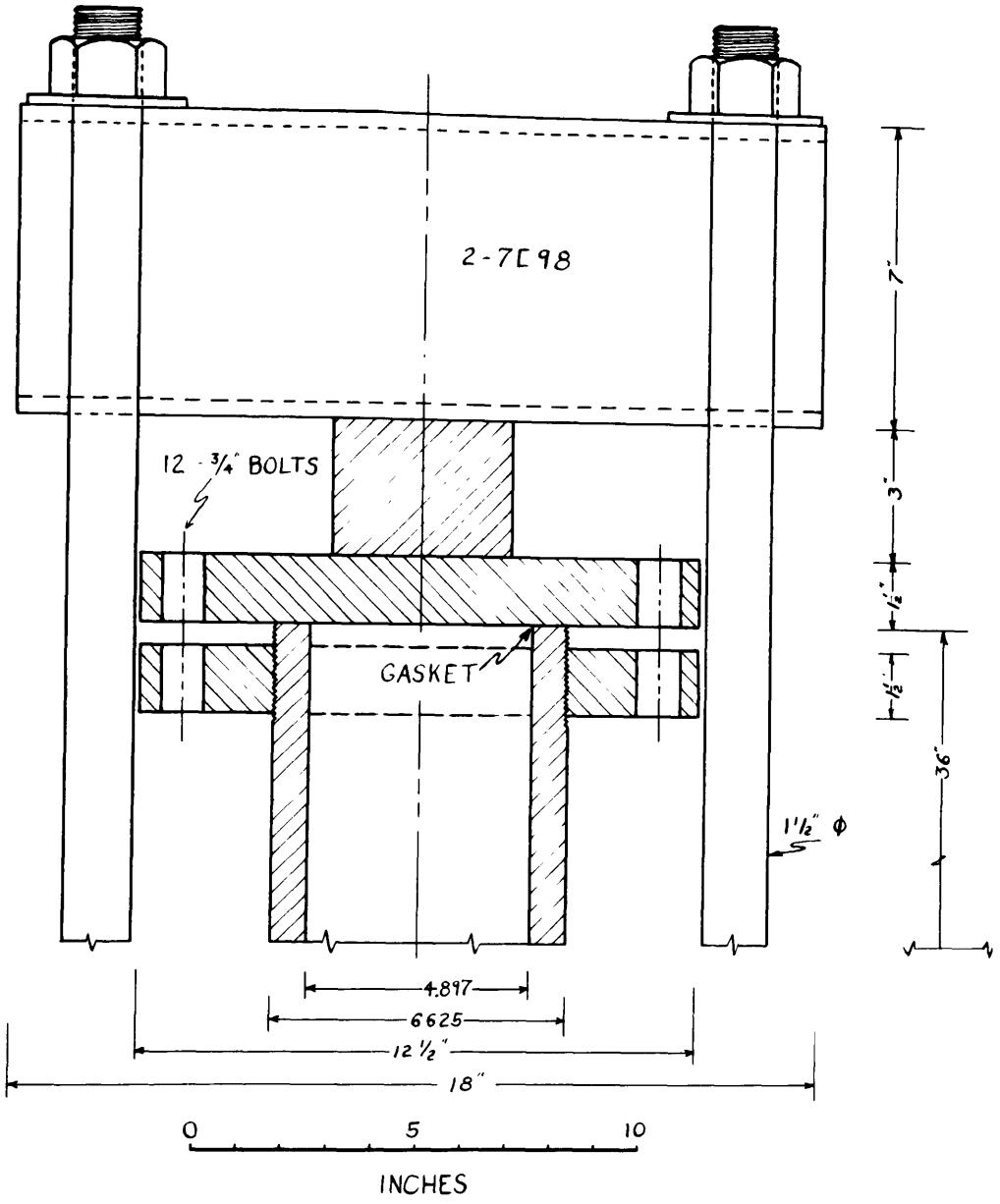
A petrofabric diagram made by universal stage from a thin section cut perpendicular to the "*b*" tectonic axis (the most common practice when the axis is known) might show a maximum number of optic axes near the center of the diagram. If this maximum area were radially symmetrical on the diagram, the rotation of the thin section in the orientation instrument would show no variation of transmitted light.

APPENDIX "B"

DESCRIPTION OF PRESSURE VESSEL

A pressure vessel was required to test Spraberry core samples to learn whether fractures could be developed along incipient planes of weakness by the sudden release of pressure. Since no pressure vessel was available which was large enough for a whole piece of core, it was decided to construct a suitable vessel. The final design is simple and economical. There are many applications for pressure vessels not only in geology but in other fields, and a description of the methods used and ways to avoid trouble may be of use in the construction of such a vessel. The actual construction of the vessel took over three weeks, but could have taken less than a week if a proper description of design considerations and methods had been available. The vessel was built entirely from commercially available parts at a cost of about $200.00.

Figure 38 is a drawing of one end of the pressure vessel showing the parts used and the dimensions; the other end is identical. The flanges and blind plates used are of forged steel while the tube itself is a 6" double-extra strong pipe. There are 12-3/4" bolts through each threaded flange and blind flange. The blind flanges were made to fit the end of the pipe by lapping the two surfaces with carborumdum. Fiber gaskets and a high pressure,



PRESSURE VESSEL

FIGURE 38

non-oil soluble gasket cement was satisfactory for pressures up to 2500 p.s.i.g., but higher pressures caused the fiber gasket to squeeze out. Finally gaskets of soft electrolytic copper were used along with a non-hardening gasket cement called "Leak-Lok."

In order to give a complete discussion of stresses in each part of the pressure vessel the numbers of the vessel itself will be analyzed without the channels or tension bars. In each case the stresses caused by a pressure of 2500 p.s.i.g. will be calculated. Other pressures will cause stresses in direct proportion.

Wall of Vessel. The 6" extra heavy pipe has an inside diameter of 4.897 inches and walls whose thickness if 0.864 inches. Stress in the walls is the vectoral sum of two components, the longitudinal tension due to pressure on the end of the vessel, and hoop tension which acts at right angles. The first is the pressure on the end divided by the area of steel in the pipe's cross section.

$$\frac{\pi \times 4.897^2 \times 2500}{4 \times 15.65} = 3{,}100 \text{ p.s.i.}$$

The hoop stress is found by the force acting on the inside diameter of the pipe for a 1" length divided by the area of steel in a 1" longitudinal section.

$$\frac{2500 \times 4.897}{2 \times .864} = 7{,}100 \text{ p.s.i.}$$

The square root of the sum of the squares of these two values gives the magnitude of the resultant which is 7,760 p.s.i. Since the elastic limit for structural steel is over 30,000 p.s.i. the vessel walls would have a factor of safety of almost 2 even under a pressure of 5,000 p.s.i.g. The stress at the threads would be higher if it were not for the fact that the threaded flange extends to the base of the threads and relieves the stress to a certain extent. A simple calculation shows that the threaded area is sufficient to carry the full stress in any case. Also when the vessel has a pressure of 5,000 p.s.i.g., the tension bars take all of the extra longitudinal stress.

Bolts. Each bolt has a cross sectional area of 0.442 sq. in., but the net area at the threads is only 0.302 sq. in. The total net area of the 12 bolts must stand the force on the end of the vessel which is $\pi/4 \times 4.897^2 \times 2500 = 47,100$ pounds.

$$\frac{47,100}{12 \times .302} = 13,000 \text{ p.s.i.}$$

Here again the longitudinal tension bars take the extra stress when higher pressures are used.

Stress in Blind Plate. The equation for the maximum bending moment at the center of a simply supported circular plate loaded uniformly over a circular central area is (adapted from Den Hartog, 1952, p. 129):

$$M = \frac{P}{4\pi} \left[(1 + m) \ln \frac{a}{b} + 1 - \frac{(1 - m) b^2}{4 a^2} \right]$$

where

M is the maximum moment - lb. in.

P is the total load - 47,100 pounds.

m is Poisson's ratio + here taken as 0.3

a is the radius of the plate - here the bolt circle represents the support a = 5.313 in.

b is the radius of the loaded area -- 2.449 in.

Calculation shows that M = 7,390 bb. in. The section modulus for a unit width of the plate is given by

$$S = 1/6\ bd^2 = 1/6 \times 1 \times 2.25 = 0.375\ in.^3$$

since d is the plate thickness and 1 1/2 inches. The extreme fiber stress in the flange is

$$\text{Stress} = 7{,}390/.375 = 19{,}700\ \text{p.s.i.}$$

Here again the channels and tension bars would be in place for pressures over 2500 p.s.i.g. and would support the center of the blind flange.

Threaded Flange. In a like manner the equation for the maximum bending moment is given by

$$M = \frac{P}{8\pi\left[(1+m)\frac{a^2}{b^2} + 1 - m\right]}\left\{2(1-m)\left(\frac{a^2}{b^2} - 1\right)+4(1+m)\frac{a^2}{b^2}\ln\frac{a}{b}\right\},$$

where all terms are the same as in the previous equation except that P is the load applied to the circumference of the hole of radius b. P is still 47,100 pounds. M is found to be 8,390 lb. in. and the stress is 22,300 p.s.i. All of the load carried by the threaded flange is carried by the bolts and

the blind flange. Under higher stresses the tension rods and channels would be in place.

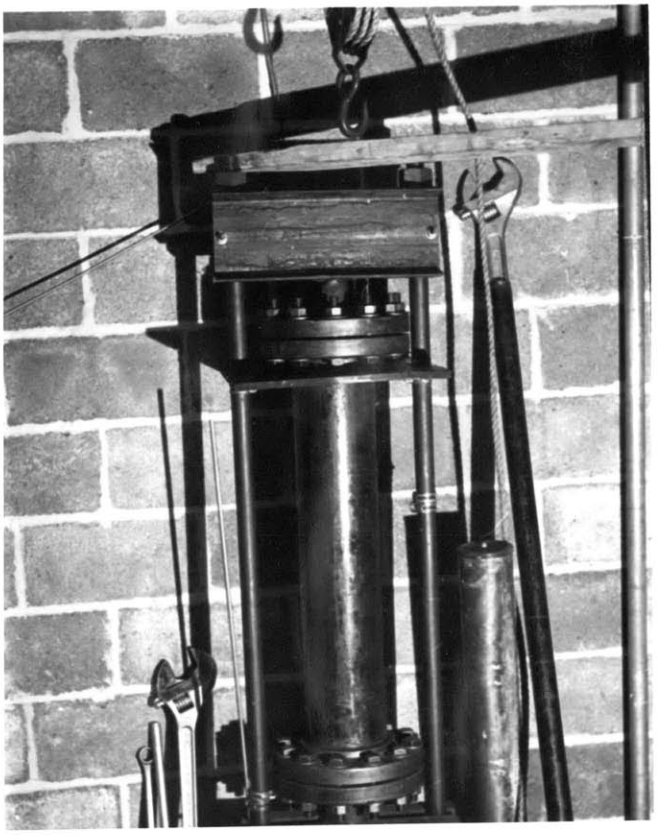
In the calculation of stresses in the flanges it was assumed that the stresses in the bolts were no greater than that required to hold the pressure of 2500 p.s.i.g. in the vessel. Actually the bolts must have a greater stress than this so that there is always some compression on the gasket. Thus the blind flange must withstand the pressure of the fluid plus the pressure of the end of the pipe acting through the gasket. The sum of these stresses is transmitted by the bolts to the threaded flange and the pipe. The additional stress caused by this extra force is not considered great.

Threads of Pipe. The longitudinal tension carried by the pipe must be transmitted to the threaded flange by the threads which thus have a shear stress. The area at the base of the threads is taken as 0.8 of the total thread width.

$$\text{Shearing stress} = \frac{47{,}100}{6.625 \times \pi \times 1\ 1/2 \times 0.8} = 1890 \text{ p.s.i.}$$

The factor of safety here is at least 5.

When the vessel is to be used at higher pressures reinforcement is added in the form of two "U" channels and 1 1/2 inch round tension bars which run the full length of the vessel. Again each end of the vessel is the same. The channels which are back to back and separated by the 1 1/2 inches



PRESSURE VESSEL

PLATE 20

required for the tension bars, bear against the centers of the blind flanges through bars of steel 4 inches in diameter and three inches long. The details of this arrangement are shown on the photographs of Plate 20. Since the short bar of metal acts over almost the same diameter as the fluid of the vessel, it can be assumed that negligible moment is imparted to the blind flange by transmission of force from the fluid through the flange to the short bar and channels. In other words the forces from pressures in excess of 2500 p.s.i.g. can be considered to act directly on the channels. Since it is desired to use the vessel at 5000 p.s.i.g. the stresses caused by the additional force of 47,100 pounds will be analyzed to see the stresses caused in the channels and 1 1/2" bars.

Channels. It is assumed that the force applied by the short metal bar acts at the center of the channel which in turn transmits half the force to each of the tension bars. The channels are 7 inch 9.8 channels with a section modulus S of 6.0 in.^{3} (Steel Construction, 1947). The tension bars are 14 inches apart center to center.

$$\text{Stress} = \frac{P}{2} \times \frac{l}{2} \Big/ 2S = 14{,}000 \text{ p.s.i.}$$

where P = 47,100 pounds and l = 14 inches and S = 6.0 in.^{3}.

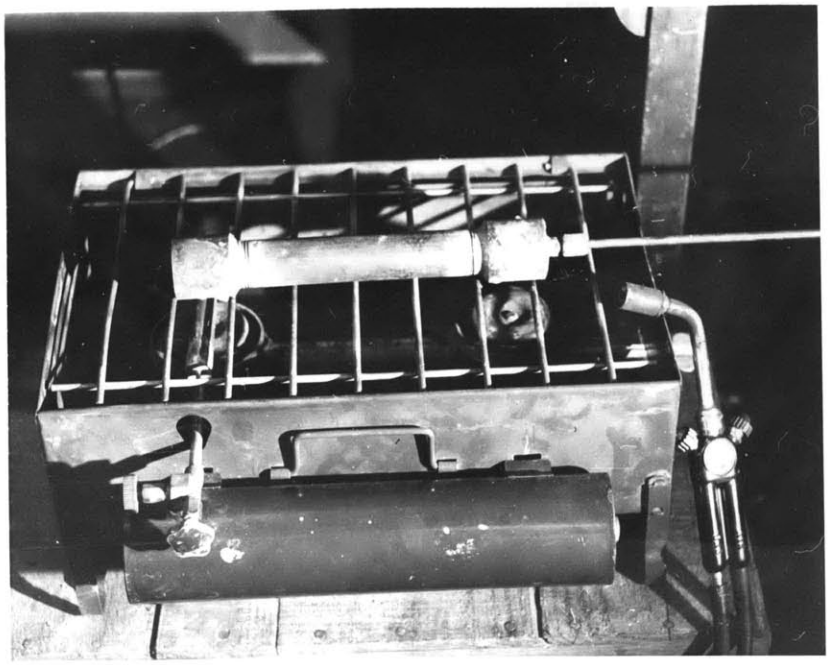
Tension Bars. The 1 1/2 inch tension bars each have a gross area of 1.767 sq. in. and a net area of 1.294 sq. in. at the threads.

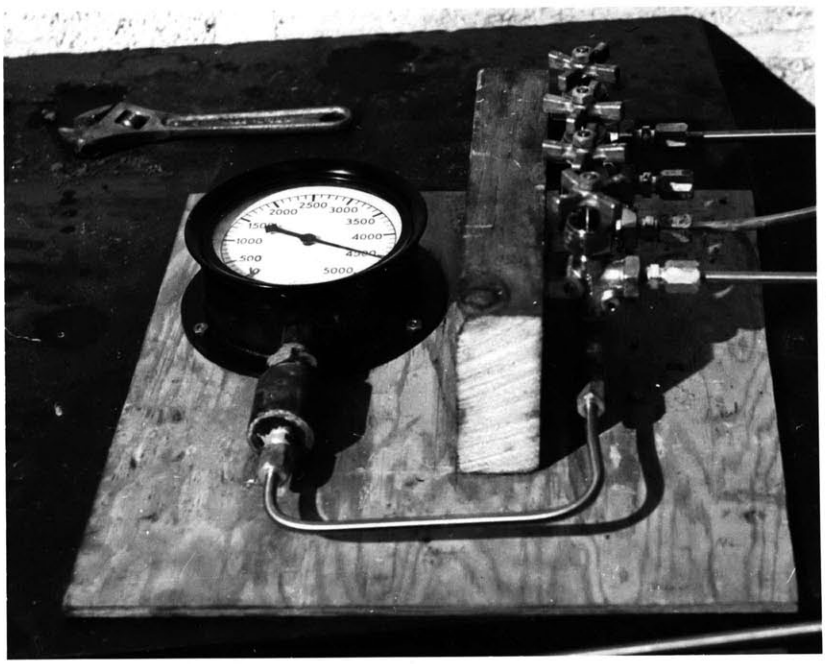
$$\text{Stress} = \frac{47{,}100}{2 \times 1.294} = 18{,}210 \text{ p.s.i.}$$

The channels and tension bars can stand the extra stress with a good margin of safety. In order for the bars to carry the necessary load they must be pre-stressed. The bars are about 60 inches long which means that they must be stretched about 0.040 inches to develop a stress of 20,000 p.s.i. The blind flanges of the pressure vessel would not deflect more than about 0.002 inches each which would stress the bars to only 2,000 p.s.i. (E = 30,000,000 p.s.i.). To measure the tension in the bars an extensometer was attached to each tension bar. These were later dispensed with since the necessary stress was developed in the bars by applying the writer's full strength to the heavy wrenches shown in the photograph.

The stress in the tension bars and in the 12 small bolts causes a total compressive force on each gasket of over 100,000 pounds before the pressure is applied to the vessel. As the fluid pressure in the vessel increases the force is transferred to the fluid.

Pressures up to 2,300 p.s.i.g. were obtained directly from a nitrogen bottle. Higher pressures were obtained by means of a small device here called a "booster." The booster is merely a piece of extra strong 1 1/2 inch pipe with very high pressure caps. See Plate 21. The booster is filled with water and then connected to the pressure vessel and the nitrogen bottle by a system of high pressure valves.





Upper Picture: Booster
Lower Picture: Valve Arrangement

AUXILIARY VESSEL EQUIPMENT

Plate 21

Nitrogen at over 2000 p.s.i.g. is introduced into the system. Since the whole vessel and the booster and all the lines are filled with fluid as much as possible, the quantity of nitrogen introduced is small. The booster is then heated to drive off the nitrogen dissolved in the water along with a small amount of steam and this raises the pressure. The heat applied does not decrease the strength of the steel in the booster since structural steel reaches its maximum strength at 500° F. and at 800° F is back to about the strength at room temperature.

Plate 21 at the bottom shows the valve arrangement used. The four needle valves shown are all connected into a common manifold into which the 5000 p.s.i.g. gage is connected permanently. In order from back to front the valves are connected as follows:

1) To the pressure vessel

2) No connection - used to release pressure

3) To nitrogen bottle

4) To booster.

The sequence of operations is as follows in raising the pressure.

1) Seal and tighten pressure vessel.

2) Fill vessel full of kerosine through fitting and then attach tubing.

3) Fill booster with water through fitting and then attach tubing.

4) Shut valves 2 and 3 and open 1 and 4.

5) Open valve 3 for about a minute and close it again.

6) Heat booster till desired pressure is reached and then close valve 1 and turn heat off booster immediately. If desired pressure is not reached by first booster treatment vessel pressure will level off and the following steps taken:

7) Cool the booster slowly by drops of water to a point where quenching is safe, then quench. The gage will read a few hundred pounds after this but the vessel will be at the highest pressure reached since valve 1 is still closed.

8) Open valve 3 for a minute to again saturate the water in the booster and close it again.

9) Heat the booster till the gage reads the value of pressure which the vessel reached on the first trial and then open valve 1.

10) Continue heating booster till desired pressure is reached. If it is not, then steps 7 to 10 can be repeated over again until the pressure is reached. In some cases the manifold pressure may have to be released completely to put more water into the booster.

The difficulty in raising the vessel to any desired pressure is proportional to the lost volume in the system which is not filled with liquids. An efficient method of filling the system was finally discovered. After step 4 a hydroaspirator was connected to valve 2 which was opened.

After a time this valve was closed maintaining a partial vacuum in the parts of the system not filled with liquid. The hydroaspirator connection was then disconnected and placed under water. On opening valve 2 water rushed into the voids in the system. These steps were generally repeated twice and usually enabled the system to be brought to a pressure of almost 5000 p.s.i.g. with only two booster cycles.

All lines were 1/4 inch steel tubing except for the line to the nitrogen bottle which never was subjected to over 2300 p.s.i.g. Parker "Ferrulok" fittings were used throughout and were very satisfactory.

Plate 20 shows the completed vessel under pressure as well as the inner liner which was inserted into the vessel for experiments with acetone. Tools and equipment used in assembling and disassembling the vessel are also shown. The block and tackle were required to raise the vessel onto the lower channels since the total weight of the apparatus was 486 pounds of which the channels, tension bars, and short 4" bars were 146, and the vessel itself was 340 pounds.

BIOGRAPHICAL NOTE

William B. Farrington was born in New York City on March 10, 1921. He received the degree Bachelor of Civil Engineering from Cornell in 1947 and the degree Master of Science in 1949 also from Cornell. The thesis for his Master's degree was "Depth of Burial, the Major Cause of Changes of Carbon Ratio in West Virginia." Mr. Farrington worked as a radio engineer for one year during the war, and for one year prior to entering M.I.T. he was a plant engineer with a company engaged in light steel fabrication.